ELECTROCHEMICAL DETECTION OF HERBICIDES AND ANTIOXIDANTS USING NANOMATE
RIAL-MODIFIED ELECTRODE

Miss Kanokwan Charoenkitamorn

A Dissertation Submitted in Partial Fulfillment of the Requirements

for the Degree of Doctor of Philosophy in Chemistry

Department of Chemistry

FACULTY OF SCIENCE

Chulalongkorn University

Academic Year 2018

ELECTROCHEMICAL DETECTION OF HERBICIDES AND ANTIOXIDANTS USING NANOMATE
RIAL-MODIFIED ELECTRODE

Miss Kanokwan Charoenkitamorn

จุฬาลงกรณ์มหาวิทยาลัย
CHULALONGKORN UNIVERSITY

A Dissertation Submitted in Partial Fulfillment of the Requirements
for the Degree of Doctor of Philosophy in Chemistry
Department of Chemistry
FACULTY OF SCIENCE
Chulalongkorn University
Academic Year 2018
Copyright of Chulalongkorn University

Dissertation Title	ELECTROCHEMICAL DETECTION OF HERBICIDES AND ANTI OXIDANTS USING NANOMATERIAL-MODIFIED ELECTRODE
By	Miss Kanokwan Charoenkitamorn
Field of Study	Chemistry
Thesis Advisor	Orawon Chailapakul

Accepted by the FACULTY OF SCIENCE, Chulalongkorn University in Partial Fulfillment of the Requirement for the Doctor of Philosophy

.... Dean of the FACULTY OF SCIENCE

(Polkit Sangvanich)

DISSERTATION COMMITTEE

.... Chairman

(Vudhichai Parasuk)

.... Advisor

(Orawon Chailapakul)

.... Examiner

(Nattaya Ngamrojanavanich)

.... Examiner

(Narong Praphairaksit)

.... External Examiner

(Weena Siangproh)

กนกวรรณ เจริญกิจจอมร : การตรวจวัดทางเคมีไฟฟ้าของสารกำจัดศัตรูพืชและสารต้านอนุมูลอิสระโดยใช้ขั้วไฟฟ้าดัดแปรด้วยวัสดุระดับนาโนเมตร. (ELECTROCHEMICAL DETECTION OF HERBICIDES AND ANTIOXIDANTS USING NANOMATERIAL-MODIFIED ELECTRODE) อ.ที่ปรึกษาวิทยานิพนธ์หลัก : อรวรรณ ชัยลภากุล

วิทยานิพนธ์ฉบับนี้มุ่งเน้นการพัฒนาเซนเซอร์ทางเคมีไฟฟ้าร่วมกับวัสดุระดับนาโนเมตรสำหรับการประยุกต์ใช้ในทางเภสัชกรรมและสิ่งแวดล้อม โดยแบ่งออกเป็น 2 ส่วนหลัก ส่วนแรกคือการพัฒนาเซนเซอร์ที่มีราคาถูกแบบใช้แล้วทิ้งสำหรับการตรวจวัดโดยพร้อม ๆ กันของโคเอนไซม์ คิวเท็น และ กรดอัลฟาลิโปอิก โดยใช้ขั้วไฟฟ้าพิมพ์สกรีนกราฟีนดัดแปรด้วยแมงกานีสออกไซด์ การผสมผสานของแมงกานีสออกไซด์ลงบนขั้วไฟฟ้าพิมพ์สกรีนกราฟีนช่วยเพิ่มประสิทธิภาพในการเกิดออกซิเดชั่นของ โคเอนไซม์ คิวเท็น และ กรดอัลฟาลิโปอิก เป็นอย่างมาก ไซคลิกโวลเมตตรีและสแควร์-เวฟแอโนดิกสตริปปิงโวลแทมเมตรี ถูกนำมาใช้ในการตรวจสอบพฤติกรรมทางเคมีไฟฟ้า และการวิเคราะห์เชิงปริมาณของเซ็นเซอร์ต่อ โคเอนไซม์ คิวเท็น และกรดอัลฟาลิโปอิก เซ็นเซอร์ที่พัฒนาขึ้นมานี้มีราคาถูกและสามารถใช้แล้วทิ้งสำหรับการตรวจวัดโคเอนไซม์ คิวเท็น และกรดอัลฟาลิโปอิก นอกจากนี้ เซนเซอร์ทางเคมีไฟฟ้าร่วมกับวัสดุระดับนาโนเมตรสามารถนำไปใช้ร่วมกับวิธีการวิเคราะห์อื่น ๆ เพื่อเพิ่มประสิทธิภาพของวิธีวิเคราะห์ ซึ่งงานวิจัยนี้ได้นำเสนอในส่วนที่สอง อนุภาคทองคำระดับนาโนเมตรดัดแปรบนขั้วไฟฟ้าพิมพ์สกรีนคาร์บอนร่วมกับเทคนิคอัลตราไฮเพอร์ฟอร์แมนซ์ลิควิดโครมาโตกราฟี ได้ถูกพัฒนาขึ้นเพื่อการตรวจวัดสารกำจัดวัชพืชประเภทไดไทโอคาร์บาเมต จากผลการทดลองการใช้อนุภาคทองคำระดับนาโนเมตรแสดงถึงการปรับปรุงการทำงานของการเร่งปฏิกิริยาออกซิเดชันของสารประกอบไดไทโอคาร์บาเมต เทคนิคแอมเพอโรเมตรีถูกนำมาใช้เป็นวิธีตรวจวัดหลังการการแยกสารประกอบด้วยเทคนิคอัลตราไฮเพอร์ฟอร์แมนซ์ลิควิดโครมาโตกราฟี พารามิเตอร์ต่างๆ ของระบบการตรวจวัดทั้งสองงานวิจัยได้ถูกศึกษาเพื่อให้ได้ภาวะที่เหมาะสมที่สุด ความไว ความจำเพาะและประสิทธิภาพในการตรวจวัดของเซนเซอร์ทั้งสองได้ถูกอภิปราย ภายใต้ภาวะที่เหมาะสมที่สุด พบว่าความถูกต้องเซนเซอร์ที่พัฒนาขึ้นอยู่ในช่วงที่สามารถยอมรับได้โดยให้ขีดจำกัดต่ำสุดของการตรวจวัดอยู่ในระดับไมโครกรัมต่อมิลลิลิตร ท้ายนี้เซนเซอร์ที่ถูกนำเสนอยังประสบความสำเร็จในการประยุกต์ใช้ในการตรวจวัดสารที่สนใจในตัวอย่างจริง เช่น ตัวอย่างทางเภสัชกรรม ผลไม้ และผัก เซนเซอร์ที่พัฒนาขึ้นในทั้งสองส่วนแสดงถึงศักยภาพสูงในการใช้งานในทางปฏิบัติ

ภาควิชา	ภาควิชาเคมี	ลายมือชื่อนิสิต ....
สาขาวิชา	เคมี	ลายมือชื่อ อ.ที่ปรึกษาวิทยานิพนธ์หลัก ....
ปีการศึกษา	2561	

5472801023 : DOCTOR OF PHILOSOPHY

ELECTROCHEMICAL DETECTION, ULTRA-HIGH PERFORMANCE LIQUID CHROMATOGRAPHY, NANOMATERIALS, HERBICIDES, ANTIOXIDANTS

Kanokwan   Charoenkitamorn   :
ELECTROCHEMICAL DETECTION OF HERBICIDES AND ANTIOXIDANTS USING NANOMATERIAL-MODIFIED ELECTRODE. ADVISOR: Orawon Chailapakul

This dissertation focused on the development of a novel nanomaterial-based electrochemical sensors for pharmaceutical and environmental applications. The research is divided into two parts. In the first part, a low-cost and disposable sensor for the simultaneous determination of coenzyme Q10 (CoQ10) and α-lipoic acid (ALA) using manganese (IV) oxide-modified screen-printed graphene (MnO_2/SPGE) electrode was developed. The incorporated MnO_2 in the SPGE can greatly enhance the detection performance towards the oxidation of CoQ10 and ALA. The cyclic voltammetry (CV) and square-wave anodic stripping voltammetry (SWASV) were employed to investigate the electrochemical behavior of the developed sensor and also to perform the quantitative analysis of the analytes. This developed sensor provides an inexpensive and disposable sensor for the detection of CoQ10 and ALA. Furthermore, the nanomaterial-based electrochemical sensor exhibits the potential to integrate with other analytical methods for improving the analytical performance. The detail was demonstrated in part 2. In this part, the gold nanoparticle-modified screen-printed carbon electrode (AuNP/SPCE) integrated with ultra-high performance liquid chromatography (UHPLC) was developed for the detection of dithiocarbamate herbicides. Based on the obtained results, AuNPs play a catalytic activity towards the oxidation of dithiocarbamate compounds. The amperometric detection was performed after separation using UHPLC technique. The experimental parameters of both researches were optimized to obtain the best condition. The sensitivity, selectivity and analytical performance of both proposed sensors were discussed. Under the optimal conditions, the proposed sensors showed an acceptable range of accuracy and precision with low limits of detection in the micro-gram levels. Finally, the proposed sensors were successfully applied to detect target analytes in pharmaceutical, fruit, and vegetable samples. These developed systems exhibit the high potential to be useful methodologies for practical applications.

Department:	Department of Chemistry	Student's Signature ....
Field of Study:	Chemistry	Advisor's Signature ....
Academic Year:	2018	

ACKNOWLEDGEMENTS

TABLE OF CONTENTS

จุฬาลงกรณ์มหาวิทยาลัย

CHULALONGKORN UNIVERSITY

LIST OF TABLES

LIST OF FIGURES

LIST OF ABBREVIATIONS

°C	degree Celsius
µF	micro-farad
µm	micro-meter
µM	micro-molar
A	electrode area
A	Ampere
AE	auxiliary electrode
Ag/AgCl	silver/silver chloride
ALA	α-lipoic acid
ASV	anodic stripping voltammetry
AuNPs	gold nanoparticles
BDD	boron doped diamond
C	concentration
C_{dl}	double layer capacitance
CFME	cylindrical carbon fiber microelectrode
C_m	concentration of solute in the mobile phase
cm	centi-meter
CMCPE	carbon paste electrode modified with nickel (II)-cyclohexylbutyrate
C_o	concentration of the oxidized form
CoQ10	coenzyme Q10
C_R	concentration of the reduced form

C_s	concentration of solute in the stationary phase
CV	cyclic voltammetry
D	diffusion coefficient
D_0	diffusion coefficient
DEDMTDS	*N,N*-diethyl-*N',N'*-dimethylthiuram disulfide
DHALA	dihydrolipoic acid
DPV	differential pulse voltammetry
DTCs	dithiocarbamate compounds
E	Potential
E^0	standard potential for the redox reaction
E_{pa}	anodic peak potential
E_{pc}	cathodic peak potential
F	Faraday constant
FL	fluorescence
FTO	fluorine-doped tin oxide electrode
G	Graphene
GC	glassy carbon
H	plate height
h	Hour
HDME	hanging mercury drop electrode
Hz	Hertz
$i_{average}$	average current from the forward and reverse sweeps

i_{pa}	anodic peak current
i_{pc}	cathodic peak current
K	partition coefficient
k'	capacity factor
$K_3Fe(CN)_6$	potassium ferricyanide
kg	kilo-gram
KNO_3	potassium nitrate
L	length of column
LOD	limit of detection
LOQ	limit of quantitation
M	Molar
mg	milli-gram
min	Minute
mL	milli-liters
mm	milli-meter
mM	milli-meter
MS	mass spectrometry
mV	milli-volt
n	number of electron
N	number of theoretical plates
ng	nano-gram
nm	nano-meter
nM	nano-molar

pg	pico-gram
PG/CoPc	a pyrolytic graphite electrode modified with cobalt phthalocyanine
PVC	polyvinylchloride
R	gas constant
RE	reference electrode
rpm	revolutions per minute
RSD	relative standard deviation
S	sensitivity of method
s	Second
S/B	signal-to-background ratio
S_{bl}	standard deviation of blank
SD	standard deviation
SEM	scanning Electron Microscope
SPCE	screen-printed carbon electrode
SPE	screen-printed electrode
SPGE	screen-printed graphene electrode
SPGE	screen-printed graphene electrode
SWASV	square wave anodic stripping voltammetry
SWV	square-wave voltammetry
T	temperature
t'_r	adjusted retention time
t_m	retention time of unretained mobile phase

t_r	retention time
UHPLC	ultra-high performance liquid chromatography
UHPLC-ED	ultra-high performance liquid chromatography coupled with electrochemical detection
UHPLC-UV	ultra-high performance liquid chromatography coupled with ultraviolet detection
u_v	volume flow rate of the mobile phase
u_x	linear flow rate
v	potential scan rate
v/v	volume by volume
V_m	volume of mobile phase
V_r	retention volume
V_s	volume of stationary phase
w	peak width at the base
$w_{1/2}$	width at half-height
WE	working electrode
x	distance traveled
σ	standard deviation of the Gaussian band
Ω	Ohm
V	Volt

CHAPTER I:

INTRODUCTION

1.1 Introduction

Nowadays, numerous approaches have been introduced in analytical chemistry for various applications. However, electrochemical sensor demonstrates the most rapidly growing class of chemical sensor in applications due to its unique properties. Electrochemical sensor has been extensively used for monitoring of interested analytes especially in clinical diagnosis, industrial and environmental monitoring, as well as agricultural area.

An electrochemical measurement directly relates to oxidation-reduction reactions and other charge-transfer phenomena. Electrochemical method has received great interest and had high demand in analytical field because of their simplicity, low cost, short analysis time, and high sensitivity [1-3]. Over the past few years, many researchers have focused on the development of the portable electrochemical sensor. They aim to miniaturize the conventional electrochemical cell for on-site applications. The design of electrochemical sensors has been developed for simplifying the preparation step and ease of use. Disposable sensors have received great attention in many applications, such as clinical, environmental and industrial analysis. The screen-printing technology represents a well-known and the most popular technique for the fabrication of the disposable electrochemical sensor on economical substrates. Screen-printed electrode (SPE) is an alternative choice that can possibly use instead of using the traditional electrodes. SPE has been extensively extended from rigid materials to many flexible substrates such as paper, plastic sheets, wearable clothes, gloves, and etc., to further widen use in the various applications [4-6].

Screen-printed carbon electrode (SPCE), one of a carbon-based material, is the most widely used as working electrode in electrochemical sensor. The preparation of SPCE is simple and able to use only once and then discarded. This makes the use

of SPCE can eliminate the surface fouling problem in comparison to those conventional electrodes. However, the limitation of SPCE is lack of sensitivity and selectivity. Therefore, to make SPCE properties meet the detection requirements, the modification is necessary [7, 8]. Nanomaterials, such as metals, alloys, inorganic substances, polymers, and composites, are extensively employed as the modifier of electrode surface in electrochemical applications. These mentioned materials can enhance conductive property, selectivity and surface area of the modified material [9-12]. Based on the several unique properties of nanomaterials, the SPCE incorporating with various nanomaterials offers the improvement of electrochemical efficiency.

As literature reviews, the aim of this dissertation is to develop novel electrochemical sensors incorporating with nanomaterial for pharmaceutical and environmental applications. In addition, to make a novel electrochemical sensor more flexible use, we also demonstrated the integration of this developed sensor with other analytical methods for widening further application.

First, the development of the disposable electrochemical sensor for the pharmaceutical application was proposed. Coenzyme Q10 (CoQ10) and α-lipoic acid (ALA) are the powerful anti-oxidant that normally present in many dietary supplements. The disposable electrochemical sensor using screen-printed graphene electrode (SPGE) and metal oxide for the detection of CoQ10 and ALA was developed. Graphene is a one-atom-thick planar sheet of sp^2 bonded carbon atoms in a honeycomb crystal lattice, and has recently attracted interest as a material for the fabrication of sensors. The unique property of graphene allows applications in various fields such as sensing and biosensing, energy conversion and storage, catalysis, composites and coatings, electronics and the biomedical field. Graphene has the ability to promote electron transfer in some species and also has excellent electrocatalytic activity [1, 13]. To further improve the electrochemical efficiency, metal oxides are another interesting material that can be used as a modifier on an electrode surface. Metal oxides such as MnO_2, Fe_3O_4, FeO, SnO_2, CuO, and Fe_2O_3

exhibit a high electrocatalytic activity toward compounds that show a slow redox process a low over-potential for the oxidation or reduction of analytes at bare electrodes [1, 14]. Among the metal oxides, MnO_2 has gained considerable attention as a modifier because of its low cost, wide abundance, and environmental friendliness [15, 16]. Therefore, the combination of MnO_2 and graphene as a novel effective material for electrochemical sensing was proposed. This is the first application of the use of MnO_2/SPGE for the determination CoQ10 and ALA. Finally, to demonstrate the capability of the proposed sensor, this introduced sensor was applied to determine CoQ10 and ALA in dietary supplements from the local market.

The combination of electrochemical detection with other analytical methods is also presented in this dissertation. Ultra-high performance liquid chromatography coupled with electrochemical detection (UHPLC-ED) for the environmental application was proposed. Thiram (tetramethyl thiuram), disulfiram (tetraethyl thiuram), and their intermediate of *N,N*-diethyl-*N',N'*-dimethylthiuram disulfide (DEDMTDS) are chosen as representative compounds of dithiocarbamates (DTCs) fungicides because they are extensively used to control a variety of pest in agriculture [17]. Because of the similar functional group of their structures, only electrochemical detection could not be used to distinguish their electrochemical signal when the simultaneous detection of a mixture component was performed. To overcome this challenge, the UHPLC was combined in order to separate the compounds prior to the measurement by the electrochemical technique. In this work, the disposable sensor was developed using a carbon-based material modified with metal nanoparticles. Based on the literature reviews, gold nanoparticles (AuNPs) are widely used for the modification of electrode surface since it provides distinguish properties including high effective surface area and conductivity, and can also use as the catalyst of the reaction. In addition, AuNPs exhibits a strong specific interaction with the sulfur-containing compounds which contain in the structure of DTCs [18]. According to these mentioned properties, AuNPs were selected to use as modifier onto SPCE to improve the electrochemical efficiency

of DTCs detection. This is the first report for UHPLC-ED using AuNPs modified SPCE to analyze thiram, DEDMTDS, and disulfiram, the DTCs in fruits and vegetables collected from local markets. Fortunately, the result obtained from this proposed UHPLC-ED system is acceptable and reliable compared those standard UHPLC-UV methods without any derivatization.

1.2 Objective of the thesis

There are two targets of this dissertation

(1) To develop and apply a novel, low-cost and disposable sensor for the simultaneous determination of CoQ10 and ALA using MnO_2-modified SPGE.

(2) To develop and apply AuNP/SPCE to integrate with UHPLC for simultaneous determination of DTC herbicides with high sensitivity, specificity, and rapid analysis for an environmental application.

1.3 Scope of the thesis

To achieve research objectives, the below scopes were set.

(1) The in-house SPE was fabricated on polyvinylchloride (PVC) substrate. The different configurations of SPE were custom designed depending on their application. The various types of nanomaterials for the modification of electrode surface were investigated relating to the analytes of interest. The method and type of nanomaterials for electrode modification were carefully selected. Moreover, the relevant parameters were optimized to obtain the best electrochemical efficiency.

(2) The disposable electrochemical sensor for simultaneous determination of CoQ10 and ALA using MnO_2/SPGE was developed to obtain the low limit of detection. Square wave anodic stripping voltammetry (SWASV) was used for the quantitative determination of CoQ10 and ALA. The parameters of SWASV were optimized to obtain

the highest performance of the proposed electrode. The foreign substances were investigated to confirm the applicability of the method to detect the target compounds for practical use in pharmaceutical samples.

(3) Combination of AuNP-modified SPCE for electrochemical detection and UHPLC technique was developed for sensitive and selective determination of DTCs. The ratio of organic solvent and supporting electrolyte was studied to provide the best separation performance. The electrochemical detection was operated using amperometry. The performance of the proposed UHPLC-ED was verified with conventional UHPLC-UV.

(4) Finally, the capability of both systems was evaluated for practical sample applications.

1.4 Research utilization

(1) Obtain a novel electrochemical sensor for the simultaneous determination of CoQ10 and ALA using MnO_2/SPGE.

(2) Obtain the alternative system for the determination of DTCs using AuNP/SPCE in UHPLC-ED.

(3) Succeed in improving electrochemical efficiency in term of sensitivity, accuracy, cost, and disposability for the determination of CoQ10 and ALA, and DTCs.

(4) Succeed in applying the developed system in pharmaceutical and environmental applications.

There are five chapters in this dissertation. Chapter I is an introduction to give an overview of the dissertation. Chapter II is a theory that describes to a fundamental of electrochemical technique, and the principle of UHPLC. In chapter II also includes the literature reviews of the previous study related to the detection of the analytes.

Chapter III contains an experimental part, referring to the all chemicals, reagents, and instruments used in the detection of the analytes as well as the procedure for the measurement. Chapter IV, results and discussion, that consists of two main parts. First is the electrochemical detection of CoQ10 and ALA, and second is UHLPC-ED for the determination of DTCs. Last is Chapter V which is a conclusion and future perspectives.

CHAPTER II:

THEORY AND LITERATURE REVIEWS

2.1 Electrochemistry

Generally, there are two kinds of electrochemical cells which are galvanic cell and electrolytic cell. Galvanic cell produces an electric current from energy released by a spontaneous redox reaction. On the other hand, electrolytic cell requires an external source of electrical energy to induce a chemical reaction. Electrolytic method has many advantages, for instance, high sensitivity with a wide linear dynamic range of concentration for both inorganic and organic species, simplicity, rapid analysis time, and simultaneous detection of various target analytes. The selection of the electrochemical techniques depends on the nature of ions or compounds of interest and its interferences in surrounding environment [19, 20]. Electrochemistry can be used to study the oxidation (loss of electrons) or reduction (gain of electrons) that a material undergoes during the electrical stimulation. These redox reactions (reduction and oxidation reactions) can provide information about the concentration, reaction mechanisms, kinetics, chemical status, and other behaviors of a species in solution.

2.1.1 Fundamental of electrochemistry

The controlled-potential of electrochemical experiment aims to obtain the current which is related to the concentration of target analytes. To approach the aim, the transfer of electron(s) at the working electrode surface during redox reaction of the analyte was monitored [19-25].

$$O + ne^- \quad \rightleftharpoons \quad R \qquad \qquad \text{(Equation 2.1)}$$

Where O and R are the oxidized and reduced forms, respectively, of a redox reaction. The redox reaction occurs in the potential region that the electron transfer is favorable thermodynamically or kinetically. For the thermodynamically controlled system, the concentration of the electroactive species [$C_o(0,t)$ and $C_R(0,t)$]

can be established by the potential of the electrode according to the Nernst equation.

$$E = E^0 + \frac{2.3\ RT}{nF}\ \log \frac{C_O(0,t)}{C_R(0,t)}$$
(Equation 2,2)

Where E^0 = standard potential for the redox reaction.

R = gas constant (8.314 $JK^{-1}mol^{-1}$).

T = temperature in Kelvin.

n = number of electrons transferred in the redox reaction.

F = Faraday constant (96,487 coulombs).

$C_o(0,t)$ = concentration of the oxidized form

$C_R(0,t)$ = concentration of the reduced form.

2.1.2 Mass transfer-controlled reaction

Mass transfer process is one of the main fundamental electrochemistry to describe charge transfer on the surface of the electrode. There are three different modes of mass transfer of redox reaction as shown in figure 2.1.

2.1.2.1 Diffusion

Diffusion is the spontaneous movement of the ions or molecules in solution influenced by the concentration gradient. The ions move from the high concentration region to low concentration region to minimize the different concentration.

2.1.2.1 Convection

Convection is the physical movement in fluids by hydrodynamics. The main driving force of convection is generated from the external mechanical energy such as flowing or stirring of solution, and vibrating or rotating of electrode, as well as the nature of density gradient.

2.1.2.3 Migration

Migration is the movement of charge under the electrical field. The positive charge will be attached by negative charge while the negative charge will be also attracted to opposite way. The potential at the surface of electrode effected on the increased or decreased velocity of ions. Migration of all ion species in the system can take place; therefore, the current of ions from analyte might be suppressed. To decrease the effect of migration, the addition of a high concentration of supporting electrolyte usually applies.
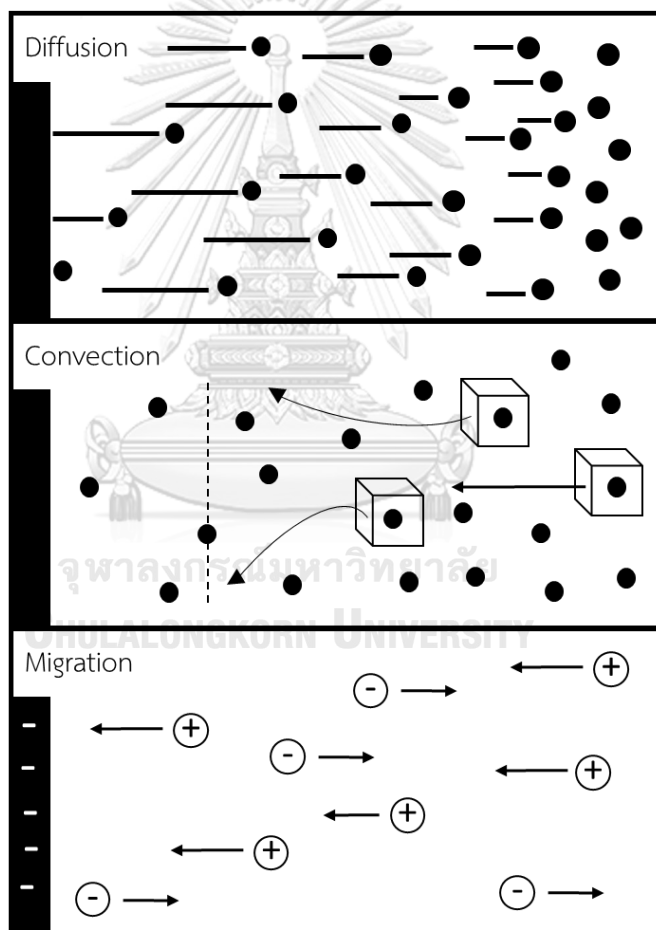
Figure 2.1 *The three modes of mass transport*

2.1.3 Voltammetry

Voltammetry is one category of electrochemical methods for the qualitative and quantitative analysis in analytical chemistry. Voltammetry provides the information of the analyte by applying the varied potential to electrode surrounding with a supporting electrolyte containing electro-active species and measuring the current response through the electrode. Voltammetric electrochemical cell consists of three or two electrodes including working, reference, and auxiliary electrodes (optional). First, working electrode (WE) is the electrode where the redox reaction occurs at the surface. WE is the most important electrode which indicated the signal response to the analytes. Second is reference electrode (RE). The potential of RE is well-known and remains constantly since no electron flow through. The last electrode is auxiliary electrode (AE) which is the optional electrode for three-electrode system. An electrical current of other reaction apart from WE is expected to flow. A time-dependent potential (waveform) is applied to WE resulting in the change of its potential corresponds to the constant potential of RE. The resulting flow-current between WE and RE is measured as a function of applied potential, and called as "voltammogram". Figure 2.2 shows the Time-dependent potential waveforms used in various voltammetry and resulting voltammogram.

Linear-sweep voltammetry

Cyclic voltammetry

Differential pulse voltammetry

Square-wave voltammetry
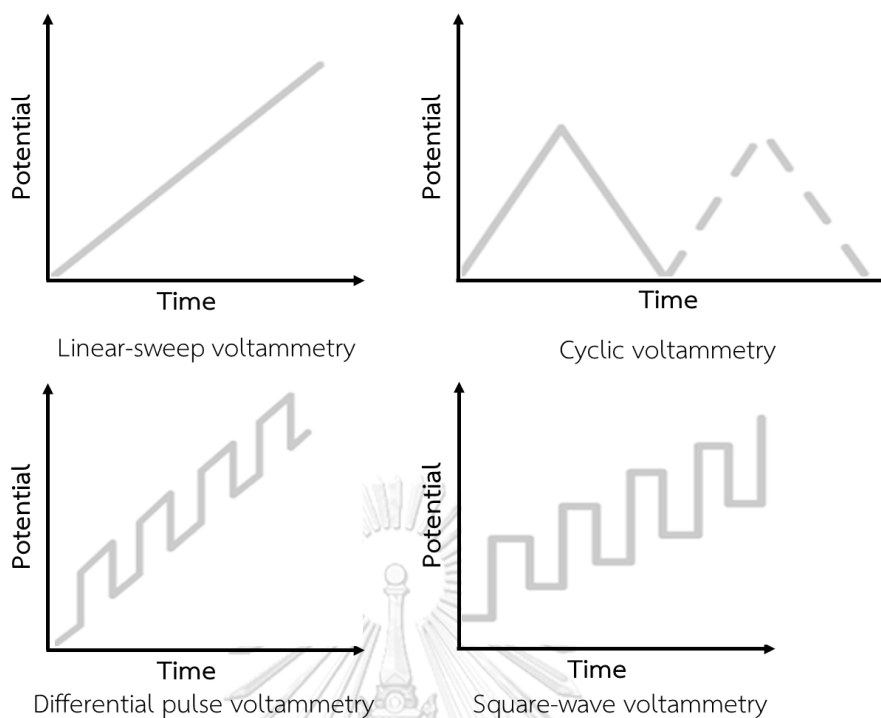
Figure 2.2 *Time-dependent potential waveforms used in various voltammetry*

In this dissertation, three types of voltammetry techniques were utilized for the simultaneous detection of CoQ10 and ALA including cyclic voltammetry, square-wave voltammetry, and stripping voltammetry. All of these techniques will be described detail more in the following section.

2.1.3.1 Cyclic Voltammetry (CV)

Cyclic voltammetry (CV) is the most widely used electrochemical technique. CV acquires much qualitative information of the interested electro-active species including the thermodynamics of redox processes and the kinetics of heterogeneous electron transfer reactions, and on coupled chemical reactions or absorption processes. CV is the preliminary technique for the electroanalytical study before the quantitative measurement using other voltammetric techniques. In CV, the potential is scanned linearly to the working electrode using the triangular potential waveform. During the scanning of potential, the current is measured resulting from

the applied potential via potentiostat. The plot of current-potential is called "cyclic voltammogram".

In a reversible redox couple, the expected voltammogram of a single potential cycle is illustrated in figure 2.3. In the initial is assumed that only the oxidized form (O) is presented. Therefore, the first half-cycle is scanned in negative-going potential where no reduction occurs. When the potential is approached to the characteristic E^0 for redox process, the increasing of cathodic current is observed, until reached as a peak. During this process, the reduced form (R) is generated near the electrode surface. After the traversing of potential at least 90/n mV beyond the cathodic peak, the potential is scanned in reverse direction that the reduction of R process. i_{pa} and i_{pc} represent the maximum anodic and cathodic peak currents, and measure by baseline extrapolation as shown in voltammogram in figure 2.3. E_{pc} and E_{pa} indicate the cathodic and anodic peak potentials at which the i_{pa} and i_{pc} are acquired, respectively.   The peak current for a reversible process is given by the Randles-Sevcik equation.

$$i_p = \left(2.69 \times 10^5\right) n^{3/2} A C D^{1/2} v^{1/2} \qquad \text{(Equation 2.3)}$$

where   n = number of electrons

A = electrode area (cm^2)

C = concentration (mol cm^{-3})

D = diffusion coefficient (cm^2 s^{-1})

v = potential scan rate (V s^{-1})

According to the Randles-Sevcik equation, i_p is directly proportional to the concentration of the analyte, and a scan root of scan rate. Thus, the linear relationship of i_p and scan root scan rate can be used to prove the mass-transfer process of

electroactive species towards the electrode surface. The E_p is related to the formal potential (E^O) of redox process. For the reversible process, E^O is located at the center between E_{pa} and E_{pc}.

$$E^O = \frac{E_{pa}+E_{pc}}{2}$$ (Equation 2.4)

In addition, the separation of Ep for the reversible process is given by the by equation 2.5

$$\Delta E_p = E_{pa} - E_{pc} = \frac{0.059}{n} \ V$$ (Equation 2.5)

Using the equation 2.5, the number of electrons (n) transferred in reversible redox process can be determined as a criterion for Nernstian behavior.
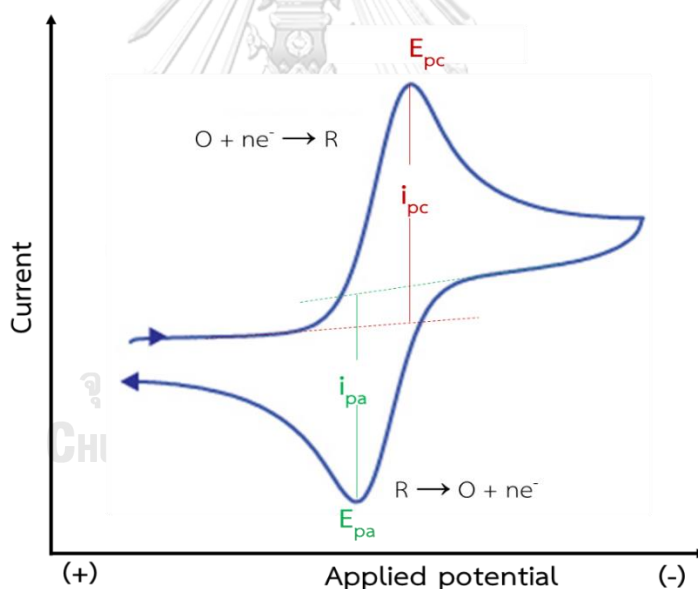
Figure 2.3 Typical cyclic voltammogram for a reversible redox process.

2.1.3.2 Pulse voltammetry

To improve the sensitivity and to reduce the limit of detection for voltammetric analysis, the pulse voltammetry is developed for increasing the ratio between faradaic and non-faradaic currents by applying a potential as a pulse and sampling current at late in the pulse life. Using the mention sampled-current/

potential-step experiment, an effective discrimination against the charging current is achieved. There are various types of pulse voltammetry including normal-pulse voltammetry, differential pulse voltammetry, square-wave voltammetry, and staircase voltammetry which are dependent on the excitation waveform and sampling regime. In this dissertation, the square-wave voltammetry is selected to use as detection technique for the quantitative analysis of the analytes.

2.1.3.2.1 Square-wave voltammetry (SWV)

SWV is one of pulse voltammetry that is popularly used for the quantitative analysis. The potential is applied a symmetrical square-wave form which is superimposed on a base stair-case potential to the working electrode as shown in figure 2.4. The current is sampled twice for each square-wave cycle once at the end of the forward pulse (forward current: i_F) and once at the end of the reverse pulse (reverse current: i_R). The net current is obtained from the different current (Δi) between i_F and i_R, and plotted against the base stair-case potential value of the applied potential. The directly proportional of peak high to the concentration of analytes is observed. Excellent sensitivity is acquired attributed to the fact that the final current is larger than either the forward or reverse compositions. The main advantages of SWV are the decreasing of the analysis time, the complete voltammogram is recorded within a few seconds.
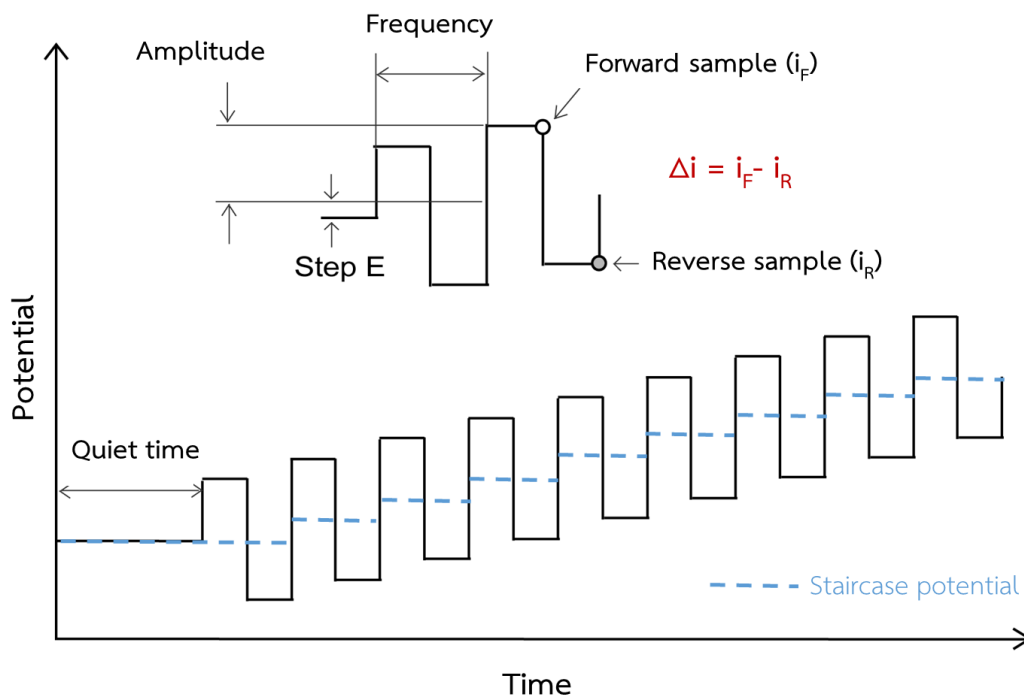
Figure 2.4 *Waveform and measurement scheme of SWV*

2.1.3.3 Stripping voltammetry

Stripping voltammetry is the most popular voltammetric technique for the determination of many substances. Stripping voltammetry consists of two steps. First is preconcentration step, the analytes in the test solution are electrolytic deposition on electrode surface for preconcentration of the analytes by applying the constant potential. Second is stripping step or measurement step. In this step, the potential is scanned in the direction that the deposited analyte is dissolution from the electrode surface. The different stripping voltammetry mode can be employed depending on nature of the analytes.

In this dissertation, anodic stripping voltammetry (ASV) was selected for the simultaneous determination of CoQ10 and ALA. Thus, the applied potential in preconcentration step is performed in the more negative potential than standard potential (E^0) to complete the cathodic deposition of the analytes. In this preconcentration step, the analytes have already accumulated onto working electrode

surface. Before starting the stripping step, a quiet period or equilibration time is set to decrease the forced convection, maintain a uniform concentration distribution, and confirm that the solution is in quiescent solution before the stripping step. After that, the potential is scanned in the anodic direction, any waveform can be used. The accumulated analytes are oxidized and dissolved to a supporting electrolyte. The anodic peaks are observed, and the quantitative analysis is usually interpreted from the anodic peak current (i_{pa}). The potential waveform and obtained voltammogram are shown in figure 2.5.
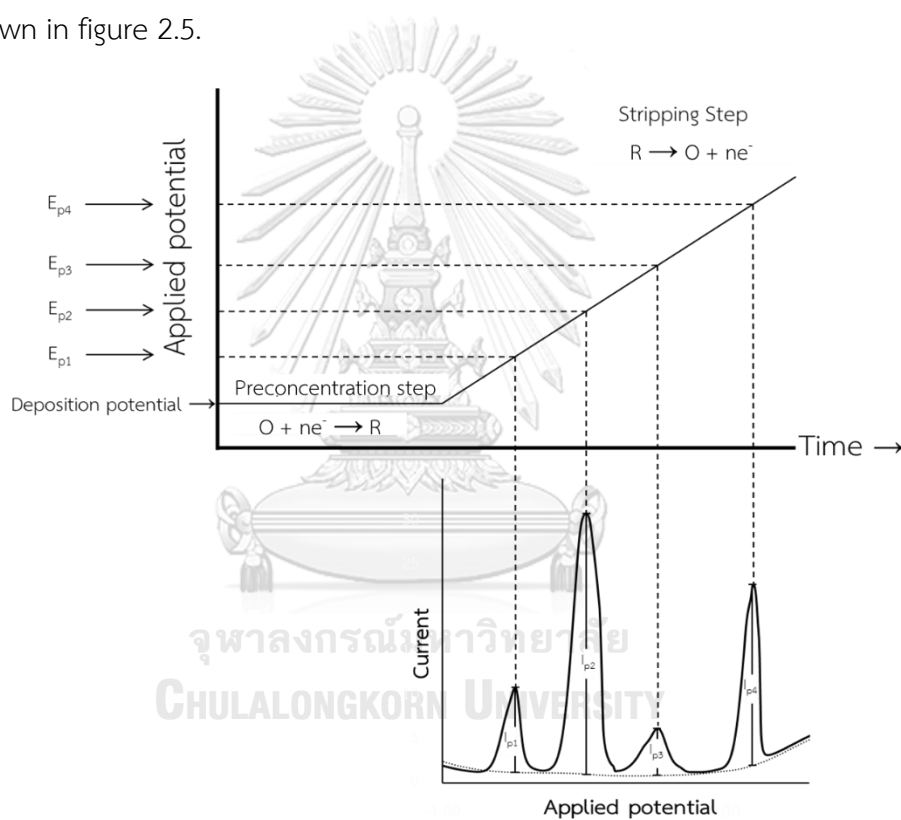
Figure 2.5 *Diagram of ASV: the potential-time waveform (top) and voltammogram (bottom)*

2.1.4 Amperometry

Amperometry is one of the most used electrochemical technique from the quantitative analysis. In this technique, the current is measured between a pair of working and reference electrodes that are driven by an electrolysis reaction. The potential is applied constantly. The amperogram is the plot between the measured current versus time. The resulting current is directly related to the concentration of the analytes in bulk solution. In this dissertation, amperometry is used as detection techniques for ultra-high performance liquid chromatography (UHPLC).

2.1.5 Working electrode (WE)

WE is the most important electrode in an electrochemical system on which the reaction of interest is occurring. The occurring redox reaction at WE can be either cathodic or anodic. The applied potential is a specific value related to the target analyte. The small surface area of WE in voltammetry is applied to increase the polarization and minimize the depletion of the analyte. The performance of electrode is strongly depended on the material of WE. The factors that should be considered for the WE are sensitivity, conductivity, reproducibility of the surface, working potential window, and cost of production.

2.1.5.1 Screen printed-carbon electrode (SPCE)

Screen printing is the technology used for fabrication of biosensors and chemical sensors instead of using large-scale electrodes. Their various advantages such as miniaturization, versatility, and low cost of production are really attractive. In addition, many laboratories use the screen-printing for in-house production of sensors. Screen-printed carbon electrode (SPCE) is an alternative material used instead of using the traditional electrodes based on an economic substrate such as ceramic, plastic sheet, and paper. Recently, SPCEs have successfully used as the electrochemical sensors for various researches due to the simplicity to produce and still give the rapid

responses. Moreover, the main advantage of SPCE is able to use only once and then discarded. This advantage can be used to solve the problems of surface fouling compared with those of conventional electrodes. However, to enhance the performance of SPCE towards the target analytes, electrode modification is required [5, 26].

2.1.5.2 Modifiers

2.1.5.2.1 Graphene (G)

Graphene (G) is a one-atom-thick planar sheet of sp^2 bonded carbon atoms in a honeycomb crystal lattice, and has recently attracted interest as a material for the fabrication of sensors. Graphene is a basic building block of other graphitic materials depending on how it is manipulated (figure 2.6.). The unique property of graphene allows applications in chemical sensing and biosensing, energy conversion and storage, catalysis, composites and coatings, electronics and the biomedical field. Graphene has the ability to promote electron transfer in some species and also has excellent electrocatalytic activity. In addition, graphene has been used as a popular nanomaterial in electrochemistry because it presents many desirable electrochemical properties including large surface area, high electrical conductivity, and rapid electron transfer [1, 13, 27, 28].
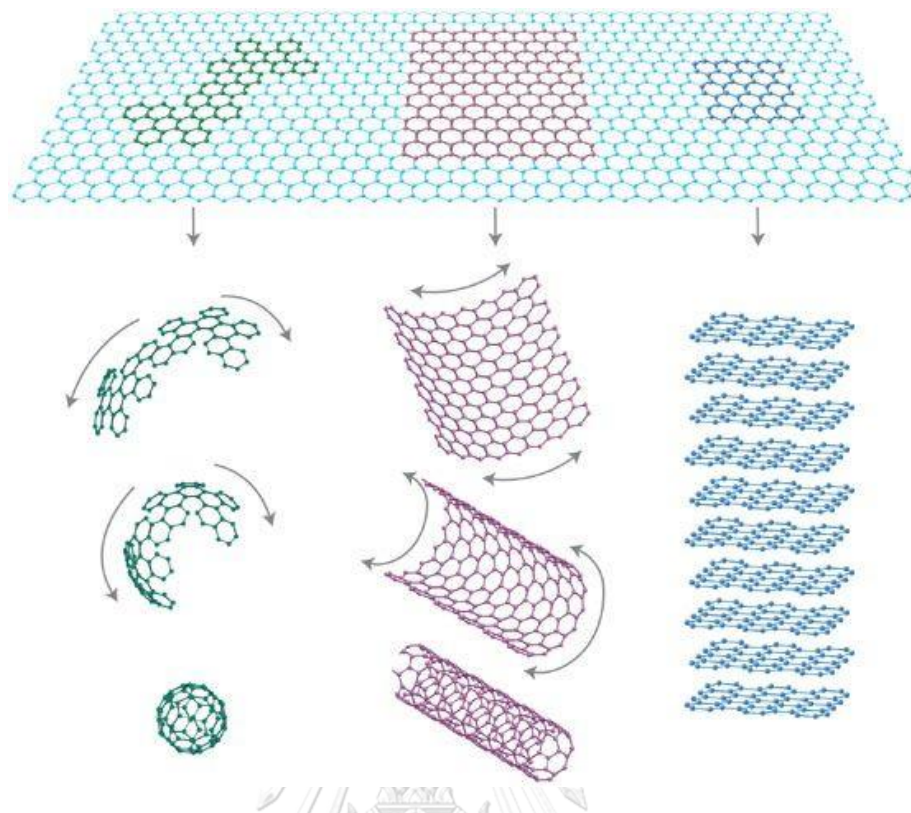
Figure 2.6 *Graphene as a building block for other carbon materials [28]*

2.1.5.2.2 Metal oxide

Metal oxides have been interesting materials in the development of sensor because of their unique properties in optical, electrical, and molecular fields. Metal oxides have been extensively applied in many applications such as gas sensors, catalyst, adsorbent, lithium-ion batteries, supercapacitors, and energy storage. Metal oxides are another interesting material to use as a modifier on an electrode surface. Metal oxides such as MnO_2, Fe_3O_4, FeO, SnO_2, CuO, and Fe_2O_3 show a high electrocatalytic activity toward compounds that exhibit a slow redox process and a low over-potential for the oxidation or reduction of analytes at bare electrodes. Among the metal oxides, MnO_2 has gained considerable attention. MnO_2 is widely used as the catalyst and electrode material for supercapacitors as well as a modifier of electrode surface in the electrochemical sensor. Because of owing to its low cost, wide abundance and environmental friendliness, MnO_2 is used as a modifier

with incorporated with other nanomaterials to raise up the performance of electrochemical sensor towards the target analytes [14-16].

2.1.5.2.3 Gold nanoparticles (AuNPs)

Metal-nanoparticles are an attractive catalyst in the electrochemical applications. Transition metals, especially precious metals, show very high catalytic abilities for catalyzing the redox process of some interesting molecules, making the use of electroanalytical techniques for applications is extended. Particularly, gold nanoparticles (AuNPs) have been received significant attention in recent years. AuNPs are widely used in many fields due to their unique optical and physical properties, such as surface plasmon oscillations for labeling, imaging, and sensing. For the electrochemical fields, AuNPs have been widely used for modification of electrode because of their benefits including catalysis, mass transport, and high effective surface area. AuNPs have the ability to improve the detection signal, electron transfer, which make the limit of detection in electrochemical sensor is reduced. Moreover, the most important is AuNPs showed the strong specific interaction with the sulfur-containing compounds. Therefore, AuNPs became an interesting nanomaterial used as modifier onto working electrode for electrochemical detection of sulfur-containing compounds [7, 18, 29, 30].

2.2 Chromatography

Chromatography is the technique for separation of mixture substances into its individual components. Chromatography operates on the same principle as extraction, but one phase is held in place while the other moves past it. The solvent moving through the column is called "mobile phase". In chromatography, the mobile phase is either a liquid or a gas. The stationary phase, the one that stays in place inside the column, is most commonly a viscous liquid chemically bonded to the inside of a capillary tube or onto the surface of solid particles packed in the column. The partitioning of solutes between mobile phase and stationary phase gives rise to

separation. Chromatography is divided into categories on the basis of the mechanism of the interaction of the solute with the stationary phase. There are mainly five types of chromatography including adsorption chromatography, partition chromatography, ion-exchange chromatography, molecular exclusion chromatography (gel filtration or gel permeation), and affinity chromatography. This dissertation focuses on the use of liquid chromatography which is the one of absorption chromatography for the separation of the analytes [25, 31-33].

2.2.1 Basic technical terms in chromatography

2.2.1.1 Flow rate

The speed of the mobile phase passing through a chromatography column is expressed either as a volume flow rate or as a linear flow rate. The volume flow rate tells how many milliliters of solvent per minute travel through the column. The linear flow rate tells how many centimeters are traveled in 1 min by the solvent.

2.2.1.2 Chromatogram

Solutes eluted from a chromatography column are observed with various detectors. A chromatogram is a graph showing the detector response as a function of elution time (figure 2.7).
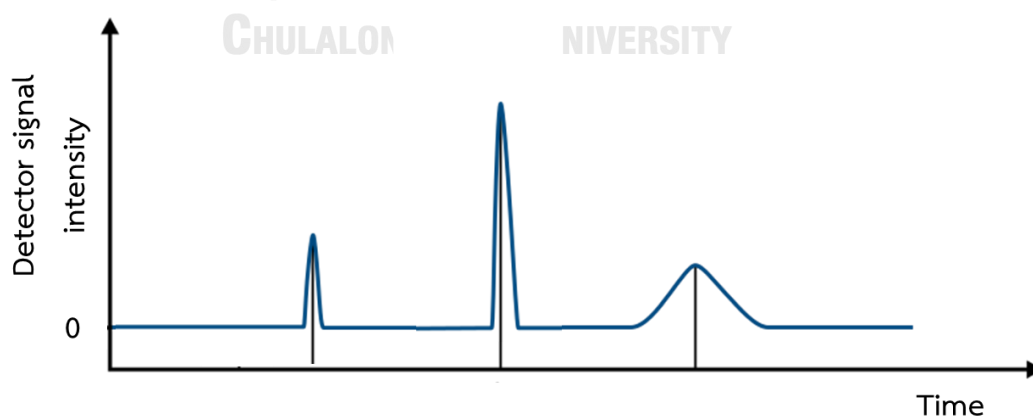
Figure 2.7 Schematic chromatogram

2.2.1.3 Retention time

The retention time (t_r) for each component is the time needed after the injection of the mixture onto the column until that component reaches the detector. Retention volume (V_r) is the volume of mobile phase required to elute a particular solute from the column. Unretained mobile phase travels through the column in the minimum possible time, called t_m. The adjusted retention time (t'_r) for a solute is additional time required for the solute to travel the length of the column beyond the time required by the unretained solvent.

$$t'_r = t_r - t_m \qquad \text{(Equation 2.6)}$$
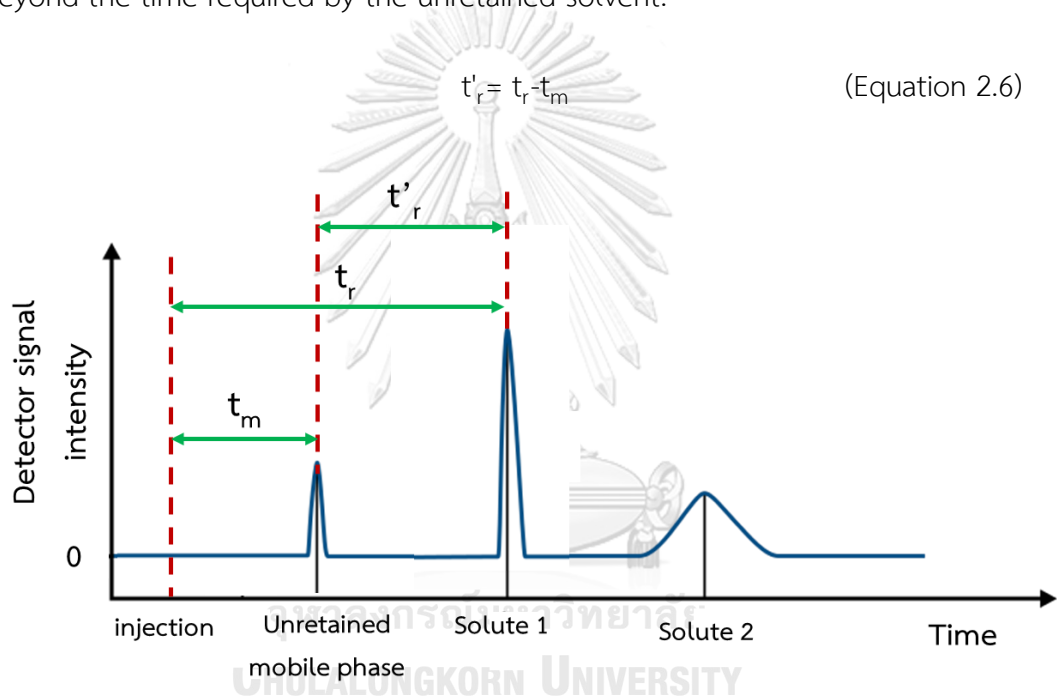
Figure 2.8 Schematic chromatogram showing measurement of retention time

For any two components 1 and 2, the relative retention (α) is the ratio of their adjusted retention time:

$$\alpha = \frac{t'_{r2}}{t'_{r1}} \qquad \text{(Equation 2.7)}$$

where $t'_{r2} > t'_{r1}$, so $\alpha > 1$. The grater of the relative retention offers the greater separation between two components. Relative retention time is fairly independent of the flow rate and can be used to help identify peaks when the flow rate change.

For each peak in chromatogram, the capacity factor (k') is defined as:

$$k' = \frac{t_r - t_m}{t_m}$$ (Equation 2.8)

The longer retained component by the column provides the greater capacity factor. To monitor the performance of a particular column, it is good practice to periodically measure the capacity factor of a standard, the number of plates, and peak asymmetry. Changes in these parameters indicate degradation of the column.

The capacity factor is equivalent to

$$k' = \frac{\text{time solute spends in stationary phase}}{\text{time solute spends in mobile phase}}$$

$$= \frac{\text{moles of solute in stationary phase}}{\text{moles of solute in mobile phase}}$$

$$= \frac{C_s V_s}{C_m V_m}$$ (Equation 2.9)

where C_s is the concentration of solute in stationary phase, V_s is the volume of stationary phase, C_m is the concentration of solute in mobile phase, and V_m is the volume of mobile phase. The quotient C_s/C_m is the ratio of concentration of solute in the stationary and mobile phase. If the column is run slowly enough to be near equilibrium, the quotient C_s/C_m is the partition coefficient (K).

$$k' = K\frac{V_s}{V_m} = \frac{t_r - t_m}{t_m} = \frac{t'_r}{t_m}$$ (Equation 2.10)

which relates the retention time to the partition coefficient and the volumes of stationary and mobile phase. Because of $t'_r \, \alpha \, k' \, \alpha \, k$, relative retention can also be express as

$$\text{Relative retention: } \alpha = \frac{t'_{r2}}{t'_{r1}} = \frac{k'_2}{k'_1} = \frac{K_2}{K_1}$$ (Equation 2.11)

The relative retention of two solutes is proportional to the ratio of their partition coefficients.

Retention volume (V_r) is the volume of mobile phase required to elute a particular solute from the column:

$$V_r = t_r\, u_v \qquad \text{(Equation 2.12)}$$

where u_v is the volume flow rate (volume per unit time) of the mobile phase. The retention volume of a particular solute is constant over a range of flow rate. Volume is proportional to time, so any ratio of times can be written as the corresponding ratio of volume.

$$k' = \frac{t_r - t_m}{t_m} = \frac{V_r - V t_m}{V_m} \qquad \text{(Equation 2.13)}$$

where V_r is the retention volume for solute and V_m is the elution volume for an unretained component, V_m is equal to the volume of mobile phase in the column.

2.2.1.4 Resolution

Solute moving through a chromatography column tends to spread into a Gaussian shape with standard deviation σ. The longer a solute spends passing through a column causing the broader band. The resolution of two peaks from each other is defined as

$$\text{Resolution} = \frac{\Delta t_r}{w_{av}} = \frac{\Delta V_r}{w_{av}} = \frac{0.589 \Delta t_r}{w_{1/2av}} \qquad \text{(Equation 2.14)}$$

where Δt_r or ΔV_r is the separation between peaks (in units of time or volume), w_{av} is the average width of the two peaks in corresponding units, and $w_{1/2av}$ is the width at half-height of Gaussian peaks. For the quantitative analysis, a resolution > 1.5 is highly desirable.

2.2.1.5 Plate height (H) and number of theoretical plates (N)

Plate height (H) is also called "the height equivalent to a theoretical plate". Plate height is approximately the length of column required for one equilibration of solute between mobile and stationary phase. The smaller plate height is given the narrower bandwidth. The ability of column to separate components of a mixture is improved by decreasing plate height. An efficient column has more theoretical plates than an inefficient column.

$$H = \frac{\sigma^2}{x} = \frac{L}{N} \qquad \text{(Equation 2.15)}$$

where σ is the standard deviation of the Gaussian band, x is the distance traveled, L is the length of column, and N is the number of plates in the entire column. The number of theoretical plates can be calculated using the following equation:

$$N = \frac{16t_r^2}{w^2} = \frac{5.55t_r^2}{w_{1/2}^2} \qquad \text{(Equation 2.16)}$$

where t_r is the retention time of peak, w is the peak width at the base, and $w_{1/2}$ is the width at half-height.

2.2.1.6 The van Deemter equation

Plate height, H, is proportional to the variance of chromatographic band. The smaller plate height provides the narrower the band. The van Deemter equation tells how the column and flow rate affect the plate height. The van Deemter equation is shown in equation 2.17.

$$H = A + \frac{B}{u_x} + Cu_x \qquad \text{(Equation 2.17)}$$

where u_x is the linear flow rate. A, B, and C are constants given by the stationary phase and column. Figure 2.9 shows the van Deemter plot relating to the van Deemter equation. Changing stationary phase and column changes A, B, and C terms. The van

Deemter equation is band-broadening mechanisms. In a packed column, there are three terms contribute to band broadening.

Van Deemter equation

$$H = A + \frac{B}{u_X} + Cu_X$$

Figure labels: Plate Height (H), Mobile Phase Velocity (u), Actual plot, C term, A term, B term, Optimum efficiency
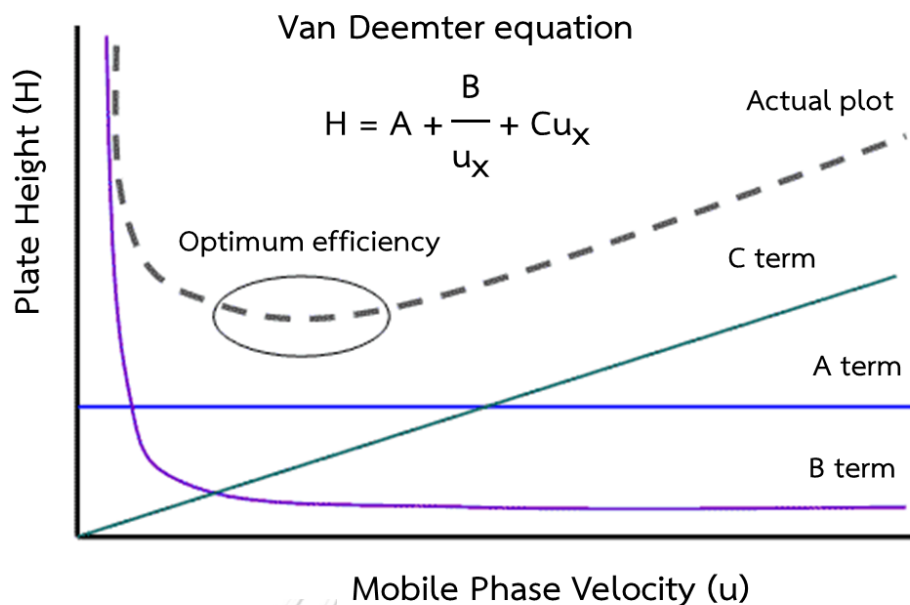
Figure 2.9 *The Van Deemter plot*

Term A: eddy diffusion

Term A in van Deemter equation refers to the peak broadening causing by the stationary phase particles in the column. The difference in shape and size of stationary phase effects to the flow rate of mobile phase, the analyte molecules pass through the column in different flow paths.

Term B: longitudinal diffusion

Term B, longitudinal diffusion, refers to the diffusional broadening of band. It takes place along the axis of the column, occurs while the band is transported along the column by flow of solvent. The faster linear flow, the less time is spent in the column and the less diffusional broadening occurs.

Term C: resistance against mass transfer

The plate height from finite equilibration time called the mass transfer term (term C) which is referred to the mass transfer of analyte between the stationary phase and mobile phase during separation. Decreasing the stationary phase thickness reduced the plate height and increased efficiency because solute can diffuse faster from the farthest depths of stationary phase into the mobile phase. Decreasing column radius, the plate height reduces by decreasing the distance through which solute must diffusion to reach the stationary phase. Moreover, the increase of temperature also decreases plate height due to the increasing of the diffusion coefficient of the solute in stationary phase.

2.2.2 Ultrahigh-Performance liquid chromatography (UHPLC)

Liquid chromatography is one category in absorption chromatography and is important because most compounds are not sufficiently volatile for gas chromatography. High-performance liquid chromatography (HPLC) uses high pressure to force solvent through closed column containing very fine particles that give high-resolution separation. Recently, ultrahigh-Performance liquid chromatography (UHPLC) has been developed to achieve fast separation for high-throughput analysis. The main configuration and basic principle of UHPLC are similar to HPLC. UHPLC concerns to the development of short column packed with small particles for working at high pressures (> 400 bar). The use of UHPLC can enhance chromatographic performances in terms of efficiency, resolution, and analysis time. The efficiency of a packed column increases as the decreasing of the size of stationary phase. Typical particle sizes in HPLC are 3- 5 µm. In UHPLC, the size of stationary phase decreases to approximately lower than 2 µm, plate number increases. The peaks are shaper with smaller particle size. The decreasing of particle size allows to improve resolution or to maintain the equivalent kinetic performance while decreasing analysis time.

2.2.3 Instrument for UHPLC system

The component of UHPLC is not different from HPLC. There are mainly five parts which comprise of UHPLC system as shown in figure 2.10.
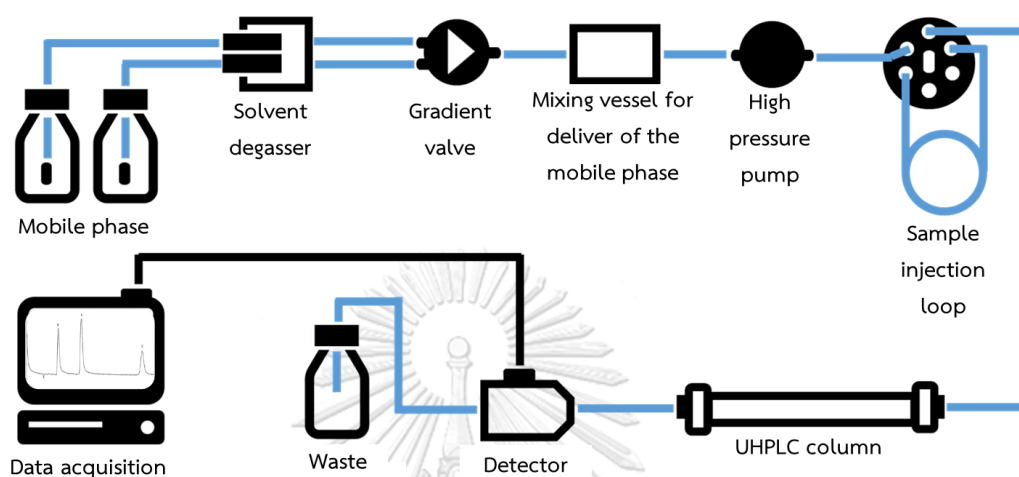
Figure 2.10 *Schematic of instrument for UHPLC system*

(1) Pump

The pump of UHPLC is employed at higher pressure than conventional pump in HPLC. The main function of pump is to deliver a mobile phase at specific flow rate. The quality of pump is measured by how steady and reproducible a flow it can produce. A fluctuating flow rate can create detector noise that obscures weak signal. There are two modes of pump including isocratic and gradient modes. In the isocratic mode, pump delivers a constant mobile phase composition to UHPLC system. Gradient mode is constructed by proportioning each liquid through a multiple-way value at low pressure and then pumping the mixture at high pressure into a column. The gradient is electrically controlled and programmable.

(2) Injector

The injection valve has interchangeable sample loop, each of which holds and fixed volume. In the loading position, a syringe is used to wash and load the loop with fresh sample at atmospheric pressure. High-pressure flow from the pump to the column passes through the segment of valve. When the valve is rotated, the content of the sample loop is injected into the column at high pressure.

(3) Column

Column is considered as the most important part in UHPLC. The analytes are separated in the column using physical and chemical parameters. Column comprised of steel or plastic tube packed with the fine particles. The mobile phase containing the analytes flows through the column and interacts with the stationary phase. The different molecular structures cause them to migrate through the column in different velocities, and then separated. The columns of UHPLC use of short and small particles size of stationary phase for productive of rapid analysis. Normally, the particles size of stationary phase in HPLC is around 5 μm while the particles size of stationary phase in UHPLC is reduced to sub 2 μm. Thus, UHPLC attains high efficiency and high resolution with the theoretical number of plates up to 35,000 for 150 mm column length. It also demonstrates the versatility of UHPLC to provide ultrafast, and very high-resolution analysis.

(4) Detector

An ideal detector is sensitive to low concentrations of every analyte, provides linear response, and does not broaden the eluted peaks. It is also insensitive to change in temperature and solvent composition. To prevent peak broadening, the volume of detector should be less than 20% of the volume of the chromatographic band. Gas bubbles in the detector create noise, so back pressure

may be applied to the detector to prevent bubble formation during depressurization of elute.   There are various types of detector such as ultraviolet, fluorescence, refractive index, mass spectrometry, Fourier transform, electrochemical, and etc.   In this dissertation, the electrochemical detection is selected to couple with UHPLC and used as detector for the quantitative analysis.

(5) Data system

All the modules UHPLC system is controlled by computer.   The data are collected and interpreted via specific software.   The retention time of the sample components and the amount of sample are determined and shown to obtain the qualitative and quantitative analysis.

2.3 Analytes
2.3.1 Coenzyme Q10 (CoQ10) and α-lipoic acid (ALA)

Coenzyme Q10 (CoQ10), known as ubiquinone or ubidecarenone, is a hydrophobic molecule containing 10 isoprenoid units in the side chain.   CoQ10 is a powerful antioxidant and also serves an essential cofactor for energy production.   CoQ10 is normally found as a ubiquinone/ubiquinol redox couple, which plays an important role in mitochondrial electron transfer and energy metabolism.   The reduced form of CoQ10 (ubiquinol) acts as an antioxidant, which inhibits lipid peroxidation in biological membranes and protects the body from damage caused by harmful molecules.   A deficiency of this antioxidant in one's diet has been related to several diseases, such as heart failure, obesity, cancer, chronic pain, and neurological disorders.   Normally, CoQ10 levels are particularly high in the hearts, livers, and kidneys of mammal species, as well as in soy oil, sardines, mackerel, and peanuts.   Although CoQ10 can be obtained from different foods and animal tissues, nevertheless many CoQ10 dietary supplements are commercially available.   Because ubiquinol (the reduced form of CoQ10) is easily oxidized in the air, most CoQ10 in dietary

supplements is therefore converted into ubiquinone (the oxidized form of CoQ10) to facilitate the sampling and holding processes [34-38].

In addition to CoQ10 dietary supplements, many companies have produced multi-dietary supplements, which contain CoQ10 and other useful substances. α-Lipoic acid (ALA) is the most popular substance that can be found in CoQ10 dietary supplements. ALA (1,2-dithiolane-3-pentanoic acid, 1,2-dithiolane-3-valeric acid, or thioctic acid) is a sulfur-containing cofactor that occurs in human mitochondria. This substance plays an essential role in various biological processes, such as mitochondrial dehydrogenase reactions, and energy metabolism. ALA and its reduced form (dihydrolipoic acid, DHALA) are powerful antioxidants and have shown the ability to protect against free radical attack both in vitro and in vivo.   Their properties are considered to approach the 'ideal' or 'universal' antioxidant. ALA presents a wide variety of therapeutic applications, including the treatment of human immunodeficiency virus (HIV) infection, age-associated neurodegenerative disease, type II diabetes, diabetic polyneuropathies, Alzheimer-type dementia, liver pathologies of diverse origin from alcoholism to chemical poisoning, and heavy metal poisoning. ALA is widely found in yeast, and organ meats, such as the liver and heart, spinach, broccoli, and potatoes. However, ALA received from foods is not enough to noticeably increase the level of free ALA in the body. Therefore, many people take supplements as a drug to improve a variety of health conditions. With the medical importance of CoQ10 and ALA in both toxicological and acceptance criteria, the development of fast, sensitive, selective, and accurate methods for the quantitative analysis of concentrations of CoQ10 and ALA in dietary supplements is in high demand [39-46].

CoQ10: Coenzyme Q10   **ALA: α**-Lipoic acid

Figure 2.11 Structure of CoQ10 and ALA

2.3.2 Dithiocarbamate compounds (DTCs)

Dithiocarbamates (DTCs) are a well-known organosulfur compound in the group of fungicides. They have been used in agriculture as fungicides in foliage vegetable and fruit. Besides these agricultural applications, DTCs are also used in industry such as vulcanization accelerator and antioxidant in rubber. All the European Union (EU) member states and many other counties register the DTCs as the main group of fungicides that used to control approximately 400 pathogens of more than 70 crops. In EU, regulations tolerances for DTCs are drafted as 2-7 mg kg^{-1}. However, the use of DTCs results in their released into the environment causing the contamination in food and water which leads to a hazardous effect in the living organisms through diverse pathways. Environmental problem resulting from the uncontrollable use of fungicides in agriculture is one of the most important evidence. Therefore, it is necessary to continuously develop the simple, selective, and sensitive methods for analysis of fungicides [47-51].

In this dissertation, thiram (tetramethyl thiuram) and disulfiram (tetraethyl thiuram) are chosen as representative compounds of DTCs because they are importantly applied to control a variety of pest [17]. When thiram and disulfiram are mixed together, the intermediate of *N, N*-diethyl-*N', N'*-dimethylthiuram disulfide (DEDMTDS) appears as the derivative of thiram and disulfiram. This compound is one

of the DTCs that affected human health as the same effect as thiram and disulfiram. The presence of DEDMTDS can use to monitor thiram and disulfiram in samples. Therefore, the detection of DEDMTDS is important. The derivative compound is also determined along with the measurement of thiram and disulfiram.
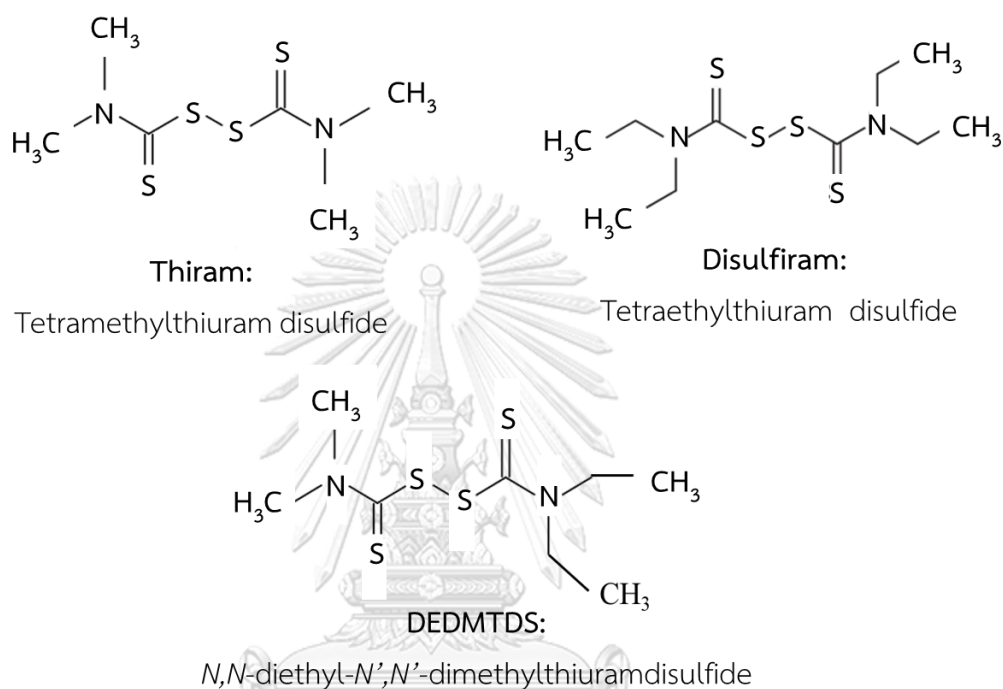
Figure 2.12 *Structure of DTCs*

2.4 Literature reviews

2.4.1 Electrochemical detection of CoQ10 and ALA

2.4.1.1 Conventional methods for the detection of CoQ10 and ALA

Various analytical methods have been developed for the determination of CoQ10 and ALA in a variety of biological, drug and food samples. The most regularly utilized techniques for CoQ10 detection are liquid chromatography. HPLC is one of the most popular analytical techniques and can be used in combination with various detection systems such as ultraviolet (UV), fluorescence (FL), and mass spectrometry (MS).

In 2011, Nohara and co-workers [52] developed the post column fluorescence for derivatization of CoQ10 before separation by HPLC. CoQ10 can produce a fluorescence under alkaline solution when reacted with 2-cyanoacetamide. Therefore, the post column containing 2-cyanoacetamide was proposed. The results showed that the derivative CoQ10 by 2-cyanoacetamide gave a fluorescence at an excitation wavelength of 442 nm, and an emission wavelength of 549 nm. Using the developed post column integrated with HPLC-FL system, a linear response was observed in the range of 0.32-1276 ng, and the detection limit (S/N = 3) was 0.16 ng.

In 2013, Franke et al. [53] proposed a fast, affordable, and accurate HPLC assays for simultaneous determination of 15 micronutrients of circulating lipid-phase such as 25-hydroxylated D vitamers, retinol, tocopherols, carotenoids including their isomers, and coenzyme Q10 in a single run using the C18 and C30 columns in series with a UV-Vis detector. All 15 analytes of interest were completely separated within 42 min, and are feasible for routine operations with fast turn-around times at an affordable cost.

In 2014, pracaxi oil-core nanocapsules were developed by Mattiazzi and co-workers [54] for selective, rapid, and simple reverse phase-HPLC-UV system. CoQ10 content and its encapsulation efficiency in nanocapsules containing pracaxi oil were determined. The proposed RP-HPLC-UV system showed linearity over the range of 5.0 - 25.0 mu g mL^{-1} with a satisfied specificity, accuracy, and precision.

In 2015, the determination of CoQ10 in cheese sample was developed [55]. Before analysis, the sample was digested in alkaline and extracted with hexane/ethyl acetate (9:1 v/v). The rapid determination was obtained under Phenomenex Kromasil 5 mu m Si 250 x 4.6 mm column and UV-Vis detector, and eluted with an isocratic mobile phase of 2-propanol 1% in n-hexane. The limit of detection was found to be 0.024 mu g mL^{-1}.

In the same year, Martano and co-authors [56] also proposed the determination of CoQ10, and other sterol and prenol lipid molecules in zebrafish embryos using high-performance liquid chromatography-high resolution mass spectrometry methodology (HPLC-HRMS). Using the developed system, a fast and selective high resolution were obtained, and could be applied to wild-type and mutant biological samples.

In 2018, Clementino et al. [57] have reported the first RP-HPLC-UV method for simultaneous determination of simvastatin, the statin hydroxy acid form, and coenzyme Q10 co-encapsulated into hybrid nanoparticles of lecithin/chitosan. Dual wavelength-UV detection at 238 nm and 275 nm was used to monitor the simvastatin and CoQ10, respectively. Linear in the range of 0.5–25 µg mL^{-1} was obtained with LOD lower than 0.2 µg mL^{-1}.

Considering all of the detectors mentioned, FL detectors exhibit low detection limits using fluorogenic labeling reagents, leading to a low enough sensitivity to detect CoQ10 in biological samples. However, this technique requires sample preparation and high reagent costs. In the case of MS, very high sensitivity and selectivity are provided, but the instrument cost is very high.

In the case of the quantitative analysis of ALA, HPLC coupled with spectrometry has been widely used.

In 2012, Montero et al. [58] have presented the utilize of liquid chromatography-tandem mass spectrometry with negative electrospray ionization (HPLC-ESI-MS/MS) in an ion-trap mass spectrometer for the simultaneous determination of lipoic acid, trolox methyl ether, and tocopherols. Multiple reaction monitoring method was accomplished for detection and quantitation using specific

transitions from precursor ion to produce ion for each analyte. The low limit of quantification of ALA was observed at 1.22 ng.

In 2014, HPLC-UV method was proposed by Chwatko and co-workers [59]. Prior HPLC analysis, ALA was conversed to its thiol counterpart - dihydrolipoic acid (DHLA) using reductive cleavage of tris (2-carboxyethyl) phosphine hydrochloride. Then dihydrolipoic acid was introduced to precolumn derivatization with 1-benzyl-2chloropyridinium bromide, followed by ion-pairing RP-HPLC-UV detection of its 2-S-pyridinium derivative at 321 nm. The proposed method was successfully applied for ALA detection in urine and dietary supplement tablets, and showed satisfied sensitivity, simplicity, and inexpensiveness.

In 2016, Campos and co-authors [60] reported the measurement of ALA and DHLA extracted from skin using HPLC with UV, electrochemical (EC), and evaporative light scattering (ELS) detection. They found that this method observed the different linear ranges, and the use of ELS as detector showed the highest sensitivity compared to the other studied detector. The HPLC coupled with three detection methods offered a simple, rapid and reliable determination of LA in human skin.

In 2018, the direct quantification of trace biologically important carboxyl compounds in body fluids including ALA, 2-(beta-carboxyethyl)-6-hydroxy-2,7,8-trimethylchroman, prostaglandin E-2, cholic acid, and chenodeoxycholic acid was proposed [61]. The detection consists of 2 steps, (i) fast and direct labeling the target analytes with N-(3-dimethylaminopropyl)-N'-ethylcarbodiimide and (ii) ultrahigh-performance liquid chromatography-tandem mass spectrometry (UHPLC-MS/MS) analysis. The wide linear range from 2.5 to 2500 pg mL^{-1} was observed with LOD of 0.10 pg mL^{-1}. This work showed the advantages of simple pretreatment, use of a small sample volume, and a short analysis time.

However, all of the mentioned methods require a complicated operation that entail a lengthy analysis. Moreover, all HPLC-based methods require a bulky instrument, high purchase and maintenance costs, and specially trained professionals.

2.4.1.2 Electrochemical detection of CoQ10 and ALA

To overcome such disadvantages as mentioned above, electrochemical methods can be a candidate for a detection and can overcome such drawbacks.

For the quantitative analysis of CoQ10, the electrochemical detection was applied as a detector after separation with HPLC. The following literature will focus on the detail of the electrodes used for detection.

In 2011, the thin-layer cell dual electrode using packed carbon bed electrodes was proposed by Dorris's team [62]. The reduced and oxidized forms of CoQ10 were monitored simultaneously and selectively with the dual-electrode. Its formation was investigated using the ratios of peak current and half wave potentials from previously generated hydrodynamic voltammograms, using the oxidized form with electrodes in a series configuration. The LOD was found to be 5 nM. This proposed analytical system was successful to determine the basal concentration of oxidized and reduced forms of CoQ10 in human plasma.

In 2013, the coulometric detection was applied as a detector in HPLC for detection of CoQ10 in swine tissue [63] including lung, skeletal muscle, brain, liver, kidney, and heart muscle. The total concentration of CoQ10 was determined along with CoQ9 as internal standard. The method offers linear, sensitive, and reproducible for total CoQ10 detection.

In 2015, Yubero et al. [64] have developed the analysis of CoQ10 in excretory systems. The developed system showed the satisfied results compared to the establishment of reference values from two age groups of the pediatric population (2-10, and 11-17 years). This work is a noninvasive, reliable, and reproducible method to determine urinary tract CoQ status.

In ALA detection, many electrochemical sensors have been developed as follow;

In 2010, Siangproh and co-workers [41] have applied the boron-doped diamond electrode (BDD) coupled with HPLC for sensitive detection of ALA. The highly sensitive detection was observed at LOD of 3.0 ng mL^{-1} without any derivatization or application of pulse waveform. Moreover, the use of BDD as working electrode exhibited a high reproducibility and simplicity detection with a low background, a wide working potential window, and a lack of adsorption. Finally, BDD was successfully applied for the determination of ALA in dietary supplements.

In 2014, the differential pulse voltammetric determination of ALA on the platinum electrode (Pt) was investigated by Marine et al. [45]. The oxidation of ALA on Pt electrode was examined compared to the use of glassy carbon (GC) electrode. It was observed that a better electrocatalytic activity and higher sensitivity were obtained using Pt as working electrode. The LOD was found at 13.15 µM without any interfering from ascorbic acid, dopamine, and uric acid.

In the same year, Ferreira and co-workers [65] have proposed the use of cobalt phthalocyanine modified pyrolytic graphite electrode as working electrode for the detection of ALA. The proposed electrode exhibited the lower positive peak potential and higher anodic peak current compared to the use of bare pyrolytic graphite. The LOD was found in nM level.

In 2016, Stankovic et al. [66] have applied the use of BDD for detection of ALA without any separation by HPLC. Amperometric and differential pulse voltammetric detection were performed for the quantitative analysis of ALA. The linearity was found in the range of 0.3 to 105 mu M with LOD of 0.088 mu M. For the interference study, this work exhibited no interference from common compounds such as ascorbic acid, uric acid, and dopamine. Moreover, it could be applied for the determination of ALA in human body fluids.

Later, fast quantification of ALA using batch injection analysis (BIA) with amperometric detection was developed [67]. BIA with amperometric detection was employed using cobalt phthalocyanine modified pyrolytic graphite electrode. A sampling rate of 180 injections per hour was attained. The LOD of 15 nM was observed.

From the literature reviews for the detection of CoQ10 and ALA, the main advantages of electrochemical methods over other detection methods are their high sensitivity, selectivity, instrument portability, low cost, and fast response times. In addition, there is no report of the use of electrochemical sensors for simultaneous detection of CoQ10 and ALA. Therefore, a part of this dissertation aims to develop a low-cost and disposable novel sensor for the simultaneous determination of CoQ10 and ALA with a simple and inexpensive fabrication procedure.

2.4.2 UHLPC-ED for the determination of DTCs
2.4.2.1 Conventional methods for the detection of DTCs

Various methods have been developed for analysis of DTCs as shown below.

In 2009, the spectrophotometric method has been developed for the determination of zineb (zinc (II) ethylenebisdithiocarbamate) [68]. Before the detection, zineb was formed blue complex with sodium molybdate in an acidic medium and detected at 956 nm. The LOD was found to be 0.006 μg mL^{-1}. Zineb was

successfully determined without any interferences in the presence of other dithiocarbamates like ziram, thiram, ferbam etc.

In 2011, Gonzálvez et al. [69] have developed the methodology for the determination of non-volatile DTCs based on the vapor phase (VP) generation of carbon disulfide. DTCs was decomposed by reacted by addition of tin chloride in acid media, and then the generated CS_2 was extracted and preconcentrated by liquid phase microextraction (LPME). Finally, the quantitative analysis was performed using transmission infrared measurements. The LOD of 0.3 µg was obtained.

In 2012, a simple and inexpensive HPLC-UV system for DTCs in greenhouse and non-greenhouse tomatoes was proposed by Jafari and co-workers [70]. The detected wavelength for the determination of mancozeb (EBDs), propineb (PBDs) and thiram was set at 272 nm. The presented method showed the success of simultaneously determine residues of the three main subclasses of dithiocarbamate fungicides in tomatoes.

In the same year, gold nanorods were developed as a substrate for surface-enhanced Raman spectroscopy and applied to detection of thiram, ferbam, and ziram at ultra-low level [71]. Gold nanorods substrate has the ability to tune the surface plasmon resonance of the nanoparticles to the laser excitation wavelength. This work was successfully detected the DTCs in nanogram level with the LODs of 11.00 nM, 8.00 nM, and 4.20 nM for thiram, ferbam, and ziram respectively.

Later, the determination of residues of 15 pyrethroids and two metabolites of DTCs was performed using UHPLC-MS-MS, and was proposed by Stephen and co-authors [72]. The isolation and sample clean-up of the sample were developed in a single step using a modified QuEChERS (quick, easy, cheap, effective, rugged, and safe) procedure. The electrospray and atmospheric pressure chemical

ionization were performed, and then detected using UHPLC-MS-MS. This multi-residue method gives quantitative results for the target pesticides and pesticide metabolites tested at low levels.

In 2013, the selective determination of thiram residues in fruit and vegetables by hydrophilic interaction LC-MS was proposed by Ringli et al. [73]. The surface extraction was used to reduce thiram into its anion prior separation. Mass selective detection was performed on a single quadrupole mass spectrometer coupled to an electrospray ionization interface operating in negative mode. The LOD of 0.6 µg kg^{-1} was obtained.

Recently, in 2018, a novel detector of miniaturized dielectric barrier discharge–microplasma molecular emission spectrometer and an online microwave-assisted hydrolysis reactor for liquid chromatography (LC) is presented by Han and co-workers [74]. DTCs including mancozeb, thiram, zineb, propineb, and metiram were converted to CS_2 by tin (II) chloride solution, then separated from the liquid phase and transformed for the detection of the specific molecular emission at 257.49 nm by the spectrometer. The presented method could be detected at the microgram level.

As mention in the literature reviews, spectrometry and gas chromatography have been widely used as the method for the determination of DTCs after their decomposition to CS_2. From these methods, most of DTCs can degrade to CS_2. Therefore, they are unable to distinguish among different DTCs. HPLC was one of the popular technique used for simultaneous determination of DTCs by coupled with UV or MS detector, because HPLC is the simple technique used for easy separation the disulfide substance. However, they still need the derivatization that is made the complicated procedure.

2.4.2.2 Electrochemical detection of DTCs

Electrochemical detection became an important choice for the determination of disulfides. The main advantage of electrochemical detection is no need derivatization step, which makes the analysis time and cost reduced.

In 1996, Fernández et al. [49] presented the determination of thiram and disulfiram in the presence of ziram using composite graphite-poly(tetrafluoroethylene) (Teflon) electrodes as amperometric indicator electrodes in HPLC detection. Teflon-graphite composite electrode was applied the first time for used in the detection of DTCs.

In 1999, glassy carbon electrodes have been applied as working electrodes for amperometric and coulometric detections after separation with RP-HPLC [75]. General thiuram disulfide, salts of alkyl-dithiocarbamates, and alkylenbis-dithiocarbamates were evaluated. For the comparison of two detection techniques, the results showed that the coulometric detection provided better detection limits than amperometric detection, due to better efficiency in the oxidation processes.

The utilization of disk and cylindrical microelectrodes for determination of DTCs in low-permittivity organic solvents has been proposed in 2000 by Hernández-Olmos and co-authors [47]. The electrochemical behavior of thiram was investigated on Au microdisk electrode and at cylindrical carbon fiber microelectrodes (CFMEs) in low-permittivity organic solvents such as toluene and ethyl acetate. The results showed that CFMEs provided the better voltammetric signal with LOD of 4.3×10^{-7} M. This work demonstrated that the electroanalysis of organic compounds such as thiram can be directly accomplished in low- permittivity organic solvents.

In 2008, Qiu and co-workers have reported the determination of ziram on a hanging mercury drop electrode using SWV [76]. The good linearity was

found in the range of 0.01 to 0.19 µg mL^{-1}.   However, the mercury electrode is toxic that is caused the health problem to users and environments.

CHAPTER III:

EXPERIMENTAL

3.1 Chemicals and materials

3.1.1 Electrochemical detection of CoQ10 and ALA

Table 3.1 *List of chemicals used for electrochemical detection of CoQ10 and ALA*

Chemicals/materials and reagents	Suppliers
Coenzyme Q10 (CoQ10)	Sigma-Aldrich, USA
α-lipoic acid (ALA)	Sigma-Aldrich, USA
Potassium ferricyanide ($K_3Fe(CN)_6$)	Sigma-Aldrich, USA
Sodium acetate trihydrate ($CH_3COONa \cdot 3H_2O$)	Fluka, Switzerland)
Glacial acetic acid	Merck, Germany
Manganese (IV) oxide (MnO_2)	Merck, Germany
Ethanol	Merck, Germany
Potassium nitrate (KNO_3)	Merck, Germany
Vitamin A	Sigma-Aldrich, USA
Vitamin B_1	Sigma-Aldrich, USA
Vitamin B_9	Sigma-Aldrich, USA
Vitamin D_2	Sigma-Aldrich, USA
Vitamin D_3	Sigma-Aldrich, USA
Vitamin E	Sigma-Aldrich, USA
Vitamin K_1	Sigma-Aldrich, USA
Vitamin K_2	Sigma-Aldrich, USA

Chemicals/materials and reagents	Suppliers
Glutathione	Sigma-Aldrich, USA
Vitamin B_2	DMSc, Thailand
Vitamin C	BDH Analar, USA
Magnesium Sulfate ($MgSO_4$)	Merck, Germany
Calcium sulfate ($CaSO_4$)	Merck, Germany
Standard solution of zinc (1000 μg mL^{-1})	Merck, Germany
Graphene ink	Gwent group, United Kingdom
Carbon ink	Gwent group, United Kingdom
Silver/silver chloride ink	Gwent group, United Kingdom
Polyvinyl chloride sheet (PVC) with a thickness of 0.15 mm	Dee-craft Co. Ltd., Thailand

3.1.2 UHPLC-ED for the determination of DTCs

Table 3.2 List of chemicals used for UHPLC-ED for the determination of DTCs

Chemicals/materials and reagents	Suppliers
Thiram (tetramethyl thiuram)	Chem Service, USA
Disulfiram (tetraethyl thiuram)	Sigma-Aldrich, USA
Gold (III) chloride	Sigma-Aldrich, USA
Potassium dihydrogen phosphate (KH_2PO_4)	BDH laboratory supplies, England
Disodium hydrogen phosphate (Na_2HPO_4)	Merck, Germany
Sodium hydroxide (NaOH)	Merck, Germany

Chemicals/materials and reagents	Suppliers
Sulfuric acid (H_2SO_4)	Merck, Germany
Phosphoric acid	Merck, Germany
Acetonitrile	Merck, Germany
Chloroform	Merck, Germany

3.2 Instruments and equipment

3.2.1 Electrochemical detection of CoQ10 and ALA

Table 3.3 *List of instruments used for electrochemical detection of CoQ10 and ALA*

Instruments and equipment	Suppliers
Autolab Potentiostat 101	Methrohm, Switzerland
Solid-wax printer Color Qube8570 model	Xerox, Japan
Screen-printed template block	Chaiyaboon Co. Ltd., Thailand
Field emission scanning electron microscope (FESEM) JSM-7001F model	JEOL, England
Energy dispersive X-ray spectrometer (EDS) INCA Penta FETx3 model	Oxford Instrument, United Kingdom
Analytical balance	Mettler Toledo, Thailand
pH meter	Mettler Toledo, Thailand
Heating & drying oven	Memmert, Czech
Milli Q water system (R ≥ 18.2 MΩ cm)	Millipore, USA
Autopipette	Eppendorf, Germany

Instruments and equipment	Suppliers
Ultrasonic bath	Elma, Germany
Vortex mixer VTX-3000L	Mixer Uzusio LMS, Japan

3.2.2 UHPLC-ED for the determination of DTCs

Table 3.4 List of instruments used for UHPLC-ED for the determination of DTCs

Instruments and equipment	Suppliers
UHPLC LC-20AD XR pump	Shimadzu, Japan
UHPLC SIL-20A XR autosampler	Shimadzu, Japan
UHPLC CTO-20AC column oven	Shimadzu, Japan
UHPLC SPD-M20A diode array detector	Shimadzu, Japan
CHI 123A	CHI Instrument, USA
Scanning Electron Microscope (SEM) JSM-6400 model	JEOL, England
Kinetex™ core-shell C18 column	Phenomenex, USA
Thin-layer electrochemical flow cell	Bioanalytical System, USA
Teflon cell gasket	Bioanalytical System, USA
Stainless-steel tube	Bioanalytical System, USA
Silver/silver chloride electrode (Ag/AgCl)	Bioanalytical System, USA
Platinum wire	Bioanalytical System, USA
PEEK tubing (0.25 mm i.d.)	Upchurch, USA
Teflon tubing (1/10 inch i.d.)	Upchurch, USA

Instruments and equipment	Suppliers
Vacuum pump	GAST, USA
Nylon membrane filter papers (0.20 μm)	Vertical Chromatography, Thailand
Nylon syringe filters (0.20 μm)	ChroMex, USA

3.3 Fabrication of the electrodes

3.3.1 Electrochemical detection of CoQ10 and ALA

3.3.1.1 Screen printed-carbon electrode (SPCE), screen printed-graphene electrode (SPGE), and manganese (IV) oxide modified screen printed-graphene electrode (MnO$_2$/SPGE)

The three-electrode system was designed in a single electrode using Adobe Illustrator software. The electrode substrate was a polyvinyl chloride (PVC) sheet. The wax-pattern was printed on a PVC substrate using a solid-wax printer to limit the area of spreading solution. To fabricate the in-house screen-printed electrode, the carbon ink was first printed on the PVC substrate for use as a counter electrode. For the screen-printed carbon electrode (SPCE) and screen-printed graphene electrode (SPGE), carbon and graphene inks, respectively, were used as ink for the working electrode. For MnO$_2$/SPGE, the ink for the working electrode was prepared by adding the desired weight of MnO$_2$ (as received) into the graphene ink and carefully mixed by hand in a mortar with a pestle. The MnO$_2$ loading amount in the graphene ink was indicated in terms of the percentage of the weight of MnO$_2$ added into the graphene ink. The obtained ink was used to fabricate the working electrode in the next step. Then, the carbon, graphene, and MnO$_2$-modified graphene ink were printed to serve as a working electrode. Finally, Ag/AgCl paste was printed to use as the reference electrode and conducting pad. The finished electrode was then

allowed to dry in an oven at 55 °C for 1 h.   The design of the screen-printed electrode was shown in figure 3.1.
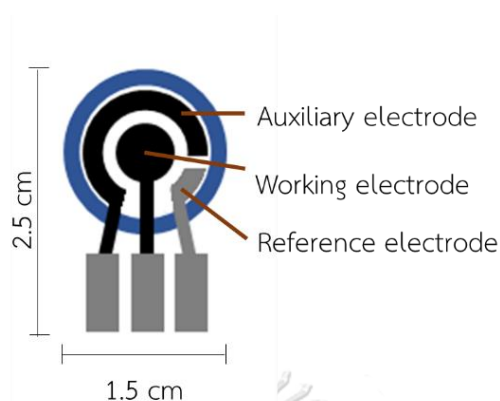
Figure 3.1 *Schematic illustration of the disposable electrode for the detection of CoQ10 and ALA*

3.3.2 UHPLC-ED for the determination of DTCs

3.3.2.1 Screen printed-carbon electrode (SPCE)

The SPCE was fabricated and produced by our laboratory using a screen printing technique. The Ag/AgCl ink was first printed on the PVC substrate for using as a conductive pad. Then, the carbon ink was printed to create a working electrode. Each step of printing electrode was allowed to dry in an oven at 55 °C for 1 h. The screen-printed carbon electrode was ready to modify in the next step.
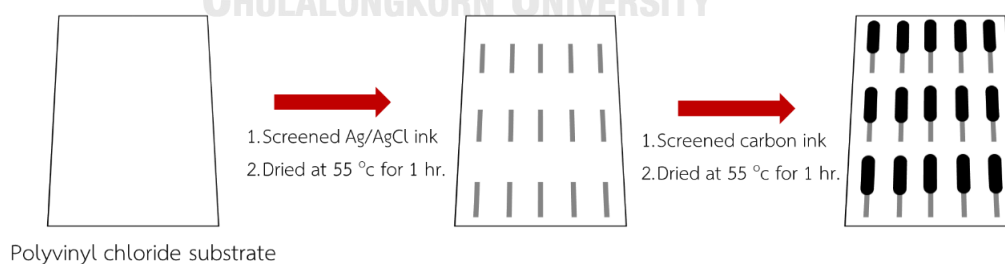
Figure 3.2 *Schematic illustration of the fabrication of an in-house screen-printed carbon electrode*

3.3.2.2 Modification of SPCE with gold nanoparticles

For the electrode modification, the 10 mM of gold (III) solution was used to modify onto electrode surface by electrodeposition technique. The three-electrode system was placed into cell containing 2 mL of solution of 10 mM of gold (III) solution in 0.5 M H_2SO_4 followed by deposition of gold onto the SPCE at a deposition potential of -0.6 V (vs. Ag/AgCl) for 50 s while the solution was stirred (by means of a mechanical stirrer bar). The gold nanoparticles (AuNPs) were obtained onto the electrode surface. After the modification, the AuNPs modified SPCE was carefully rinsed with distilled water and dried under N_2 gas prior to use.
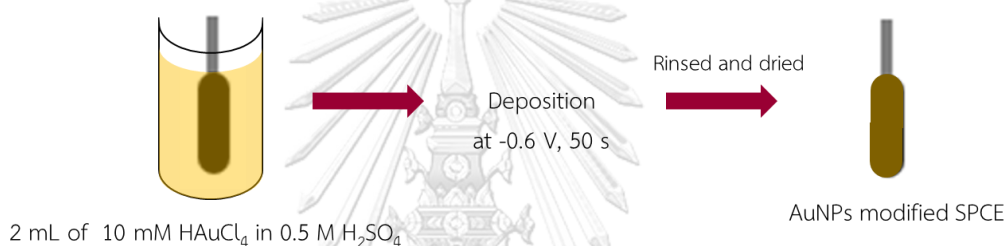
Figure 3.3 *Schematic illustration of the modification of SPCE by electrodeposition of* *AuNPs*

3.4 Chemical solution

3.4.1 Disposable electrochemical sensor of CoQ10 and ALA

3.4.1.1 Electrochemical characterization

For the electrochemical characterization, the double layer capacitance (C_{dl}) was estimated using 0.1 M KNO_3 solution. After that the electroactive surface area was performed in 1 mM of $Fe(CN)_6^{3-}$. The electrochemical performance of MnO_2/SPGE was compared with SPGE and SPCE via C_{dl} and electroactive surface area. Finally, the electrochemical behavior and mass transfer process of CoQ10 and ALA towards MnO_2/SPGE was evaluated using the mixture of 75 μg mL^{-1} of CoQ10 and 50 μg mL^{-1} of ALA in 20:80 ratio of ethanol: acetate buffer solution.

3.4.1.2 Supporting electrolyte

0.1 M acetate buffer solution was prepared by mixing 0.1 M CH_3COONa and 0.1 M CH_3COOH, and used as a supporting electrolyte. For the electrochemical detection, the ratio of ethanol and acetate buffer was optimized as well as pH of acetate buffer. The preparation of different pH of 0.1 M acetate buffer in the range of 3.5 to 6.0 (10 mL) was shown in table 3.5.

Table 3.5 *The preparation of pH in a range of 3.5 to 6.0 of acetate buffer solution*

pH	Volume of 0.1 M CH_3COONa (mL)	Volume of 0.1 M CH_3COOH (mL)
3.5	1.09	8.91
4.0	1.66	8.34
4.5	3.35	6.65
5.0	6.78	3.22
5.5	8.40	1.60
6.0	8.93	1.07

3.4.1.3 Stock standard solution and standard working solution

The 500 µg mL^{-1} of standard stock solutions of CoQ10 and ALA were prepared by dissolving in ethanol and stored at 4°C until use. Then, the standard stock solution was diluted in ethanol and 0.1 M acetate buffer at a desired ratio and used as the standard working solution.

3.4.2 UHPLC-ED for the determination of DTCs

3.4.2.1 Supporting electrolyte

Phosphate buffer solution was used as supporting electrolyte for the investigation of the electrochemical behavior and the measurement in UHLC-ED. Phosphate buffer solution was prepared by mixing of the desired concentration of

KH_2PO_4 and Na_2HPO_4. The ratio between ethanol and phosphate buffer solution, and concentration and pH of phosphate buffer solution were optimized. Table 3.6 shows a certain volume of KH_2PO_4 and Na_2HPO_4 for the preparation of phosphate buffer solution (100 mL) at desired pH.

Table 3.6 *The preparation of pH in a range 5.0 to 8.0 of phosphate buffer solution*

pH	Volume of 0.05 M KH_2PO_4 (mL)	Volume of 0.05 M Na_2HPO_4 (mL)
j5.0	99.2	0.80
5.5	96.4	3.60
6.0	88.9	11.1
6.5	70.4	26.6
7.0	41.3	58.7
7.5	16.2	83.8
8.0	3.70	96.3

3.4.2.2 Stock standard solution and standard working solution

All of stock standard solutions (1000 μg mL^{-1}) were prepared by dissolving 10 mg of each analyte in acetonitrile. The solutions were then placed in an amber bottle and stored at 4 °C. To investigate the electrochemical behavior, the standard solution of thiram was diluted in 0.05 M phosphate buffer solution and used as working solution. To prepare working standard solution for UHPLC-ED, the standard solutions of thiram and disulfiram were mixed and diluted in suitable proportions of acetonitrile:Milli-Q water (50:50; v/v), and kept for 5 min before measurement. All solutions and solvents were filtered by 0.22 μm nylon membranes prior to use in UHPLC separation.

3.4.2.3 Mobile phase

For UHPLC-ED experiment, acetonitrile and 0.05 M phosphate buffer solution were used as the mobile phase to separate and detect DTCs. All solutions and solvents were filtered by 0.22 μm nylon membranes prior to use.

3.5 Procedure

3.5.1 Electrochemical detection of CoQ10 and ALA

3.5.1.1 Electrochemical studies of CoQ10 and ALA

Cyclic voltammetry (CV) was used for characterizing the electrochemical behavior of the CoQ10 and ALA, and investigating the capacitance and electroactive surface area of the unmodified and modified electrode surfaces. For the determination of CoQ10 and ALA, square wave anodic stripping voltammetry (SWASV) was performed at a 20:80 (v/v) ratio of ethanol:acetate buffer (0.1 M) at pH 4.0. A standard mixture solution (100 μL) of CoQ10 and ALA was added to the three-electrode system at an applied potential of -0.7 V for 100 seconds to convert the CoQ10 and ALA to their reduced forms. After 5 seconds of quiescence, a square wave stripping voltammetric measurement was scanned from 0 to +1.0 V with a step potential of 5 mV, an amplitude of 20 mV, and a frequency of 25 Hz.

3.5.1.2 Optimization

The effect of the amount of MnO_2, the ratio of ethanol in the supporting electrolyte, pH of the acetate buffer, reduction potential and time, and the SWASV parameters to the quantitative detection of CoQ10 and ALA were studied. During the optimization, the investigated parameter was varied, while the other parameters were kept constant.

3.5.1.3 Interferences study

The oxidation behaviors of some possible interferents such as vitamins A, B_1, B_2, B_9, C, D_2, D_3, E, K_1, and K_2, glutathione, Mg^{2+}, Ca^{2+}, and Zn^{2+} were investigated separately in a solution containing 50 μg mL^{-1} of CoQ10, and 1 μg mL^{-1} of

ALA. The tolerance limit was defined as the interferent that yielded a relative error less than or equal to 5% when compared to the response obtained from standard concentrations of CoQ10 and ALA.

3.5.1.4 Analytical performance

3.5.1.4.1 Calibration curve

Standard solutions and samples were analyzed, and the peak currents were integrated. A calibration curve of standard solutions was performed under optimal conditions and treated with linear least square regression analysis using the Excel software package. The limit of detection (LOD) and limit of quantification (LOQ) were determined from the $3S_{bl}/S$ and $10S_{bl}/S$, respectively, where S_{bl} is standard deviation of blank (n = 10), and S is sensitivity of method, obtained from the slope of the linearity.

3.5.1.4.2 Reproducibility and repeatability study

The repeatability and reproducibility of the proposed sensor were estimated in terms of the relative standard deviation (%RSD) of 10 measurements for repeatability and 10 different sensors for reproducibility in a mixture solution of 25 and 0.5 µg mL^{-1} of CoQ10 and ALA, respectively. The %RSD was calculated from the following formula;

$$\%RSD = \frac{standard\ deviation\ (SD)}{mean} \times 100 \qquad (Equation\ 3.1.)$$

3.5.1.4.2 Real samples analysis

CoQ10 and ALA dietary supplement tablets, and a mixture of CoQ10 and ALA in dietary supplement tablets were purchased from local markets in Thailand, and dissolved in 10 mL of ethanol. The aliquot solutions were diluted in a supporting electrolyte, and the final concentration of test solution was within a dynamic range. SWASV was recorded under optimal conditions, and the

concentrations of CoQ10 and ALA were evaluated from the calibration curves. All experiments were performed in triplicate.

3.5.2 UHPLC-ED for the determination of DTCs

3.5.2.1 Cyclic voltammetric study of DTCs

The electrochemical reaction and optimal parameters for electrodeposition step were studied by cyclic voltammetry (CV) using a CH instrument potentiostat 1232A. The working electrodes used in this work were bare SPCE and AuNP/SPCE. The reference and auxiliary electrodes were Ag/AgCl electrode and Pt wire, respectively. All experiments were done at room temperature.

3.5.2.2 UHPLC-ED

The UHPLC system was performed in reversed-phase mode with core-shell C18 column (50 mm x 4.6 mm i.d.; particle size, 2.6 μm.). The thin-layer flow cell consisted of a working AuNP/SPCE, a reference Ag/AgCl electrode, and a stainless steel tube counter electrode. The geometric area of the AuNP/SPCE in the flow cell was estimated to be $0.40 \ cm^2$ with 1 mm thick silicon rubber gasket as a spacer. An electrochemical measurement for amperometric control and signal processing was performed using CH instrument potentiostat 1232A. The UHPLC-electrochemical measurement was carried out in 45:55 (v/v) ratio acetonitrile: 0.05 M phosphate buffer solution (pH 5), which was adjusted to pH 5 with 0.1 M sodium hydroxide solution, as mobile phase with an applied potential of 1.2 V vs Ag/AgCl, an injection volume of 50 μL, and a flow rate of 1.5 mL min^{-1}. All chromatographic separations were performed at room temperature.
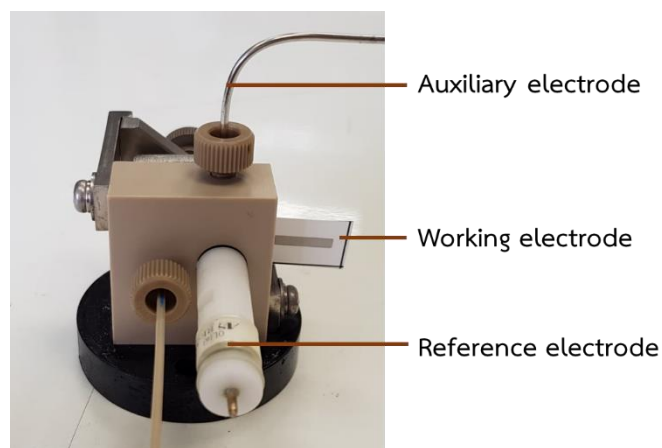
Figure 3.4 *Electrochemical flow cell including; AuNP/SPCE, silver/silver chloride (Ag/AgCl), and a stainless steel tube.*

3.5.2.3 Optimization of electrode modification

AuNPs were modified on electrode surface using the electrodeposition technique. The deposition potential and time were investigated because these parameters affect the shape and size of AuNPs on the surface resulting in the signal-to-noise ratio of the detection of the analytes. Thiram was selected as the representative compounds. To obtain the optimal condition of AuNP/SPCE, the dependence of deposition potential and deposition time were studied via CV, and the relationship between the studied parameter and the current response of thiram was plotted.

3.5.2.4 Optimization of UHPLC-ED

The effects of percentage of acetonitrile used in the mobile phase, the concentration of phosphate buffer solution, injection volume, and flow rate on the retention characteristics were evaluated to obtain the best separation characteristic. During the optimization, the investigated parameter was varied, while the other parameters were kept constant.

Finally, the amperometric detection potential was investigated because it effects to the peak current of analytes as well as background signal.

Therefore, the peak current after background subtraction was plotted to observe the optimal detection potential.

3.5.2.5 Analytical performance

3.5.2.5.1 Calibration curve

Standard solutions and samples were analyzed, and the currents were integrated. A calibration curve of standard solutions was performed under optimal conditions and treated with linear least square regression analysis using the Excel software package. The limit of detection (LOD) and limit of quantification (LOQ) were determined from the $3S_{bl}/S$ and $10S_{bl}/S$, respectively, where S_{bl} is standard deviation of blank (n = 10), and S is sensitivity of method, obtained from the slope of the linearity.

3.5.2.5.2 Reproducibility and precision study

The stability of the AuNP/SPCE was studied in multiple analyses 30 replicates without the replacement of the electrode under the optimal conditions. The reproducibility was investigated from 10 different electrodes. The precision of the analytical process was evaluated by the repeatability of the process. The spiked concentrations in the dynamic linearity between 1 to 15 µg mL^{-1} were studied to calculate the RSD percentage. The precision of intra-day and inter-day, three concentrations of DCTs (1, 6, and 12 µg mL^{-1}) were observed three times within a day and three different days.

3.5.2.5.3 Method validation

To validate the developed method, UHPLC-ED was compared to the standard method of UHPLC coupled with ultraviolet detection (UHPLC–UV) using the paired *t-test* under the same separation condition.

3.5.2.5.4 Real samples analysis

The three real samples including apple, grape and lettuce were obtained from local markets in Thailand. For analysis, 50 g of cut sample was weighed accurately and transferred to a blender. Then 50 µL of 500 µg mL^{-1} of standard mixture solution and chloroform were added. The mixture was homogenized with blender and transferred into centrifuge tubes. After centrifugation at 4000 rpm for 10 min, all of the organic phases were filtered through a Buchner funnel with Whatman filter paper No. 4 and transferred to 250 mL vessel of the rotary vacuum evaporator for evaporation to dryness at room temperature. The residues were dissolved in 4.5 mL of acetonitrile using ultrasonic stirring, filtered through the 0.2 µm pore size of nylon membrane, and collected in 5 mL of volumetric flask. After that, acetonitrile filtered through the 0.2 µm pore size of nylon membrane was added to adjust the volume to 5 mL of solution. Finally, 50 µL of the solution was injected into the UHPLC system. The determination of DTCs in samples was analyzed within the linear dynamic range that obtained by adding a different volume of 500 µg mL^{-1} of standard mixture solution into the blank sample and prepared following the above treatment.

CHAPTER IV:

RESULTS AND DISCUSSION

4.1 Electrochemical detection of CoQ10 and ALA

The development of the disposable electrochemical sensor to the pharmaceutical application was proposed. CoQ10 and ALA were the powerful anti-oxidant that presented in many dietary supplements. The disposable electrochemical sensor was developed on SPGE and MnO_2 for the detection of CoQ10 and ALA. This is the first application of the use of MnO_2/SPGE to determine CoQ10 and ALA simultaneously.

4.1.1 Morphological characterization of SPCE, SPGE, and MnO_2/SPGE

The surface morphologies of the SPCE, SPGE, and MnO_2/SPGE were investigated using a scanning electron microscopy (SEM), as shown in figure 4.1. A smooth surface was observed at the carbon surface due to a flat sheet of graphite. As expected, the surface of the SPGE exhibited isolated flakes. Additionally, separated layers were observed that indicated the presence of graphene at the surface. As seen in SEM of MnO_2/SPGE, the surface of the MnO_2/SPGE is similar to the SPGE. However, no MnO_2 was observed using SEM.

To confirm the existence of MnO_2, EDS was performed. From the EDS spectra (figure 4.2), the results show that C and Mn are the major elements found on the electrode surface. C originates from graphene, while Mn came from MnO_2, indicating that Mn remained on the surface of the MnO_2/SPGE.
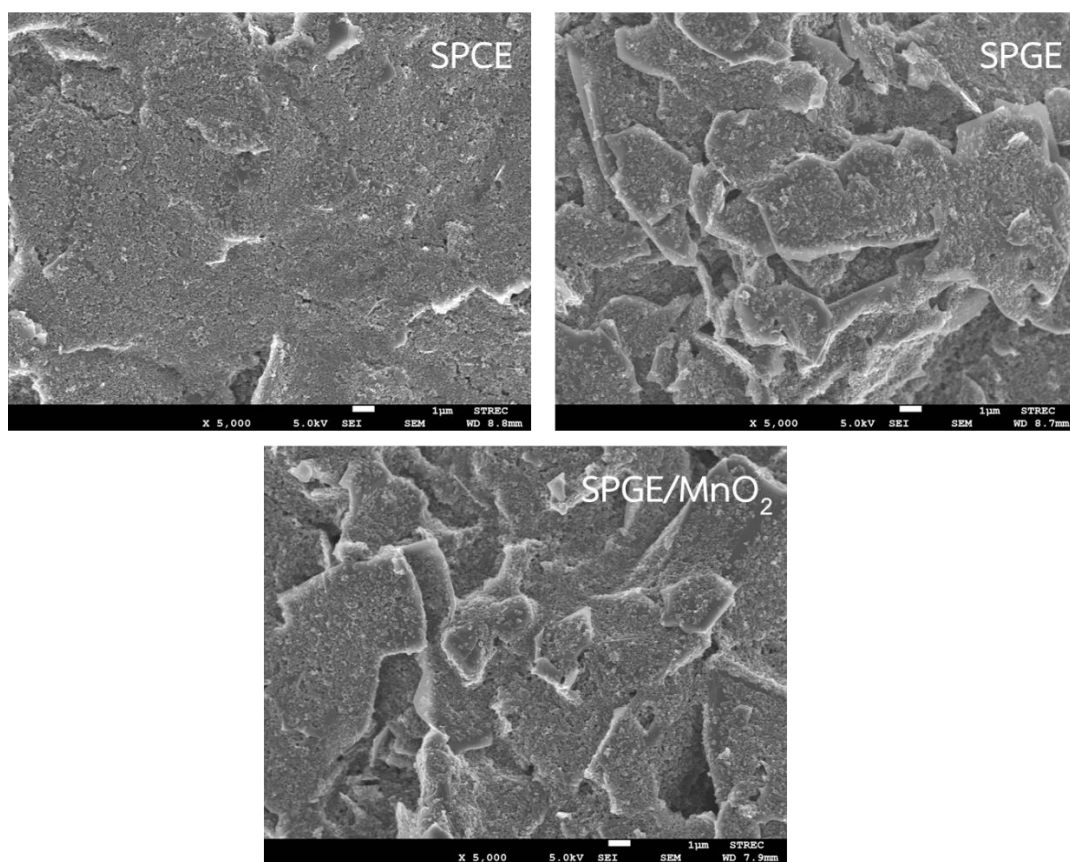
Figure 4.1 *SEM images of SPCE, SPGE, and MnO₂/SPGE*
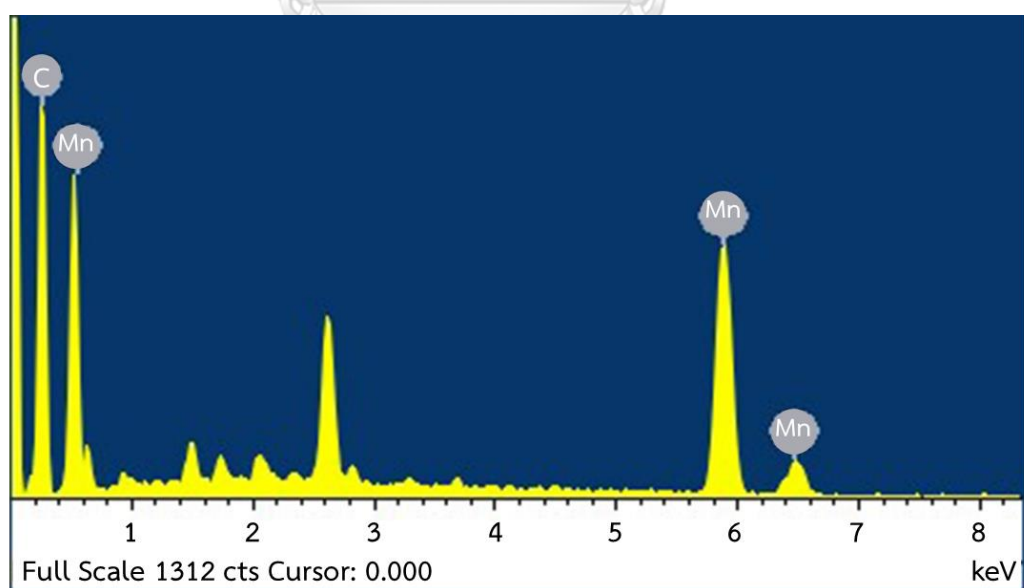
Figure 4.2 *EDS spectrum of MnO₂/SPGE*

4.1.2 Electrochemical characterization of the SPCE, SPGE, and MnO$_2$/SPGE

The performance of the SPCE, SPGE, and MnO$_2$/SPGE was evaluated via the double layer capacitance (C$_{dl}$), as shown in figure. 4.3. The CV plots were scanned between -0.2 to +0.2 V at 20 mV s^{-1} in 0.1 M KNO$_3$, and the C$_{dl}$ of each electrode was determined at 0 V. The C$_{dl}$ was calculated using equation 4.1,

$$C_{dl} \quad = \quad i_{average}/vA_{geometric} \hspace{2cm} \text{(Equation 4.1)}$$

where i$_{average}$ is the average current from the forward and reverse sweeps in amperes (A), v is the scan rate in volts per second (V s^{-1}), and A$_{geometric}$ is the geometric electrode area in square centimeters (cm^2). The capacitances of the SPCE, SPGE, and MnO$_2$/SPGE were found to be 7.33 ± 0.50, 2.61 ± 0.44, and 18.78 ± 0.74 μF cm^{-2}, respectively (n = 3 electrodes). As a result, the MnO$_2$/SPGE shows the largest capacitance due to the oxide of MnO$_2$ and demonstrates that MnO$_2$ is an ideal material for supercapacitors [77].
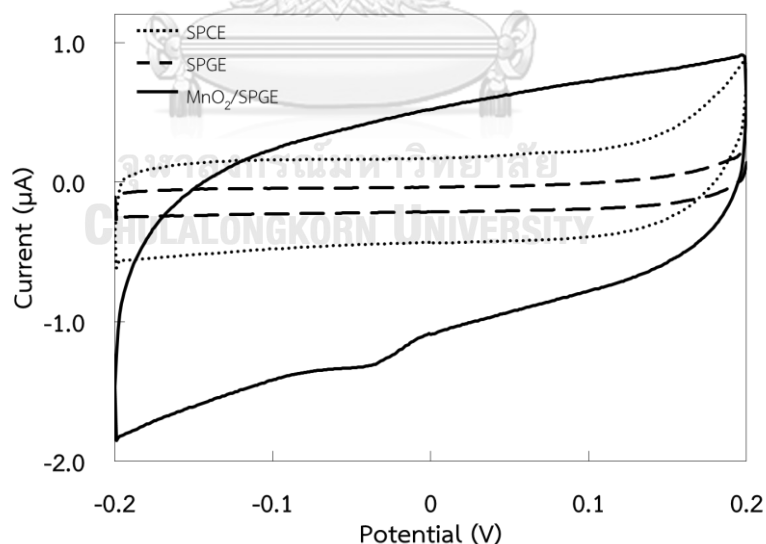
Figure 4.3 *CV data in aerated 0.1 M KNO$_3$ recorded at 0.2 V s^{-1} over the potential range of −0.2 to 0.2 V, for the SPCE (dotted line), SPGE (dashed line), and MnO$_2$/SPGE (solid line)*

The electrochemical characteristics of the electrodes were investigated using a 1 mM [Fe (CN)$_6$]$^{3-}$ solution in 0.1 M KNO$_3$ via CV. The comparison of CVs performed on SPCE, SPGE, and MnO$_2$/SPGE displays a reversible process, as shown in figure 4.4.
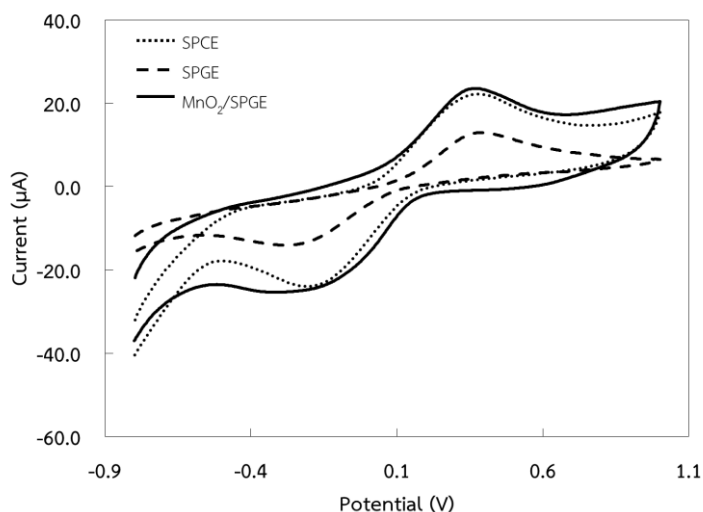
Figure 4.4 *The comparison of CVs performed on SPCE (dotted line), SPGE (dashed line), and MnO$_2$/SPGE (solid line), at 0.08 V s^{-1} using 1 mM Fe(CN)$_6^{3-}$ in 0.1 M KNO$_3$*

In addition, the electrochemical characteristics demonstrated at different scan rate were shown in figure 4.5. For the reversible process, the Randles-Sevcik equation 4.2 is applied for the calculation of the electroactive surface area.

$$I_p = (2.69 \times 10^5) \, n^3 A D_0^{1/2} v^{1/2} C_0^*$$ (Equation 4.2)

where n is the number of electrons transferred in the redox event, A is the electroactive surface area (cm^2), D$_0$ is the diffusion coefficient (cm^2 s^{-1}), v is the scan rate (V s^{-1}), and C$_0$* is the concentration (M). Based on the known parameters (n = 1, D = 7.6 × 10^{-6} cm^2 s^{-1}, I$_p$ v$^{-1/2}$ = slope obtained from the plot between square root of scan rate and current, and C = 1 × 10^{-6} M), the electroactive surface areas were 0.070 cm^2 for SPCE, 0.057 cm^2 for SPGE, and 0.091 cm^2 for MnO$_2$/SPGE. The electroactive surface area obtained from the MnO$_2$/SPGE was found to be 1.3 and 1.6 times higher

than those obtained from SPCE and SPGE, respectively. Apart from this, the differences between anodic and cathodic peak potentials (ΔE_p) at a scan rate of 80 mV s^{-1} are 0.59 V for SPCE, 0.66 V for SPGE, and 0.68 V for MnO$_2$/SPGE. These differences can be explained by the partial inhibition the electron-transfer kinetics due to the modification of the electrode surface with MnO$_2$ [15].
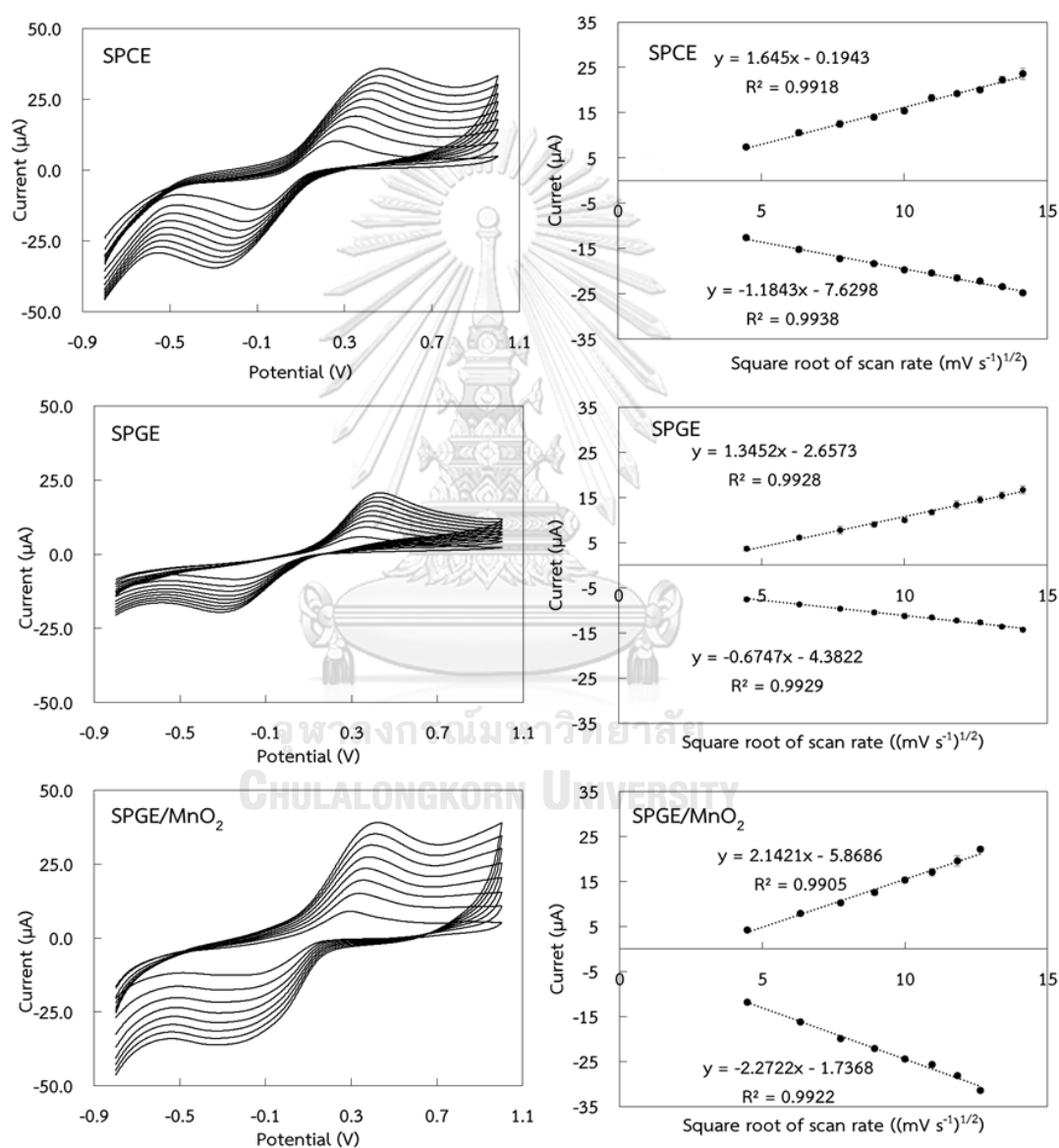
Figure 4.5 CVs of SPCE, SPGE, and MnO$_2$/SPGE in 1 mM Fe(CN)$_6^{3-}$ in 0.1 M KNO$_3$ at scan rates of 20, 40, 60, 80, 100, 120, 140, 160, 180, and 200 mV s^{-1}. In addition, the plot between the peak current and square root of the scan rate.

4.1.3 Electrochemical behavior of CoQ10 and ALA at SPCE, SPGE, and MnO$_2$/SPGE

CV was used to study the electrochemical behavior of CoQ10 and ALA on the SPCE, SPGE, and MnO$_2$/SPGE, as shown in figure 4.6A. A cyclic voltammogram of a mixture of 75 µg mL^{-1} of CoQ10 and 50 µg mL^{-1} of ALA was obtained in the potential range from -0.8 V to 1.0 V. From the CV results, the well-defined oxidation peaks of CoQ10 and ALA were clearly observed at the SPGE and MnO$_2$/SPGE in comparison to the results obtained from the SPCE. The anodic peak potentials of CoQ10 were observed at 0.26 V for the SPCE, 0.18 V for the SPGE, and 0.22 V for the MnO$_2$/SPGE. The anodic peak potentials of ALA were observed at 0.76, 0.67, and 0.64 V for the SPCE, SPGE, and MnO$_2$/SPGE, respectively. In comparison to the SPCE, the anodic peak potentials observed at the SPGE and MnO$_2$/SPGE were shifted slightly to a negative potential. The results suggest that the use of graphene facilitated electron transfer at the surface. The anodic peak current of CoQ10 at the MnO$_2$/SPGE was significantly higher than the current obtained from the SPGE. As a result, the presence of MnO$_2$ particles on the surface mainly attributed to the higher electroactive surface area. The current response obtained from the modified electrode also approves the effect of MnO$_2$ as an electrocatalyst in the electrode structure. However, for the determination of ALA, the anodic peak current obtained from the MnO$_2$/SPGE was slightly lower than that obtained from the SPGE. The low anodic peak current of ALA using the MnO$_2$/SPGE caused by the oxidation of MnO$_2$ (~0.85 V) immediately occurred after the oxidation of ALA (~0.65 V). This oxidation process caused the appearance of the high background signal at the anodic potential of ALA, resulting in a slightly lower anodic peak current. Figure 4.6B shows the SWASV data of combined solution of 75 µg mL^{-1} of CoQ10 and 50 µg mL^{-1} of ALA at a reduction potential of -0.6 V for 100 seconds. In this work, reduction step was applied to convert all of the CoQ10 and ALA in the solution to a reduced form for the determination of total CoQ10 and ALA amount in

the sample. As shown in the voltammogram of figure 4.6B, small stripping current responses were observed on the SPCE. In contrast, the stripping peak currents of CoQ10 and ALA were significantly improved, and the well-defined peaks were clearly observed and separated regarding SPGE and MnO_2/SPGE. Specifically, the use of MnO_2/SPGE exhibited an enhancement in the CoQ10 peak current. As mentioned above, the use of graphene and MnO_2 facilitated electron transfer and increased the electroactive surface area; therefore, the sensitivity can be improved for the simultaneous determination of CoQ10 and ALA.
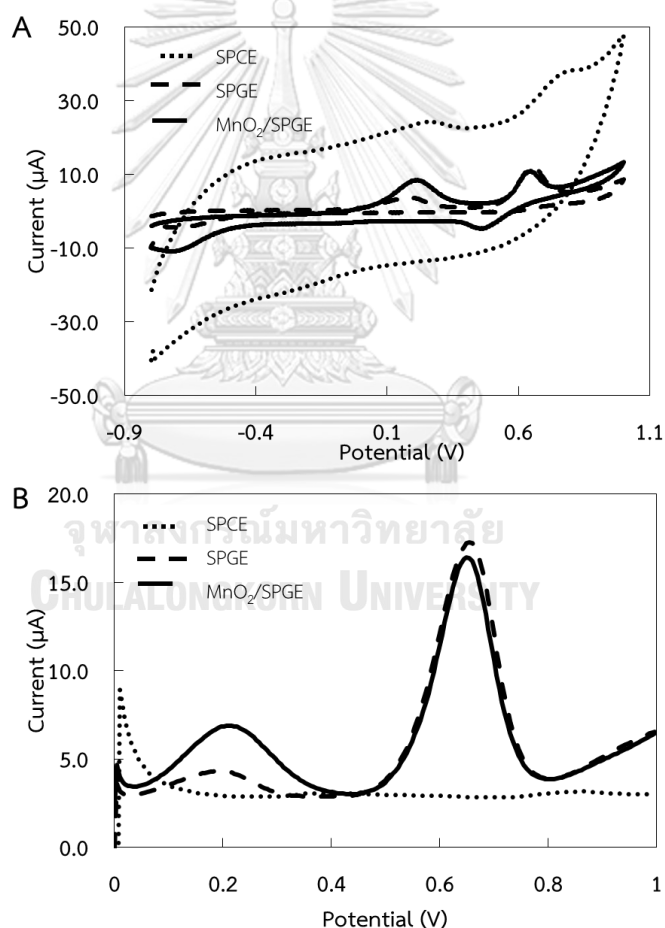
Figure 4.6 CV curves (A), and SWASV curves (B) of the SPCE (dotted line), SPGE (dashed line), and MnO_2/SPGE (solid line) using a mixture solution of 75 $\mu g\ mL^{-1}$ of CoQ10 and 50 $\mu g\ mL^{-1}$ of ALA in 20:80 of ethanol:0.1 M acetate buffer at pH 4.0 with a scan rate of 0.1 $V\ s^{-1}$.

To evaluate the mass transfer of the analytes toward the $MnO_2/SPGE$ surface, CV was performed at different scan rates. As shown in figure 4.7, the peak current increased with an increasing scan rate, as predicted. Moreover, good linearity between the square root of the scan rate and the peak current of both compounds was observed indicating that the mass transport of CoQ10 and ALA to the $MnO_2/SPGE$ surface was controlled by a diffusion process.

Figure 4.7 *CVs of 75 µg mL^{-1} of CoQ10 and 50 µg mL^{-1} of ALA on the MnO$_2$/SPGE at different scan rates of 20, 40, 60, 80, 100, 120, 140, 160, 180, and 200 mV s^{-1} (left). In addition, the plot between the peak current and square root of the scan rate (right).*

4.1.4 Optimization of experimental parameters

4.1.4.1 The amount of MnO_2

MnO_2 plays an important role in the electrocatalytic effect on the oxidation of compounds. The optimization of the amount of MnO_2 for the preparation of the MnO_2/SPGE was conducted by varying the percentage of MnO_2 in the graphene ink. The effect of the percentage of MnO_2 on the oxidation of CoQ10 (50 µg mL^{-1}) and ALA (0.5 µg mL^{-1}) was examined as shown in figure 4.8. The oxidation current of the compounds increased in correspondence with the increasing percentage of MnO_2, and the maximum current response was observed at 1.25% of MnO_2. Hence, this amount was determined to be the most suitable and was selected as the optimal value for the next experiments.
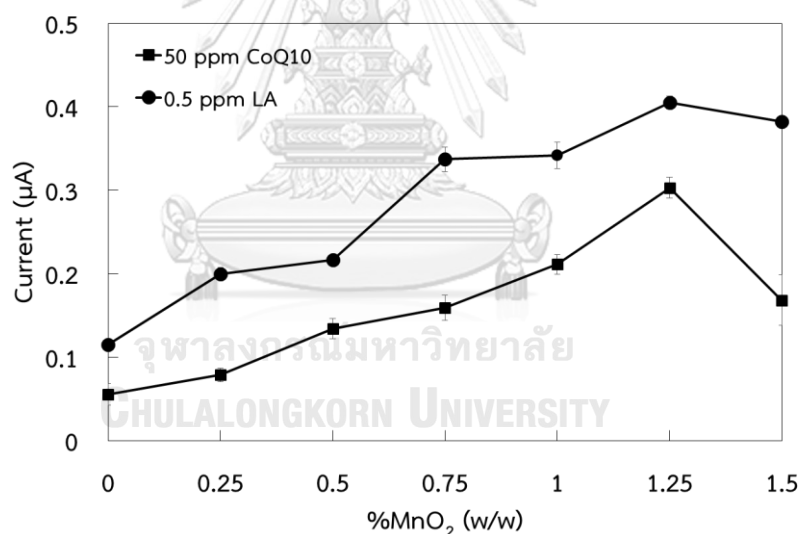
Figure 4.8 *Effect of %MnO_2 on the peak current of 50 µg mL^{-1} of CoQ10 (■) and 0.5 µg mL^{-1} of ALA (●) in 20:80 of ethanol:0.1M acetate buffer pH 4.0 on MnO_2/SPGE using SWASV at 15 mV for step potential, 20 mV for amplitude, and 25 Hz for frequency.*

4.1.4.2 The ratio of ethanol in supporting electrolyte

In this work, CoQ10 and ALA were dissolved in ethanol. The effect of the percentage of ethanol used in the supporting electrolyte on the anodic peak current was evaluated (figure 4.9). The high percentage of ethanol affected a decrease in the oxidation current of both compounds. This decrease is because of the changes in the ionic strength of the medium that exhibited a low diffusion coefficient. On the other hand, at a lower content of ethanol in the supporting electrolyte, a dissolubility of the compounds was observed. Therefore, an ethanol level of 30% was selected to achieve good sensitivity for the detection of CoQ10 and ALA.
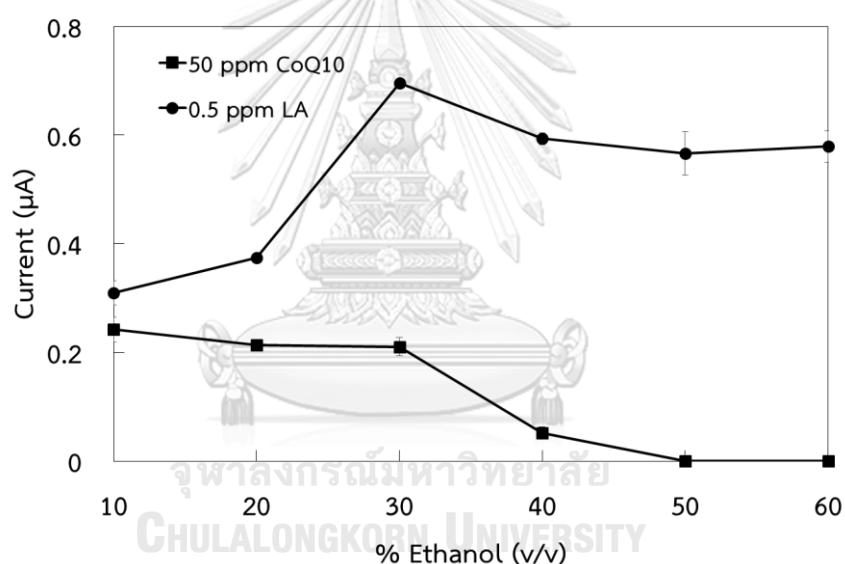
Figure 4.9 *Effect of %ethanol (in 0.1 M acetate buffer pH 4.0) on the peak current of 50 µg mL^{-1} of CoQ10 (■) and 0.5 µg mL^{-1} of ALA (●) on MnO$_2$/SPGE using SWASV at 15 mV for step potential, 20 mV for amplitude, and 25 Hz for frequency.*

4.1.4.3 The pH of acetate buffer

SWASV was used to study the effect of the pH of the supporting electrolytes. Different pH levels of the 0.1 M acetate buffer were studied in the range of 3.5 to 5.5, as shown in figure 4.10. The oxidation current of CoQ10 decreased with an increase in pH. In contrast, the oxidation current of ALA increased with an increase in pH (figure 4.10A). This phenomenon occurred because of the different nature of the compounds. In general, ALA exhibits a high stability in an acidic solution and was markedly stable when the pH increased [78]. Therefore, ALA was easily oxidized exhibits a high stripping current in a basic medium. Conversely, CoQ10 is less stable and easily oxidized in an acidic solution leading to the high stripping current at low pH. Based on this phenomenon, the acetate buffer at pH 4.0 was chosen as an optimal pH to compromise the sensitivity of both compounds. Considering a pH from 3.5 to 5.5, the peak potentials of both compounds were shifted to a more negative potential (figure 4.10B). The slopes of plot between the peak potential (E_p) and pH were 27.6 mV for CoQ10, and 28.9 mV for ALA, which were close to the theoretical value of 30 mV per pH unit for the ratio of 1 proton and 2 electrons involved in the redox reaction. Therefore, the oxidation of CoQ10 and ALA on the MnO_2/SPGE demonstrated a two-electron and one-proton transfer.
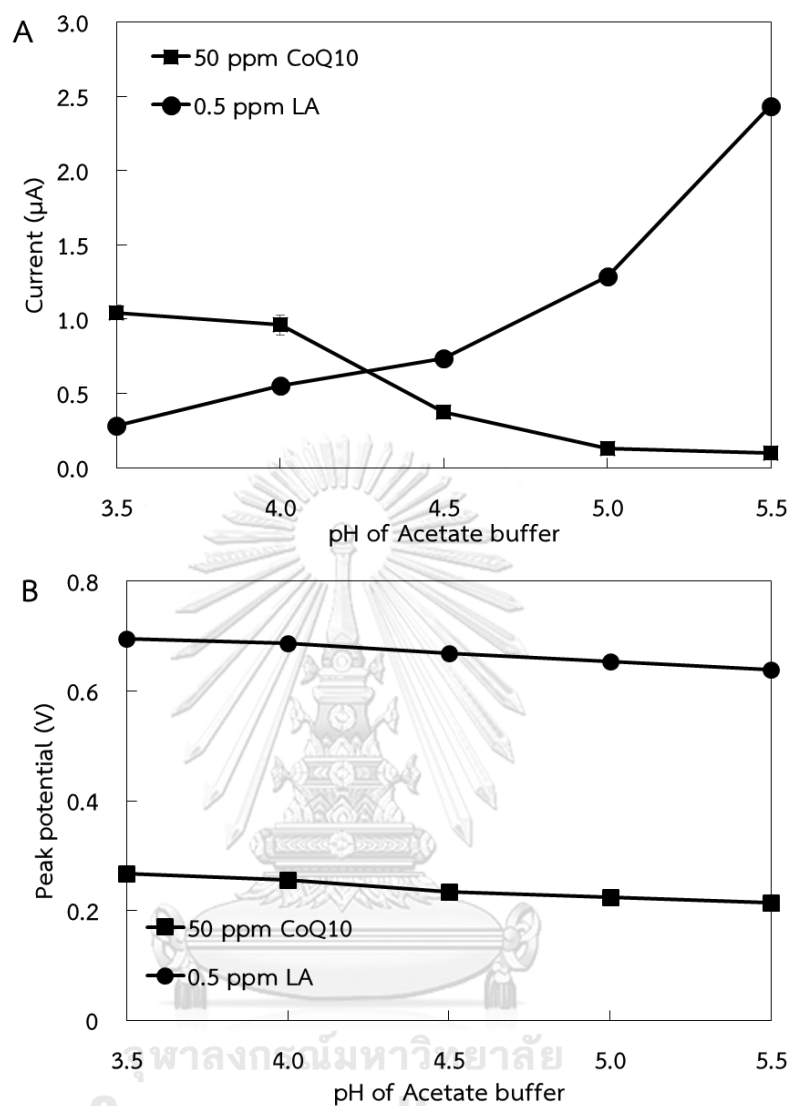
Figure 4.10 *Effect of pH on the peak current (A), and peak potential (B) of 50 µg mL^{-1} of CoQ10 (■) and 0.5 µg mL^{-1} of ALA (●) in 30:70 of ethanol: 0.1 M acetate buffer on MnO$_2$/SPGE using SWASV at 15 mV for step potential, 20 mV for amplitude, and 25 Hz for frequency.*

4.1.4.4 The reduction potential and time

The effects of the reduction potential and reduction time were evaluated in the range of -1.0 to -1.4 V, and 25 to 150 seconds, respectively (figure 4.11). As shown in figure 4.11A, the oxidation currents of both compounds increased with an applied potential from -0.4 to -1.0 V. At a reduction potential less negative

than -0.7 V, the oxidation current of CoQ10 dramatically decreased, and the peak current of ALA gradually decreased. The decreasing of peak currents occurred because of the formation of hydrogen that inhibited the reduction of both compounds. Hence, the reduction potential of -0.7 V was selected due to providing the highest current signal. In addition, the deposition time is another important factor that affected both the reduction step and stripping currents of the compounds (figure 4.11B). The anodic peak currents increased with an increase in the reduction time to 100 seconds but did not improve considerably with longer times. Therefore, the reduction time of 100 seconds was chosen as the optimal time.

4.1.4.5 The SWASV parameters

For the quantitative analysis of CoQ10 and ALA, square wave voltammetry (SWV) was performed because of the low background signal currents and its high sensitivity [14]. The SWV parameters including step potential, amplitude, and frequency were optimized because these parameters affected the sensitivity and linearity of the quantification of CoQ10 and ALA as shown in figure 4.12. During the optimization, the investigated parameter was varied, while the other parameters were kept constant. The step potential, amplitude, and frequency were studied in the range of 1 to 15 mV, 10 to 70 mV, and 5 to 75 Hz, respectively. From the experiment, the most appropriate parameters with respect to the current response of CoQ10 and ALA were 5 mV for the step potential, 20 mV for the amplitude, and 25 Hz for the frequency. All other experiments, such as interference studies, analytical performance studies, and real sample application studies, were performed under these optimized parameters.
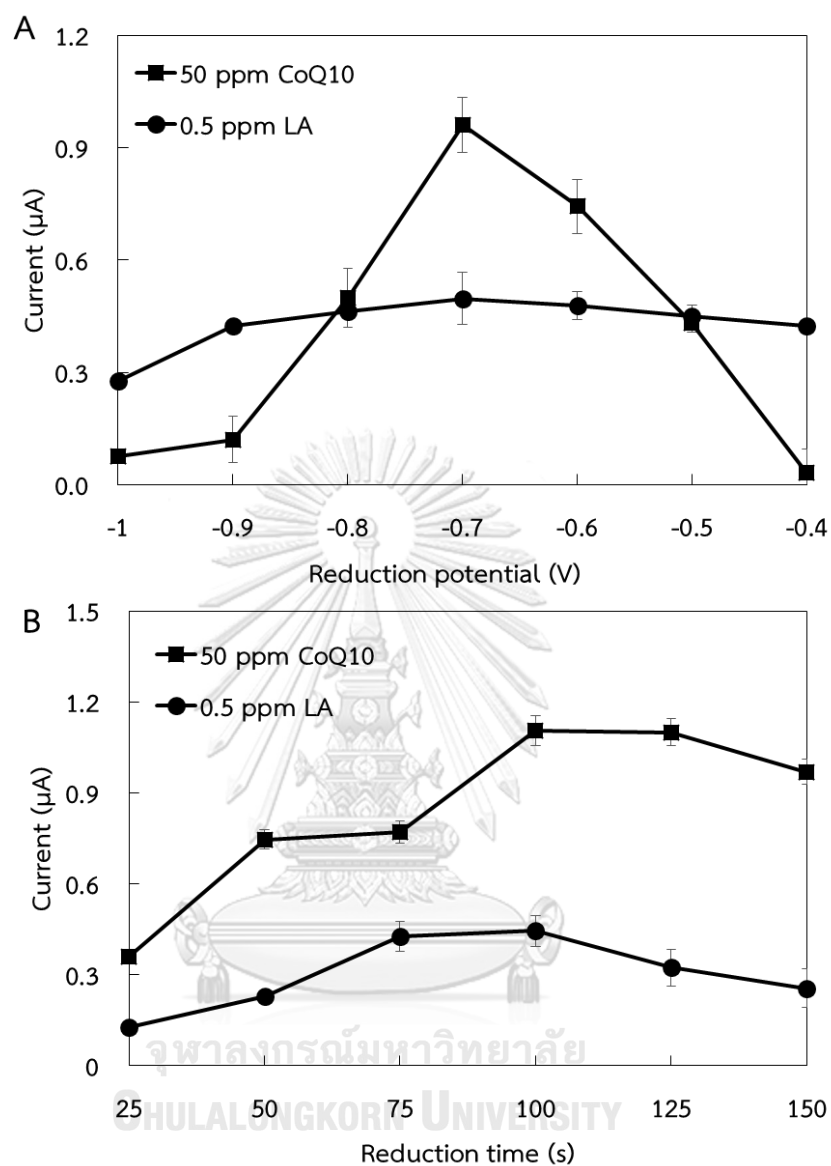
Figure 4.11 *Effect of reduction potential (left) and reduction time (right) of 50 μg mL^{-1} of CoQ10 (■) and 0.5 μg mL^{-1} of ALA (●) in 30:70 of ethanol: 0.1 M acetate buffer pH 4.0 on MnO$_2$/SPGE using SWASV at 15 mV for step potential, 20 mV for amplitude, and 25 Hz frequency.*
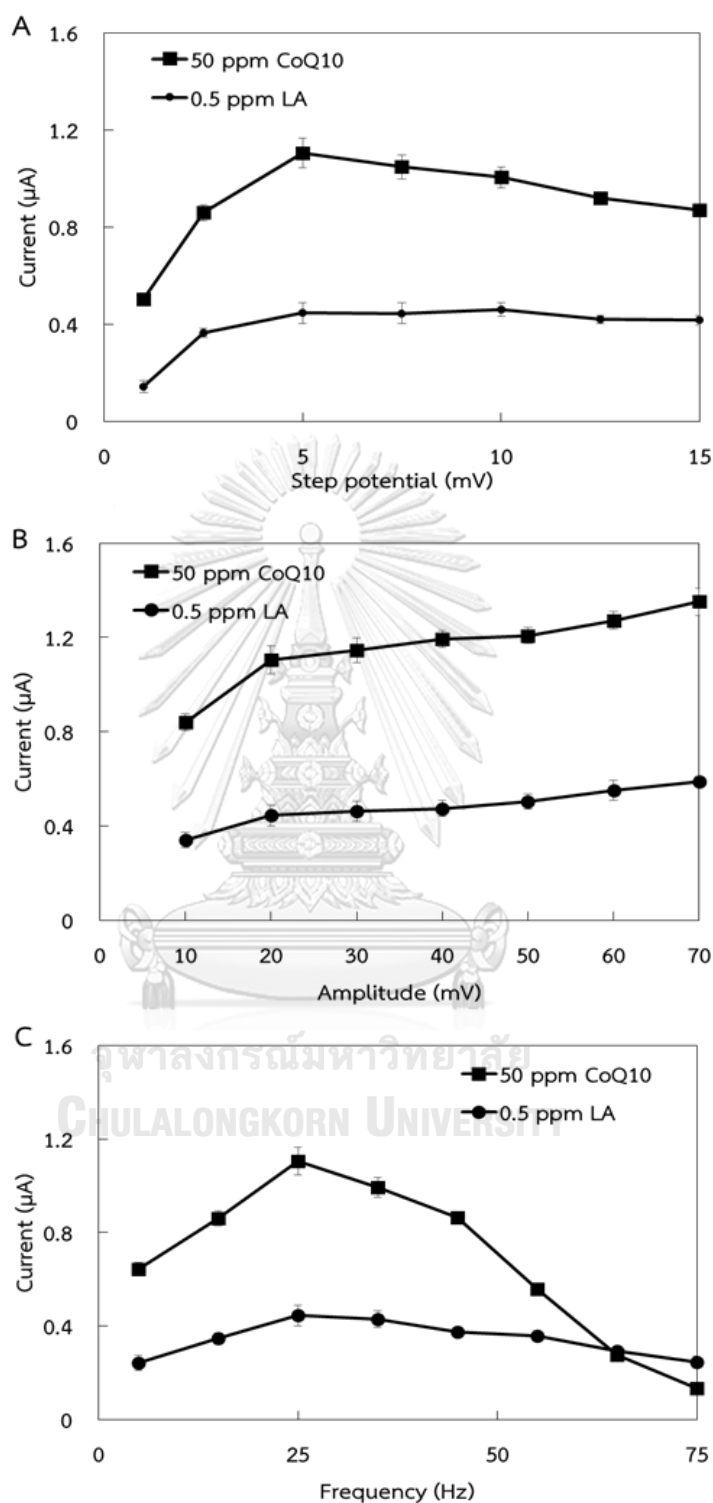
Figure 4.12 *Effect of step potential (A), amplitude (B), and frequency (C) of 50 µg mL^{-1} of CoQ10 (■) and 0.5 µg mL-1 of ALA (●) in 30:70 of ethanol: 0.1 M acetate buffer pH 4.0 on MnO$_2$/SPGE using SWASV.*

4.1.4.6 Analytical performance

The quantitative determination of CoQ10 and ALA in the mixture was performed using SWASV under the optimal conditions. The effect of ALA on the anodic peak current of CoQ10, and the effect of CoQ10 on the anodic peak current of ALA were studied as shown in figure 4.13 and 4.14. Figure 4.13 shows the voltammograms of the various concentrations of ALA from 0 to 25 µg mL^{-1} while the concentration of CoQ10 was constant. The results showed that there were no changes in the peak current of CoQ10, and the peak current of ALA was proportional to its concentration.
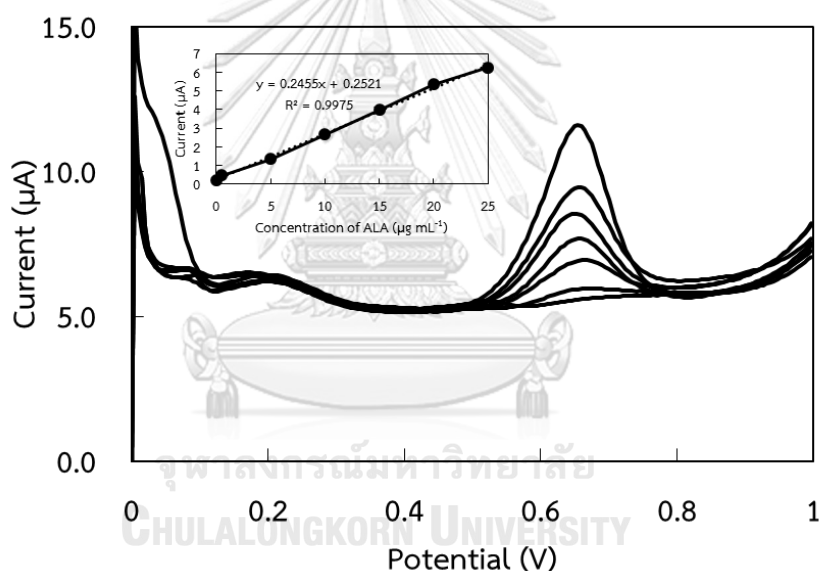
Figure 4.13 *SWASVs of ALA (A) in 20:80 of ethanol:0.1 M acetate buffer at pH 4.0 on the MnO$_2$/SPGE containing 25 µg mL^{-1} of CoQ10 and different concentrations of ALA. From inner to outer: 0, 0.25, 0.5, 1.0, 5.0, 10.0, 15.0, 20.0, and 25.0 µg mL^{-1} of ALA. Plot of the electrocatalytic peak current as a function of ALA concentration (inset).*

Figure 4.14 shows the voltammograms of a constant concentration of ALA with various concentrations of CoQ10 from 0 to 75 µg mL^{-1}. The same results were observed, indicating that both compounds did not affect each other. Therefore, the determination of two compounds could be performed simultaneously.
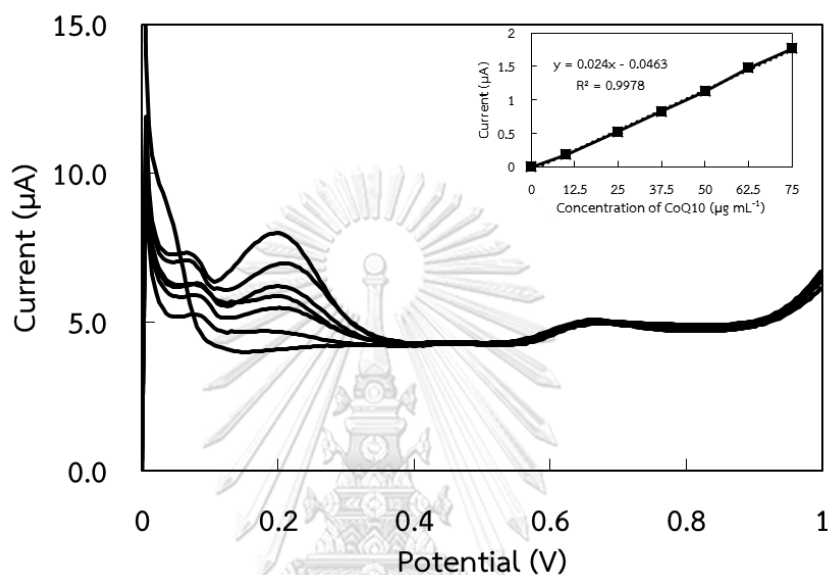
Figure 4.14 *SWASVs of CoQ10 (B) in 20:80 of ethanol:0.1 M acetate buffer at pH 4.0 on the MnO$_2$/SPGE containing 0.5 µg mL^{-1} of ALA and different concentrations of ALA. From inner to outer: 0, 5.0, 7.5, 10.0, 25.0, 37.5, 50.0, 62.5, and 75.0 µg mL^{-1} of CoQ10. Plot of the electrocatalytic peak current as a function of CoQ10 concentration (inset).*

The SWASV was performed for the quantitative determination of CoQ10 and ALA by changing the concentration of CoQ10 and ALA (figure 4.15). The data for a calibration curve were collected under optimal conditions, and the curve was constructed by plotting the anodic peak current versus known concentrations of CoQ10 and ALA (figure 4.14 inset). A linearity in the curve was observed in the range of 2.0 to 75.0 µg mL^{-1} for CoQ10, and 0.3 to 25.0 µg mL^{-1} for ALA with a correlation coefficient (r^2) higher than 0.99. The LOD and limit of quantitations (LOQ) were calculated from 3 S_{bl}/S and 10 S_{bl}/S, where S_{bl} is the standard deviation of a blank

measurement (n = 10), and S is the sensitivity of the method (slope of linearity). The

LODs were found to be 0.56 µg mL^{-1} for CoQ10, and 0.088 µg mL^{-1} for ALA.
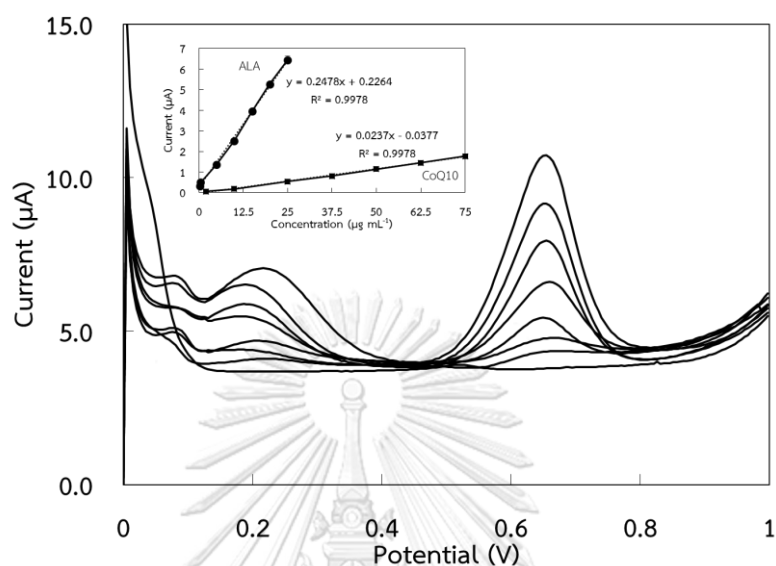
Figure 4.15 *SWASVs of CoQ10 and ALA in 20:80 of ethanol:0.1 M acetate buffer at pH*
4.0 on the MnO$_2$/SPGE containing different concentrations of CoQ10 and
ALA in µg mL^{-1}, from inner to outer: 0 + 0, 5.0 + 0.25, 7.5 + 0.5, 10.0 + 1.0,
25.0 + 5.0, 37.5 + 10.0, 50.0 + 15.0, 63.5 + 20.0, and 75.0 + 25.0 µg mL^{-1}.
Plots of the anodic peak potential vs. concentration of CoQ10 (■) and
ALA (●) (inset). Measurements were performed under optimal conditions.

In addition, the performance of the MnO$_2$/SPGE was compared to

the other previous electrodes for the detection of CoQ10 and ALA, as shown in table.

4.1. The data show that the proposed sensor provides a lower LOD than those

obtained from the glassy carbon [79], FTO [80], and platinum [45] electrodes. However,

some research studies that used other modified electrodes showed low LODs [81, 82].

Nevertheless, those electrodes could not be used for the simultaneous detection of

CoQ10 and ALA. Moreover, the measurements and modifications were performed on

high-cost commercial electrodes, such as platinum [45], silver [83], glassy carbon [79,

84], pyrolytic graphite [82] and tin oxide [80] electrodes.   Even though, higher LODs

were obtained from this work. However, the LODs are acceptable for the simultaneous detection of CoQ10 and ALA in supplements, which is the key idea of this work. Therefore, the advantages of the proposed sensor are based on lower toxicity, disposability, low-cost, simple fabrication, wide linearity, and good sensitivity. Moreover, this sensor exhibits comparable or better performance compared to the sensors in some previous studies. To our best knowledge, many researchers developed methods for the determination of either CoQ10 or ALA, and no research reported the simultaneous detection of CoQ10 and ALA. It is notable that our work is the first proposed for the simultaneous determination of CoQ10 and ALA. Additionally, this modified electrode can be an alternative electrode as a sensor for the simultaneous detection of CoQ10 and ALA.

Table 4.1 *Comparison of the reported electrodes and the proposed sensor for the determination of CoQ10 and ALA (where CMCPE is a carbon paste electrode modified with nickel (II)-cyclohexylbutyrate; FTO is a fluorine-doped tin oxide electrode, and PG/CoPc is a pyrolytic graphite electrode modified with cobalt phthalocyanine).*

Electrode	Method	Analyte	linearity (μM)	LOD (μM)	Ref.
Glassy carbon	SWV	CoQ10	0.50 to 700	0.10	[81]
Mercury	Polarography	CoQ10	0.06 to 0.25	0.01	[82]
Glassy carbon	DPV	CoQ10	120 to 1000	14	[83]
Silver	DPV	CoQ10	0.10 to 1000	0.033	[84]
CMCPE	LSASV (linear sweep ASV)	ALA	0.008 to 0.30	0.004	[85]
Glassy carbon	SWV	ALA	lower than 75	1.80	[79]
FTO	SWV	ALA	5 and 500	3.68	[80]
Platinum	DPV	ALA	10 to 800	13.15	[45]

Electrode	Method	Analyte	linearity (µM)	LOD (µM)	Ref.
PG/CoPc	Amperometry	ALA	1.30 to 100	0.015	[67]
MnO$_2$/SPGE	SWV	CoQ10	2.3 to 87 (2.0 to 75 µg mL^{-1})	0.65 (0.56 µg mL^{-1})	This work
		ALA	1.40 to 120 (0.3 to 25 µg mL^{-1})	0.42 (0.088 µg mL^{-1})	

4.1.4.7 Repeatability and Reproducibility

The repeatability and reproducibility of the proposed sensor were estimated in terms of the relative standard deviation (%RSD) of 10 measurements for repeatability and 10 different sensors for reproducibility in a mixture solution of 25 and 0.5 µg mL^{-1} of CoQ10 and ALA, respectively. The repeatability and reproducibility of both compounds were lower than 2.7% and 5.0%, respectively. These results showed that the MnO$_2$/SPGE was successfully applied for the simultaneous determination of CoQ10 and ALA with good sensitivity and repeatability. Moreover, the low cost of production of this sensor enhances its disposability.

4.1.4.8 Interferences study

To evaluate the selectivity towards CoQ10 and ALA, the tolerance limit is used as an evaluation method, which is estimated to be less than 5% of the error. Some possible interferents, such as vitamins A, B$_1$, B$_2$, B$_9$, C, D$_2$, D$_3$, E, K$_1$, and K$_2$, glutathione, Mg^{2+}, Ca^{2+}, and Zn^{2+} were tested. One-thousand-fold mass ratios of vitamins B$_2$, B$_9$, D$_2$, D$_3$, and E; and 1-fold mass ratios of vitamins A, K$_1$, and K$_2$ did not interfere with the analysis of CoQ10. For the analysis of ALA, a 1000-fold mass ratio of glutathione; 100-fold mass ratios of vitamins B$_2$, K$_1$, and K$_2$, Mg^{2+}, and Ca^{2+}; 10-fold mass ratios of vitamins C, D$_2$, and D$_3$, and Zn^{2+}; and 1-fold mass ratios of vitamins B$_9$ and E did not cause changes in the anodic peak current obtained from ALA alone. However, vitamin B$_1$ strongly interfered with the analysis of both CoQ10 and ALA. The

summary of the tolerance ratios of interfering compounds in the electrochemical determination of CoQ10 and ALA is shown in table 4.2. From these results, although some compounds in a multivitamin dietary supplement interfered with the detection of CoQ10 and ALA, most CoQ10 and ALA dietary supplements did not contain these compounds. Therefore, this sensor demonstrates good effective performance for the simultaneous determination of CoQ10 and ALA.

Table 4.2 Tolerance ratio of interfering substances in the determination of 50 µg mL^{-1} of CoQ10 and 1 µg mL^{-1} of ALA (n=3).

Interferences	Tolerance ratio ($W_{interference}/W_{analyte}$)	
	CoQ10	ALA
Vitamin A	1	10
Vitamin B$_1$	-	0.5
Vitamin B$_2$	1000	100
Vitamin B$_9$	1000	1
Vitamin C	-	10
Vitamin D$_2$	1000	10
Vitamin D$_3$	1000	10
Vitamin E	1000	1
Vitamin K$_1$	1	100
Vitamin K$_2$	1	100
Glutathione	-	1000
Mg^{2+}	-	100
Ca^{2+}	-	100
Zn^{2+}	-	10

4.1.4.9 Application to real samples

To verify the applicability of the MnO_2/SPGE, CoQ10 and ALA in supplementary formulations from local Thailand supermarkets were analyzed. The standard addition method was used to investigate the practical applicability of the sensor. The samples were prepared as per the previous description. The contents of CoQ10 and ALA were determined from the calibration curve. In terms of consistency, the RSD (n = 3) for the determined content of CoQ10 and ALA in all dietary supplements was lower than 5%. For the quantitative evaluation, three dietary supplement samples were tested. The results showed that the experimentally calculated values correspond quite well with the labeled value of the manufacturer's claim in all examined dietary supplements. In the standard addition, the estimated values were in good agreement with the added amount of CoQ10 and ALA, and a recovery experiment was used to evaluate the accuracy of the sensor (table. 4.3). The RSDs and recoveries were found in the ranges of 0.4–4.8% and 95.2–103.2%, respectively. Thus, the results clearly indicated the ability to measure CoQ10 and ALA simultaneously in dietary supplements.

Table 4.3 Determination of CoQ10 and ALA in different samples (n = 3) by the developed sensor reported here.

Samples	Added (µg mL⁻¹)		Expected (µg mL⁻¹)		Found (µg mL⁻¹)		%Recovery		%RSD	
	CoQ10	ALA	CoQ10	ALA	CoQ10	ALA	CoQ10	ALA	CoQ10	ALA
	0	0	10.0	0	9.78±0.30	ND	-	-	3.1	-
	15.0	5.0	25.0	5.0	25.0±1.19	4.95±0.09	100.3	99.00	4.8	1.8
1	27.5	10.0	37.5	10.0	37.9±0.44	9.82±0.22	101.5	98.20	1.2	2.2
	40.0	15.0	50.0	15.0	49.6±0.63	14.3±0.25	99.00	95.20	1.3	1.8
	52.5	20.0	67.5	20.0	67.8±1.01	20.6±0.07	99.20	100.5	0.4	1.5
	0	0	0	1.0	ND	1.05±0.04	-	-	-	3.6
	25.0	4.0	25.0	5.0	25.9±1.17	5.06±0.08	103.4	101.4	4.5	1.6
2	37.5	9.0	37.5	10.0	37.6±0.98	9.81±0.18	100.3	97.90	2.6	1.8
	50.0	14.0	50.0	15.0	50.9±1.00	14.3±0.27	101.9	99.20	2.0	1.8
	67.5	19.0	67.5	20.0	68.0±0.72	20.6±0.17	101.8	103.2	1.1	0.8
	0	0	5.0	5.0	5.06±0.17	4.92±0.23	-	-	3.4	4.4
	20.0	5.0	25.0	10.0	25.5±0.61	9.99±0.18	102.7	99.80	3.4	1.8
3	32.5	10.0	37.5	15.0	37.8±0.53	15.1±0.36	101.0	100.7	1.4	2.4
	45.0	15.0	50.0	20.0	50.2±1.21	20.5±0.29	100.5	103.2	2.4	1.4
	62.5	20.0	67.5	25.0	68.1±0.30	25.1±0.20	100.9	100.6	0.4	0.8

4.2 UHPLC-ED for the determination of DTCs

The development of an electrochemical sensor for using as working electrode in UHPLC-ED system was proposed in this section. DTCs are organosulfur compounds that have been used in agriculture as fungicides in foliage vegetable and fruit resulting in their release into the environment causing the contamination in food and water. Therefore, AuNP/SPCE was developed as working electrode for simultaneous determination of thiram, disulfiram, and *N,N*-diethyl-*N',N'*-dimethylthiuram disulfide (DEDMTDS), their derivative compound after their separation with UHPLC system.

4.2.1 Morphological characterization of AuNP/SPCE

Gold (III) solution was used to generate the AuNPs on the electrode surface by electrodeposition. The surface morphology of bare SPCE and AuNP/SPCE was investigated using scanning electron microscope (SEM) as shown in figure 4.16, respectively. After the modification, the well-dispersed of gold particles in nanoscale was observed (figure 4.16 right). The distribution of AuNPs on the electrode surface led to increase the surface area and improved the electrochemical sensitivity of the modified electrode.
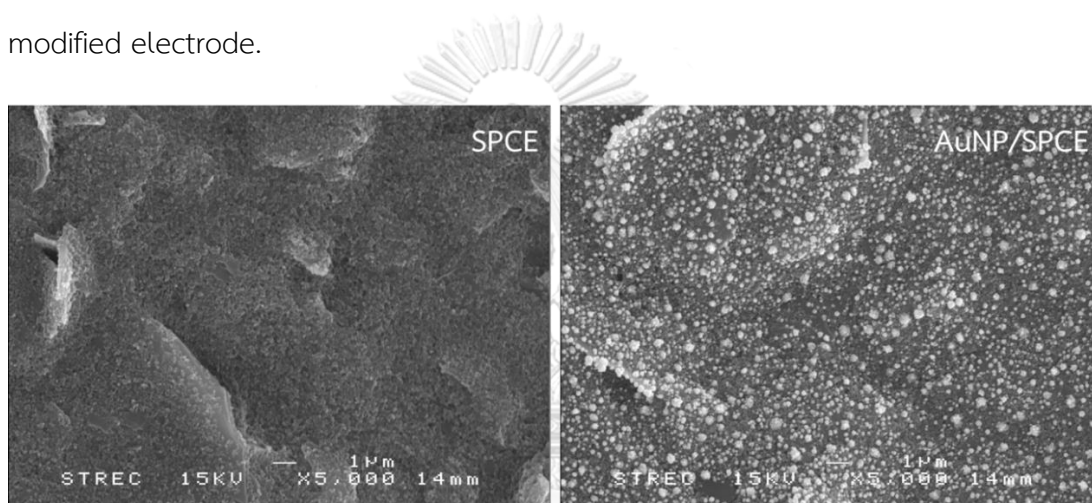
Figure 4.16 *SEM images of bare SPCE and AuNP/SPCE prepared by electrodeposition of 10 mM gold (III) solution at an applied potential of -0.6 V for 50 s.*

4.2.2 Optimization of electrodeposition of AuNPs on SPCE

For the electrode modification using electrodeposition technique, the deposition potential and deposition time were optimized because these factors can affect the analytical results. First, thiram was selected as the representative compounds because it is the best electrochemically active species at bare carbon electrode. Therefore, it is easy to observe the signal obtained from modified and unmodified electrode. To obtain the optimal condition of AuNP/SPCE, the dependence of deposition potential, deposition time, and concentration of gold (III) solution were studied using CV, and the relationship between the studied parameter and current response of thiram was plotted. The deposition potential was studied in

the range of -1.0 to 0.2 V. The current signal of thiram was initially increased as the function of deposition potential from -1.0 to -0.6 V and then decreased (figure 14.6A). For the deposition time, the current signal of thiram increased from 10 s to 50 s and then decreased (figure 14.6B). Lastly, the concentration of gold (III) solution was optimized the range of 1-20 mM. The highest current signal was observed at concentration of 10 mM. Therefore, the deposition potential of -0.6 V, the deposition time of 50 s, and the concentration of gold (III) solution of 10 mM were chosen as optimal parameters for modification of AuNPs onto the electrode surface.

4.2.3 Electrochemical behavior of thiram at AuNP/SPCE

As mentioned above, thiram is the best electrochemically active species. Thus, it was used as the representative of DTCs to study the electrochemical response. The CV of 10 µg mL^{-1} of thiram obtained from bare SPCE and AuNP/SPCE at the potential range of 0.0 to 1.4 V was shown in figure 4.18. From CV results, the anodic current of thiram was investigated, and the current at AuNP/SPCE was significantly higher than the current obtained from bare SPCE due to the distribution of AuNPs on the electrode surface. AuNPs on the electrode surface can enhance electron transfer and also improve the electrochemical determination of DTCs. For the comparison of oxidation current density between AuNP/SPCE and bare SPCE (figure 4.18B), the higher current density about 9 times was observed at AuNP/SPCE. This result indicated that the AuNP/SPCE can be assuring electrode for the detection of thiram, disulfiram, and DEDMTDS. Therefore, this modified electrode can be an alternative electrode for using as working electrode with the advantages of low-cost material, simple fabrication and high sensitivity in case of detection DTCs.
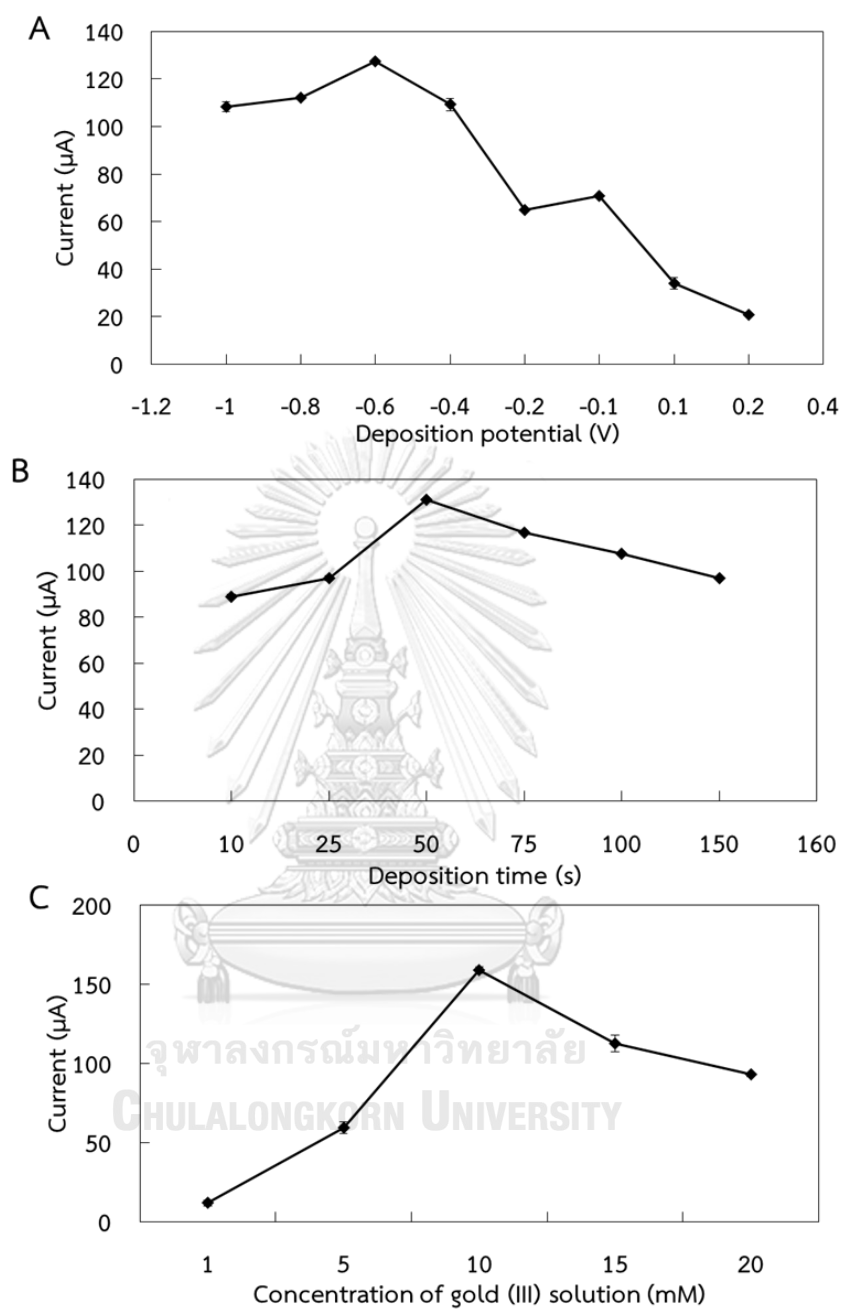
Figure 4.17 *Effect of the deposition potential (A), deposition time (B), and concentration of gold (III) solution (C) on thiram at AuNP/SPCE. Data are shown as the mean ± SD derived from three replicates.*
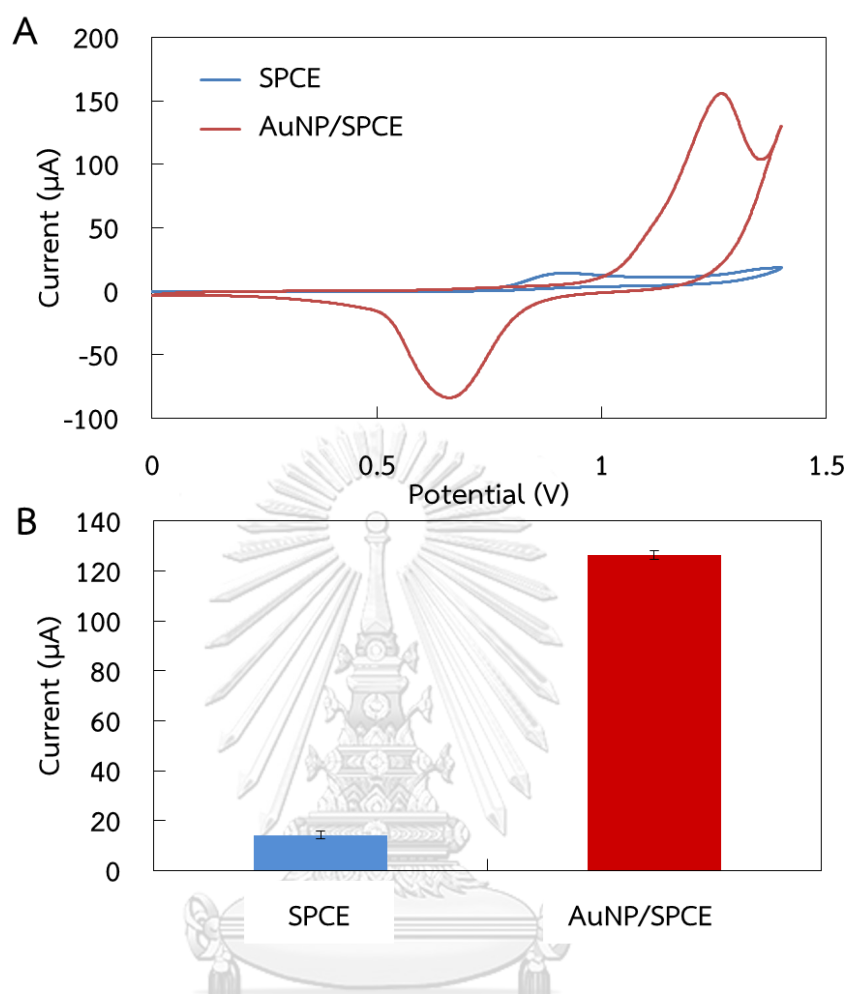
Figure 4.18 *Cyclic voltammogram (A) of thiram at the AuNP/SPCE (red line) compared to bare SPCE (blue line) and comparison of oxidation current density (B) between AuNP/SPCE (red rod) and bare SPCE (blue rod) vs. Ag/AgCl at the concentration of 10 µg mL^{-1} in 55:45 of 0.05 M phosphate solution pH 5: acetonitrile, scan rate 100 mV s^{-1}.*

4.2.4 Separation of DTCs using UHPLC

In this work, C18 column was used to separate thiram, DEDMTDS, and disulfiram by isocratic elution. The effect of percentage of acetonitrile used in the mobile phase on the retention characteristics was first evaluated. When the percentage of acetonitrile ≤ 40 was used, the separation time was higher than 20 min and peak broadening of disulfiram was observed. On the other hand, at higher content of

acetonitrile in mobile phase, the current signals of thiram, DEDMTDS, and disulfiram were decreased due to the low of diffusion coefficient with changing ionic strength of the medium. Therefore, the acetonitrile of 45% was selected as compromise to achieve the completely separated them within 6 min with good sensitivity. In addition, 0.05 M phosphate buffer solution (pH 5) was chosen as the electrolyte solution because the high concentration of salt in buffer solution was not suitable for the UHPLC system. The chromatogram for the separation of standard mixture solution was shown in figure 4.19. The retention time of thiram, DEDMTDS, and disulfiram was 1.5, 2.6, and 5.4 min, respectively. The peaks width were 11.6 s for thiram, 14.2 s for DEDMTDS, and 18.8 s for disulfiram. Therefore, this proposed system offers the rapid time for separating DTCs.
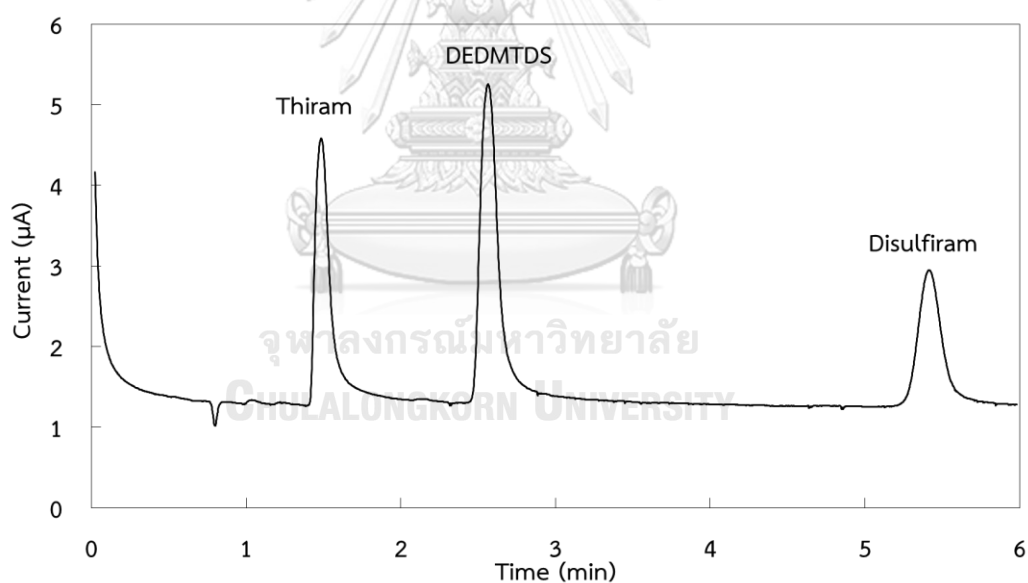
Figure 4.19 *Representative UHPLC-ED chromatogram of 12 μg mL^{-1} of thiram, DEDMTDS, and disulfiram in a mobile phase (55:45 of 0.05M phosphate solution (pH 5): acteonitrile), the detection potential of 1.2 V vs. Ag/AgCl using AuNP/SPCE, the injection volume of 50 μL, and the flow rate of 1.5 mL min^{-1}. Chromatograms are representative of at least three independent repetitions.*

4.2.5 Injection volume

The injection loop of studied UHPLC system was available in the range of 0.1-50 µL. Therefore, the injection volume was investigated because it effected to the sensitivity and band broadening of the analytes. The injection volume was studied at 10, 20, 30, 40, and 50 µL in 55:45 of 0.05M phosphate solution (pH 5): acteonitrile, the detection potential of 1.2 V vs. Ag/AgCl using AuNP/SPCE, and the flow rate of 1.5 mL min^{-1}. Figure 4.20 observed that the current responses increased with increasing of injection volume and the highest current response was observed at injection volume of 50 µL. Considering to band broadening, the increasing of injection volume trended to high band broadening. However, as shown in chromatogram of figure 4.19, it was displayed that at high injection volume of 50 µL, the sharp peak without band broadening still observed. Therefore, the injection volume of 50 µL was selected to use as optimal condition to attain the high sensitivity.
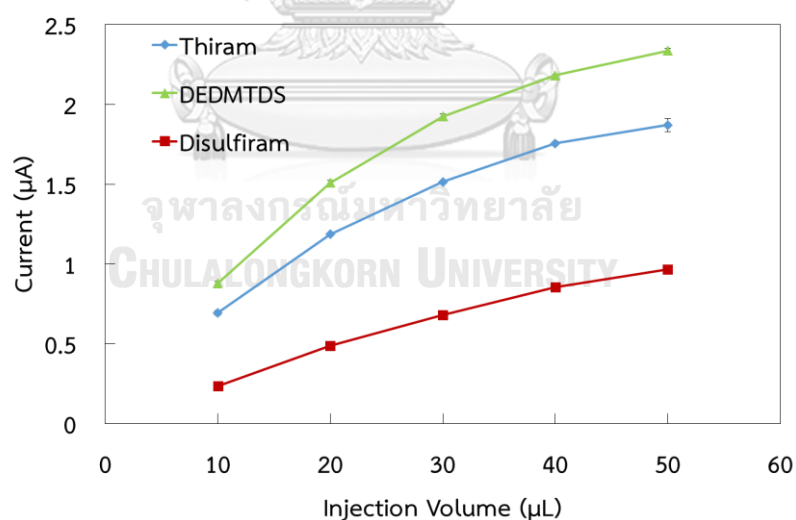
Figure 4.20 *Effect of the injection volume on thiram (blue line), DEDMTDS (green line), disulfiram (red line) at AuNP/SPCE. The other conditions are the same as in in Fig. 4.19. Data are shown as the mean ± 1 SD derived from three independent repetitions.*

4.2.6 Detection potential

Amperometry was used as detection technique. The applied potential was studied in the range of 0.8 to 1.4 V. The peak current after each injection at different potential was recorded corresponding to the background current. These data were plotted as a function of applied potential to obtain the hydrodynamic curves as shown in figure 4.21. The detection potentials significantly affected the oxidation current of the thiram, DEDMTDS, and disulfiram as well as the background current (figure 4.20A). Therefore, the net current after background subtraction was studied, and signal-to-background (S/B) ratios were plotted corresponding to the detection potential. It was found that the current increased when the potential increased up to 1.2 V for all compounds (figure 4.20B). Therefore, the detection potential of 1.2 V was selected as optimal detection potential for amperometric detection of thiram, DEDMTDS, and disulfiram after their separation with UHPLC.
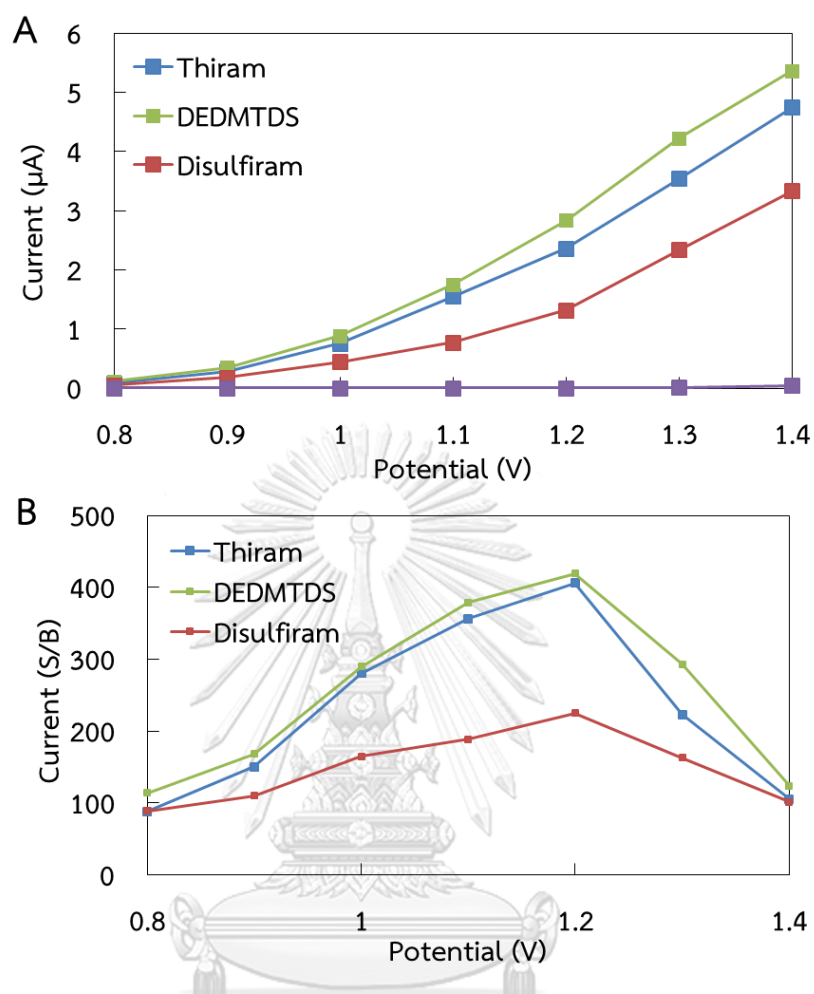
Figure 4.21 *Amperometric currents (A) at the AuNP/SPCE for a 10 μg mL^{-1} each mixture (50 μL total) of thiram and disulfiram. thiram (blue line), DEDMTDS (green line), disulfiram (red line), and background (purple line); amperometric results (B) of signal-to-background ratios. The other conditions are the same as in Fig. 4.19 Data are shown as the mean ± SD derived from three independent repetitions.*

4.2.7 Method validation

4.2.7.1 Analytical performance

The analytical performance of this proposed system was studied. The chromatogram at concentration range of 0.07 to 15 µg mL^{-1} for thiram, 0.07 to 12 µg mL^{-1} for DEDMTDS, and 0.5 to 15 µg mL^{-1} for disulfiram was shown in figure 4.22A. The calibration curve between the concentration and current response of analytes was plotted as shown in figure 4.22B. Under the optimal conditions, the linearity was observed in the range of 0.07 to 15 µg mL^{-1} for thiram, 0.07 to 12 µg mL^{-1} for DEDMTDS, and 0.5 to 15 µg mL^{-1} for disulfiram. The limit of detection (LOD) and limit of quantification (LOQ) were calculated from $3S_{bl}/S$ and $10S_{bl}/S$, where S_{bl} is the standard deviation of blank measurements ($n = 10$), and S is the sensitivity of the method or the slope of linearity. Good linearity value with $r^2 > 0.99$ was obtained. LODs and LOQs were summarized in table 4.4. In addition, when the performance of AuNP/SPCE was compared to the other previous electrodes for the detection of DTCs as shown in table 4.5. It was found that the LODs obtained from the proposed electrode were lower than using cylindrical carbon fiber [47] and graphite-poly (tetrafluoroethylene) composite electrode [49]. However, few researches used the mercury electrode to provide lower LOD than this method but the mercury is toxic [76, 86]. Therefore, the proposed electrode offers less toxicity, uncomplicated, and low cost. Additionally, the proposed electrode shows good electrocatalytic properties for DTCs detection to obtain a high electrochemical sensitivity.
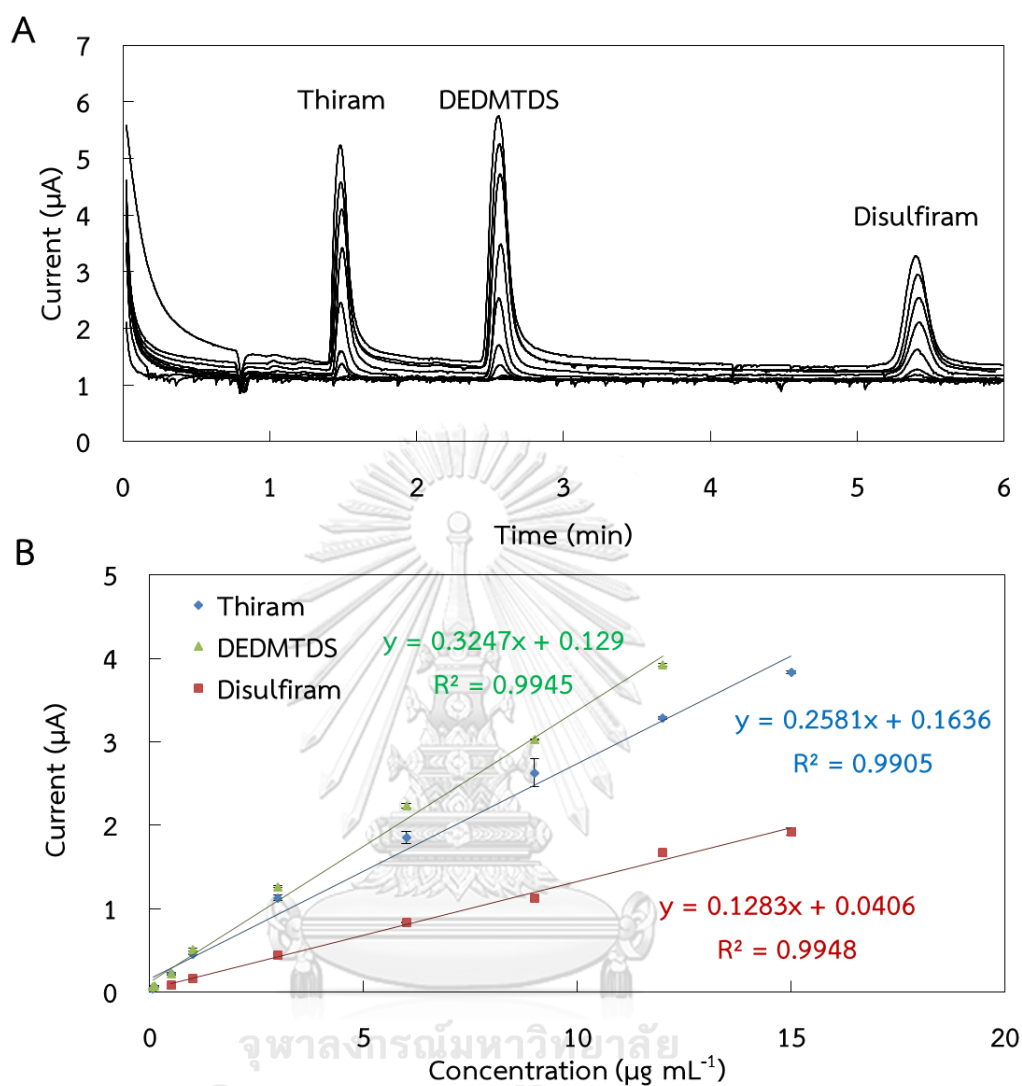
Figure 4.22 *The amperometric chromatogram (A) for different concentrations of thairam, DEDMTDS, and disulfiram (0.07 to 15 µg mL^{-1}) using AuNP/SPCE and the corresponding calibration plots (B). Measurements were performed under the optimal conditions.*

Table 4.4 Linearity, limit of detection (LOD) and limit of quantitation (LOQ) of the UHPLC-ED method (n = 3).

Analyte	Linear range (µg mL^{-1})	Slope (peak height) (µA/µg mL^{-1})	Intercept (µA)	r^2	LOD (µg mL^{-1})	LOQ (µg mL^{-1})
Thiram	0.07-15	0.2585	0.1636	0.9905	0.022	0.074
DEDMTDS	0.07-12	0.3247	0.1290	0.9945	0.023	0.076
Disulfiram	0.50-15	0.1283	0.0406	0.9948	0.165	0.551

Table 4.5 Recent report using different types of electrodes for electrochemical determination of DTCs (where CFME and HDME are cylindrical carbon fiber microelectrode and hanging mercury drop electrode, respectively).

Modified electrode	Detection method	Linearity (µg mL^{-1})	LOD (µg mL^{-1})	Analyte	Reference
CFME	SWV	0.24-144	0.10	Thiram	[47]
Teflon-graphite composite	Amperometry	2-100	0.14-1.0	Thiram and disulfiram	[49]
HDME	DPV	0.01-0.6	0.01	Ziram	[86]
HDME	SWV	0.01-0.19	0.0072	Ziram	[76]
AuNP/SPCE	Amperometry	0.07-15	0.022-0.165	Thiram, DEDMTDS and disulfiram	This work

4.2.7.2 Repeatability and Reproducibility

The repeatability and reproducibility of the proposed sensor were estimated in terms of the relative standard deviation (%RSD) of 40 measurements for repeatability and 6 different sensors for reproducibility at concentration of 10 µg mL^{-1}

of thiram, DEDMTDS, and disulfiram (figure 4.23). The repeatability and reproducibility of both compounds were lower than 5.0%. These results showed that the use of AuNP/SPCE for UHPLC-ED system was successfully applied for the determination of DTCs with good sensitivity and repeatability.
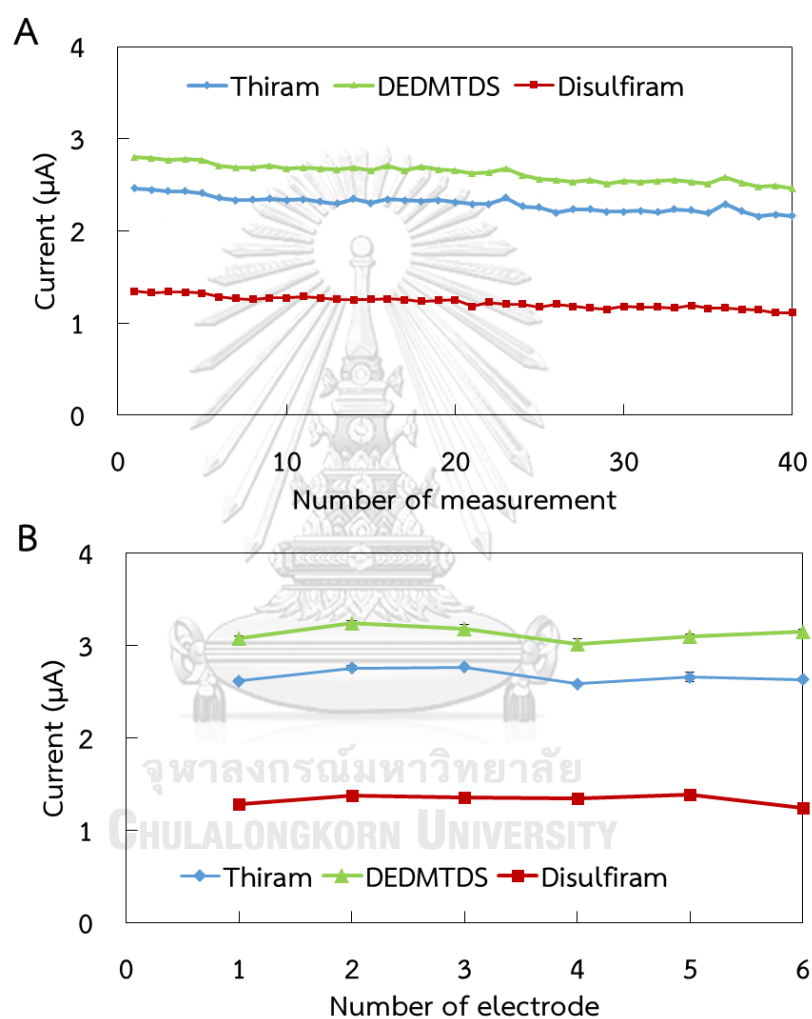
Figure 4.23 *The repeatability (A) and reproducibility (B) of AuNP/SPCE in UHPLC system under the optimal conditions.*

4.2.7.3 Application to real samples

To assess the applicability of the proposed method, target compounds in samples from local supermarkets were investigated. The proposed

method was applied for the detection of three different samples, including apple, grape, and lettuce. The standard addition method was chosen to investigate the reliability of this proposed system. The precision of the analytical process was evaluated by the repeatability of the process. The spiked concentrations in the dynamic linearity between 1 to 15 µg mL^{-1} were studied to calculate the RSD percentage. The summary of intra- and inter- day precision, and recovery that obtained from the proposed method was shown in table 4.6. The RSDs and recoveries of intra-day were found in the range of 0.1 - 3.7% and 94.3 - 108.8%, respectively, while the inter-day RSDs and recoveries were found in the range of 0.1 - 5.7% and 95.8 - 107.7%, respectively. Therefore, this method is an alternative and suitable for rapid separation and simultaneous determination of DTCs.

To validate the proposed method, UHPLC-UV was used as a standard method to compare the acceptable and reliable. The results obtained from UHPLC-ED and UHPLC-UV were compared by a paired *t*-test at the 95% confidence for three samples that spiked with three standard concentrations (1, 6, and 12 µg mL^{-1} to represent the low, medium, and high level, respectively). The critical *t*-value was significantly higher than calculated *t*-values between two assays. From the results as shown in table 4.7, the calculated *t*-values of three concentrations were found in the range of 0.243 to 3.029 and lower than critical *t*-values (4.303). It can be concluded that there is no significant difference between UHPLC–ED and conventional UHPLC–UV method. Therefore, the results obtained from UHPLC coupled with amperometric detection using AuNP/SPCE is acceptable and reliable for applying to simultaneous determination of DTCs in food.

Table 4.6 The intra- and inter-precisions and recoveries of the UHPLC-ED method (n = 3).

Samples	Analyte	Intra-day	Inter-day

Samples	Spiked level (µg mL^{-1})	Analyte	Recovery (%)	RSD (%)	Recovery (%)	RSD (%)
Apple	1	Thiram	97.10	1.1	99.00	3.7
		DEDMTDS	101.5	0.2	100.6	1.0
		Disulfiram	104.1	3.3	100.6	4.9
	3	Thiram	102.7	0.1	100.7	5.7
		DEDMTDS	102.7	0.3	102.0	1.4
		Disulfiram	108.5	0.3	103.3	4.4
	6	Thiram	109.0	0.9	104.0	4.4
		DEDMTDS	109.2	1.3	104.8	4.0
		Disulfiram	97.40	0.6	98.10	2.4
	9	Thiram	109.3	0.6	107.0	1.8
		DEDMTDS	109.2	0.3	107.7	1.7
		Disulfiram	103.6	0.6	104.2	4.9
	12	Thiram	101.5	0.2	101.9	0.7
		DEDMTDS	106.5	0.4	102.5	3.4
		Disulfiram	102.6	0.2	101.4	2.5
Grape	1	Thiram	100.1	0.2	102.3	3.3
		DEDMTDS	101.5	2.3	99.70	1.9
		Disulfiram	108.8	0.7	104.2	7.7
	3	Thiram	103.9	0.6	100.7	2.8
		DEDMTDS	105.2	0.2	102.2	2.5
		Disulfiram	107.9	0.3	104.7	2.7
	6	Thiram	103.5	1.0	103.3	2.9
		DEDMTDS	98.90	1.5	102.6	4.9
		Disulfiram	98.40	0.2	100.6	3.4
	9	Thiram	107.4	0.5	107.2	0.1
		DEDMTDS	100.4	1.0	102.6	4.7
		Disulfiram	97.50	0.4	98.00	2.6
Samples		Analyte	Intra-day		Inter-day	

	Spiked level ($\mu g\ mL^{-1}$)		Recovery (%)	RSD (%)	Recovery (%)	RSD (%)
Grape	12	Thiram	106.1	0.4	103.3	2.4
		DEDMTDS	102.1	0.7	101.9	0.8
		Disulfiram	100.5	0.3	100.9	5.0
Lettuce	1	Thiram	98.80	0.8	101.9	3.4
		DEDMTDS	102.6	1.4	101.6	1.4
		Disulfiram	102.4	1.7	100.8	4.3
	3	Thiram	105.1	0.9	99.70	4.8
		DEDMTDS	102.4	1.0	103.4	3.6
		Disulfiram	104.1	1.9	99.0	4.9
	6	Thiram	98.90	0.2	96.70	4.4
		DEDMTDS	98.70	0.5	101.7	4.7
		Disulfiram	106.0	0.5	101.3	4.1
	9	Thiram	108.0	1.8	105.8	2.5
		DEDMTDS	100.5	3.7	101.8	3.8
		Disulfiram	103.1	0.8	102.6	4.2
	12	Thiram	102.6	1.3	101.6	2.5
		DEDMTDS	100.5	2.9	101.1	0.8
		Disulfiram	100.1	0.6	102.5	2.3

Table 4.7 Determination of DTCs level in different samples (n = 3) by the traditional UHPLC-UV method and the developed UHPLC-ED method reported here.

Samples	Spiked level (μg mL^{-1})	Analyte	Amount found (μg mL^{-1}) (x ± SD)				% recovery	
			UHPLC-ED		UHPLC-UV		UHPLC-ED	UHPLC-UV
Apple	1	Thiram	0.990	± 0.04	1.02	± 0.03	99.0	102.2
		DEDMTDS	1.01	± 0.01	1.01	± 0.02	100.6	101.1
		Disulfiram	0.980	± 0.05	1.01	± 0.05	97.5	100.6
	6	Thiram	6.24	± 0.27	5.79	± 0.26	104.0	96.50
		DEDMTDS	6.15	± 0.10	6.12	± 0.19	102.5	101.9
		Disulfiram	5.89	± 0.14	5.72	± 0.13	98.10	95.40
	12	Thiram	12.2	± 0.50	11.9	± 0.36	101.9	99.20
		DEDMTDS	12.3	± 0.49	11.8	± 0.62	102.5	98.10
		Disulfiram	12.4	± 0.25	12.3	± 0.23	103.5	102.1
Grape	1	Thiram	1.02	± 0.03	1.02	± 0.02	102.3	102.2
		DEDMTDS	1.01	± 0.02	1.00	± 0.01	100.8	99.70
		Disulfiram	1.04	± 0.08	0.99	± 0.01	104.2	98.70
	6	Thiram	6.20	± 0.18	5.92	± 0.19	103.3	98.70
		DEDMTDS	6.15	± 0.30	6.01	± 0.22	102.6	100.1
		Disulfiram	6.04	± 0.21	6.04	± 0.12	100.6	100.7
	12	Thiram	12.2	± 0.34	12.1	± 0.41	101.4	100.8
		DEDMTDS	12.2	± 0.60	12.0	± 0.60	101.9	100.0
		Disulfiram	12.4	± 0.41	12.3	± 0.20	103.3	102.5

Samples	Spiked level (μg mL^{-1})	Analyte	Amount found (μg mL^{-1}) ($x \pm SD$)				% recovery	
			UHPLC-ED		UHPLC-UV		UHPLC-ED	UHPLC-UV
Lettuce	1	Thiram	1.02	± 0.03	0.98	± 0.03	101.9	98.10
		DEDMTDS	1.02	± 0.01	1.02	± 0.04	102.2	101.6
		Disulfiram	1.01	± 0.04	0.97	± 0.09	100.8	97.10
	6	Thiram	5.80	± 0.26	5.75	± 0.25	96.70	95.80
		DEDMTDS	6.10	± 0.28	5.99	± 0.22	101.7	99.80
		Disulfiram	6.08	± 0.25	5.99	± 0.13	101.3	99.80
	12	Thiram	12.2	± 0.41	12.0	± 0.27	101.6	99.90
		DEDMTDS	12.1	± 0.47	12.0	± 0.62	101.1	99.50
		Disulfiram	12.3	± 0.20	12.1	± 0.35	102.5	100.9
Paired two-tail test	t values (at 1 μg mL^{-1})	Thiram			0.104			
		DEDMTDS			0.898			
		Disulfiram			0.792			
	t values (at 6 μg mL^{-1})	Thiram			2.293			
		DEDMTDS			3.029			
		Disulfiram			1.747			
	t values (at 12 μg mL^{-1})	Thiram			2.808			
		DEDMTDS			2.989			
		Disulfiram			-0.243			
	t critical				4.303			

CHAPTER V:

CONCLUSION

5.1 Conclusions

The development of electrochemical sensors for pharmaceutical and environmental applications was presented. Firstly, the simultaneous determination of CoQ10 and ALA using a MnO_2-modified SPGE was proposed. The incorporating of MnO_2 into the SPGE greatly improved the analytical performance of the sensor towards the oxidation of CoQ10 and ALA. This improvement was attributed to the fascinating electron transfer and the increased electroactive surface area. This proposed sensor provides a simple, inexpensive, and a disposable electrochemical sensor that has the potential to be used as an alternative sensor for the determination of CoQ10 and ALA in food and supplementary samples.

In addition, the electrochemical sensor was integrated with other analytical methods for the rapid and selective detection of pesticide residues in environmental and foods. AuNP/SPCE was firstly developed for the determination of thiram, disulfiram, and DEDMTDS after the separation by UHPLC technique. The rapid separation within 6 min, and the high current response signal were obtained at AuNP/SPCE. This attributed to the strong catalytic property of the used AuNPs on the electrode surface towards the sulfur-containing compounds of DTCs. The main advantages of this developed AuNP/SPCE sensor are high sensitivity, stability and reproducibility. The fabrication of this sensor is also simple. Moreover, the obtained results using this proposed UHPLC-ED system is acceptable and reliable in comparison to those the standard UHPLC-UV method. The results were compared using a paired t-test value without any derivatization. Ultimately, the UHPLC coupled with AuNP/SPCE amperometry was successfully applied to detect the analyte of interest in practical samples. This proposed electrode could be employed as a novel or an alternative electrode in UHPLC-ED system for the simultaneous determination of DTCs in fruits and vegetables.

This dissertation shows that the electrochemical technique is the powerful tool to be used as a sensor for both qualitative and quantitative analysis. The use of SPE can successfully miniaturize the conventional electrochemical cell. This type of electrode can be easily and inexpensively prepared by in-house screen printing technique which enables mass-production of disposable sensors on flexible substrates. The sensitivity of detection can simply improve by simple modification of electrode using appropriate nanomaterials. Finally, the use of this developed electrochemical sensor for real samples application has been evaluated, and the good performance was obtained.

5.2 Future perspective

As mentioned above, the electrochemical sensor offers high sensitivity, selectivity, and low-cost detection; it is suitable for inventing as a powerful sensor. Moreover, an electrochemical sensor can also easily combine with other analytical instruments for a specific propose. Due to its versatility and flexibility, a variety of chemical sensor could be developed based on electrochemical technique for applying in diverse samples in the future.

REFERENCES

[1]   Jadon, N., Jain, R., Sharma, S., and Singh, K. Recent trends in electrochemical sensors for multianalyte detection – A review. Talanta 161 (2016): 894-916.

[2]   Ronkainen, N.J., Halsall, H.B., and Heineman, W.R. Electrochemical biosensors. Chemical Society Reviews 39(5) (2010): 1747-1763.

[3]   Stradiotto, N.R., Yamanaka, H., and Zanoni, M.V.B. Electrochemical sensors: a powerful tool in analytical chemistry. Journal of the Brazilian Chemical Society 14 (2003): 159-173.

[4]   Thiyagarajan, N., Chang, J.-L., Senthilkumar, K., and Zen, J.-M. Disposable electrochemical sensors: A mini review. Electrochemistry Communications 38 (2014): 86-90.

[5]   Li, M., Li, Y.-T., Li, D.-W., and Long, Y.-T. Recent developments and applications of screen-printed electrodes in environmental assays—A review. Analytica Chimica Acta 734 (2012): 31-44.

[6]   Taleat, Z., Khoshroo, A., and Mazloum-Ardakani, M. Screen-printed electrodes for biosensing: a review (2008–2013). Microchimica Acta 181(9) (2014): 865-891.

[7]   Albareda-Sirvent, M., Merkoçi, A., and Alegret, S. Configurations used in the design of screen-printed enzymatic biosensors. A review. Sensors and Actuators B: Chemical 69(1) (2000): 153-163.

[8]   Honeychurch, K.C. and Hart, J.P. Screen-printed electrochemical sensors for monitoring metal pollutants. TrAC Trends in Analytical Chemistry 22(7) (2003): 456-469.

[9]   Donten, M. and Stojek, Z. Nanoparticles and Nanostructured Materials Used in Modification of Electrode Surfaces. in Functional Nanoparticles for Bioanalysis, Nanomedicine, and Bioelectronic Devices Volume 1, pp. 313-325: American Chemical Society, 2012.

[10]   Akanda, M.R., Sohail, M., Aziz, M.A., and Kawde, A.-N. Recent Advances in Nanomaterial-Modified Pencil Graphite Electrodes for Electroanalysis. Electroanalysis 28(3) (2016): 408-424.

[11]   Wang, J. Nanomaterial-based electrochemical biosensors. Analyst 130(4) (2005): 421-426.

[12]   Zeng, Y., Zhu, Z., Du, D., and Lin, Y. Nanomaterial-based electrochemical biosensors for food safety. Journal of Electroanalytical Chemistry 781 (2016): 147-154.

[13]   Bollella, P., et al. Beyond graphene: Electrochemical sensors and biosensors for biomarkers detection. Biosensors and Bioelectronics 89 (2017): 152-166.

[14]   Mehmeti, E., Stanković, D.M., Chaiyo, S., Švorc, Ľ., and Kalcher, K. Manganese dioxide-modified carbon paste electrode for voltammetric determination of riboflavin. Mikrochimica Acta 183 (2016): 1619-1624.

[15]   Xu, B., Ye, M.-L., Yu, Y.-X., and Zhang, W.-D. A highly sensitive hydrogen peroxide amperometric sensor based on MnO_2-modified vertically aligned multiwalled carbon nanotubes. Analytica Chimica Acta 674(1) (2010): 20-26.

[16]   Anu Prathap, M.U., Satpati, B., and Srivastava, R. Facile preparation of polyaniline/MnO_2 nanofibers and its electrochemical application in the simultaneous determination of catechol, hydroquinone, and resorcinol. Sensors and Actuators B: Chemical 186 (2013): 67-77.

[17]   Fernández, C., Reviejo, A.J., and Pingarrón, J.M. Development of graphite-poly(tetrafluoroethylene) composite electrodes Voltammetric determination of the herbicides thiram and disulfiram. Analytica Chimica Acta 305(1) (1995): 192-199.

[18]   Agüí, L., Peña-Farfal, C., Yáñez-Sedeño, P., and Pingarrón, J.M. Electrochemical determination of homocysteine at a gold nanoparticle-modified electrode. Talanta 74(3) (2007): 412-420.

[19]   Averill, B.A. and Eldredge, P. Describing electrochemical cells. 2012, Flat World Education, Inc.

[20]   Bard, A.J. and Faulkner, L.R. Electrochemical Methods: Fundamentals and Applications, ed. 2. JOHN WILEY & SONS, INC., 2001.

[21]   Gladysz, J. and Michl, J. Electrochemistry - An Introduction. Chemical Reviews 90(5) (1990): 689-689.

[22]   Aikens, D.A. Electrochemical methods, fundamentals and applications. Journal of Chemical Education 60(1) (1983): A25.

[23]   Bard, A.J. Fundamentals of analytical chemistry (Skoog, Douglas A.; West, Donald M.). Journal of Chemical Education 40(11) (1963): 614.

[24]   Langhus, D.L. Analytical Electrochemistry, 2nd Edition (Wang, Joseph). Journal of Chemical Education 78(4) (2001): 457.

[25]   Engstron, R.C. Quantitative chemical analysis; second edition (Harris, Daniel C.). Journal of Chemical Education 65(5) (1988): A140.

[26]   Renedo, O.D., Alonso-Lomillo, M.A., and Martínez, M.J.A. Recent developments in the field of screen-printed electrodes and their related applications. Talanta 73(2) (2007): 202-219.

[27]   Novoselov, K.S., et al. Electric Field Effect in Atomically Thin Carbon Films. Science 306(5696) (2004): 666-669.

[28]   Geim, A.K. and Novoselov, K.S. The rise of graphene. Nature Materials 6 (2007): 183.

[29]   Hernández-Santos, D., González-García, M.B., and García, A.C. Metal-Nanoparticles Based Electroanalysis. Electroanalysis 14(18) (2002): 1225-1235.

[30]   Das, M., Shim, K.H., An, S.S.A., and Yi, D.K. Review on gold nanoparticles and their applications. Toxicology and Environmental Health Sciences 3(4) (2011): 193-205.

[31]   Dong, M.W. and Zhang, K. Ultra-high-pressure liquid chromatography (UHPLC) in method development. TrAC Trends in Analytical Chemistry 63 (2014): 21-30.

[32]   Fekete, S., Schappler, J., Veuthey, J.-L., and Guillarme, D. Current and future trends in UHPLC. TrAC Trends in Analytical Chemistry 63 (2014): 2-13.

[33]   Nováková, L., Solichová, D., and Solich, P. Advantages of ultra performance liquid chromatography over high-performance liquid chromatography: Comparison of different analytical approaches during analysis of diclofenac gel. Journal of Separation Science 29(16) (2006): 2433-2443.

[34]   Mortensen, S.A., et al. The Effect of Coenzyme Q10 on Morbidity and Mortality in Chronic Heart Failure: Results From Q-SYMBIO: A Randomized Double-Blind Trial. JACC: Heart Failure 2(6) (2014): 641-649.

[35]   Paliakov, E.M., Crow, B.S., Bishop, M.J., Norton, D., George, J., and Bralley, J.A. Rapid quantitative determination of fat-soluble vitamins and coenzyme Q-10 in human serum by reversed phase ultra-high pressure liquid chromatography with UV detection. Journal of Chromatography B 877(1) (2009): 89-94.

[36]   Bentinger, M., Tekle, M., and Dallner, G. Coenzyme Q – Biosynthesis and functions. Biochemical and Biophysical Research Communications 396(1) (2010): 74-79.

[37]   Román-Pizarro, V., Fernández-Romero, J.M., and Gómez-Hens, A. Automatic determination of coenzyme Q10 in food using cresyl violet encapsulated into magnetoliposomes. Food Chemistry 221 (2017): 864-870.

[38]   Souchet, N. and Laplante, S. Seasonal variation of Co-enzyme Q10 content in pelagic fish tissues from Eastern Quebec. Journal of Food Composition and Analysis 20(5) (2007): 403-410.

[39]   Packer, L., Witt, E.H., and Tritschler, H.J. Alpha-lipoic acid as a biological antioxidant. Free Radical Biology and Medicine 19(2) (1995): 227-250.

[40]   Navari-Izzo, F., Quartacci, M.F., and Sgherri, C. Lipoic acid: a unique antioxidant in the detoxification of activated oxygen species. Plant Physiology and Biochemistry 40(6) (2002): 463-470.

[41]   Siangproh, W., Rattanarat, P., and Chailapakul, O. Reverse-phase liquid chromatographic determination of α-lipoic acid in dietary supplements using a boron-doped diamond electrode. Journal of Chromatography A 1217(49) (2010): 7699-7705.

[42]   Haj-Yehia, A.I., Assaf, P., Nassar, T., and Katzhendler, J. Determination of lipoic acid and dihydrolipoic acid in human plasma and urine by high-performance liquid chromatography with fluorimetric detection. Journal of Chromatography A 870(1) (2000): 381-388.

[43]   Guo, Y., et al. Oral alpha-lipoic acid to prevent chemotherapy-induced peripheral neuropathy: a randomized, double-blind, placebo-controlled trial. Supportive Care in Cancer 22(5) (2014): 1223-1231.

[44]   Hager, K., Kenklies, M., McAfoose, J., Engel, J., and Münch, G. α-Lipoic acid as a new treatment option for Alzheimer's disease — a 48 months follow-up analysis. in, pp. 189-193. Vienna: Springer Vienna, 2007.

[45]   Marin, M., Lete, C., Manolescu, B.N., and Lupu, S. Electrochemical determination of α-lipoic acid in human serum at platinum electrode. Journal of Electroanalytical Chemistry 729 (2014): 128-134.

[46]   Gurer, H., Ozgunes, H., Oztezcan, S., and Ercal, N. Antioxidant role of α-lipoic acid in lead toxicity. Free Radical Biology and Medicine 27(1) (1999): 75-81.

[47]   Hernández-Olmos, M.A., Agüí, L., Yáñez-Sedeño, P., and Pingarrón, J.M. Analytical voltammetry in low-permitivity organic solvents using disk and cylindrical microelectrodes. Determination of thiram in ethyl acetate. Electrochimica Acta 46(2) (2000): 289-296.

[48]   Blasco, C., Font, G., and Picó, Y. Determination of dithiocarbamates and metabolites in plants by liquid chromatography–mass spectrometry. Journal of Chromatography A 1028(2) (2004): 267-276.

[49]   Fernández, C., Reviejo, A.J., Polo, L.M., and Pingarrón, J.M. HPLC-Electrochemical detection with graphite-poly (tetrafluoroethylene) electrode Determination of the fungicides thiram and disulfiram. Talanta 43(8) (1996): 1341-1348.

[50]   Rastegarzadeh, S. and Abdali, S. Colorimetric determination of thiram based on formation of gold nanoparticles using ascorbic acid. Talanta 104 (2013): 22-26.

[51]   Shaidarova, L.G., Budnikov, G.K., and Zaripova, S.A. Electrocatalytic Determination of Dithiocarbamate-Based Pesticides Using Electrodes Modified with Metal Phthalocyanines. Journal of Analytical Chemistry 56(8) (2001): 748-753.

[52]   Nohara, Y., Suzuki, J., and Kubo, H. Determination of Ubiquinone in Blood by High-Performance Liquid Chromatography with Post-Column Fluorescence Derivatization Using 2-Cyanoacetamide. Journal of Fluorescence 21(6) (2011): 2093-2100.

[53]   Franke, A.A., Morrison, C.M., Custer, L.J., Li, X., and Lai, J.F. Simultaneous analysis of circulating 25-hydroxy-vitamin D3, 25-hydroxy-vitamin D2, retinol, tocopherols, carotenoids, and oxidized and reduced coenzyme Q10 by high performance

liquid chromatography with photo diode-array detection using C18 and C30 columns alone or in combination. Journal of Chromatography A 1301 (2013): 1-9.

[54]   Mattiazzi, J., S. Pegoraro, N., R. Schaffazick, S., and Cruz, L. Validation of a RP-HPLC-UV Method for the Assay of Ubiquinone in Pracaxi Oil-core Nanocapsules. Vol. 33, 2014.

[55]   Manzi, P. and Durazzo, A. Rapid determination of coenzyme Q10 in cheese using high-performance liquid chromatography. Dairy Science & Technology 95(4) (2015): 533-539.

[56]   Martano, C., Mugoni, V., Dal Bello, F., Santoro, M.M., and Medana, C. Rapid high performance liquid chromatography–high resolution mass spectrometry methodology for multiple prenol lipids analysis in zebrafish embryos. Journal of Chromatography A 1412 (2015): 59-66.

[57]   Clementino, A. and Sonvico, F. Development and validation of a RP-HPLC method for the simultaneous detection and quantification of simvastatin's isoforms and coenzyme Q10 in lecithin/chitosan nanoparticles. Journal of Pharmaceutical and Biomedical Analysis 155 (2018): 33-41.

[58]   Montero, O., Ramírez, M., Sánchez-Guijo, A., and González, C. Determination of lipoic acid, Trolox methyl ether and tocopherols in human plasma by liquid-chromatography and ion-trap tandem mass spectrometry. Biomedical Chromatography 26(10) (2012): 1228-1233.

[59]   Gra zyna, C., Pawe l, K., and Edward, B. Determination of Lipoic Acid in the form of 2-S-pyridinium Derivative by High-performance Liquid Chromatography with Ultraviolet Detection. Current Analytical Chemistry 10(3) (2014): 320-325.

[60]   Campos, P.M., Praça, F.S.G., and Bentley, M.V.L.B. Quantification of lipoic acid from skin samples by HPLC using ultraviolet, electrochemical and evaporative light scattering detectors. Journal of Chromatography B 1019 (2016): 66-71.

[61]   Guo, C., Li, D., Liu, C., Guo, Z., and Chen, Y. Facile derivatization of ultratrace carboxylic acids in saliva for quantification by HPLC–MS/MS. Analytical and Bioanalytical Chemistry 410(18) (2018): 4293-4300.

[62]   Dorris, M.K. and Lunte, C.E. Determination of Co-Q10 in plasma samples by dual-electrode amperometric detection and liquid chromatography. <u>Analytical Methods</u> 3(1) (2011): 161-167.

[63]   Niklowitz, P., Döring, F., Paulussen, M., and Menke, T. Determination of coenzyme Q10 tissue status via high-performance liquid chromatography with electrochemical detection in swine tissues (Sus scrofa domestica). <u>Analytical Biochemistry</u> 437(1) (2013): 88-94.

[64]   Yubero, D., et al. Determination of urinary coenzyme Q10 by HPLC with electrochemical detection: Reference values for a paediatric population. <u>BioFactors</u> 41(6) (2015): 424-430.

[65]   Ferreira, A.P.M., dos Santos Pereira, L.N., da Silva, I.S., Tanaka, S.M.C.N., Tanaka, A.A., and Angnes, L. Determination of α-Lipoic acid on a Pyrolytic Graphite Electrode Modified with Cobalt Phthalocyanine. <u>Electroanalysis</u> 26(10) (2014): 2138-2144.

[66]   Stankovic, D.M., Mehmeti, E., and Kalcher, K. Development of Sensitive Analytical Approach for the Quantification of α-Lipoic Acid Using Boron Doped Diamond Electrode. <u>Analytical Sciences</u> 32(8) (2016): 847-851.

[67]   Santos Pereira, L.N.d., da Silva, I.S., Araújo, T.P., Tanaka, A.A., and Angnes, L. Fast quantification of α-lipoic acid in biological samples and dietary supplements using batch injection analysis with amperometric detection. <u>Talanta</u> 154 (2016): 249-254.

[68]   Kaur, M., Kaur, V., Malik, A.K., Verma, N., Singh, B., and Rao, A.L.J. Development of a derivative spectrophotometric method for the determination of fungicide zinc ethylenebisdithiocarbamate using sodium molybdate. <u>Journal of the Brazilian Chemical Society</u> 20 (2009): 993-998.

[69]   Gonzálvez, A., Garrigues, S., Armenta, S., and de la Guardia, M. Determination at low ppm levels of dithiocarbamate residues in foodstuff by vapour phase-liquid phase microextraction-infrared spectroscopy. <u>Analytica Chimica Acta</u> 688(2) (2011): 191-196.

[70]   Jafari, A., et al. Monitoring dithiocarbamate fungicide residues in greenhouse and non-greenhouse tomatoes in Iran by HPLC-UV. <u>Food Addit Contam Part B Surveill</u> 5(2) (2012): 87-92.

[71]   Saute, B., Premasiri, R., Ziegler, L., and Narayanan, R. Gold nanorods as surface enhanced Raman spectroscopy substrates for sensitive and selective detection of ultra-low levels of dithiocarbamate pesticides. <u>Analyst</u> 137(21) (2012): 5082-5087.

[72]   Chung, S.W.C. and Lam, C.H. Development and validation of a method for determination of residues of 15 pyrethroids and two metabolites of dithiocarbamates in foods by ultra-performance liquid chromatography–tandem mass spectrometry. <u>Analytical and Bioanalytical Chemistry</u> 403(3) (2012): 885-896.

[73]   Ringli, D. and Schwack, W. Selective determination of thiram residues in fruit and vegetables by hydrophilic interaction LC-MS. <u>Food Addit Contam Part A Chem Anal Control Expo Risk Assess</u> 30(11) (2013): 1909-17.

[74]   Han, B., Li, Y., Qian, B., He, Y., Peng, L., and Yu, H. A novel liquid chromatography detector based on a dielectric barrier discharge molecular emission spectrometer with online microwave-assisted hydrolysis for determination of dithiocarbamates. <u>Analyst</u> 143(12) (2018): 2790-2798.

[75]   da Silva, M.d.P., Procopio, J.R., and Hernández, L. ELECTROCHEMICAL DETECTION IN THE DETERMINATION OF SEVERAL DITHIOCARBAMATES BY REVERSE-PHASE LIQUID CHROMATOGRAPHY. <u>Journal of Liquid Chromatography & Related Technologies</u> 22(3) (1999): 463-475.

[76]   Qiu, P. and Ni, Y.N. Determination of ziram in vegetable samples by square wave voltammetry. <u>Chinese Chemical Letters</u> 19(11) (2008): 1337-1340.

[77]   Jian-Shan, Y., Ying, W., Wei-De, Z., Hui Fang, C., Guo Qin, X., and Fwu-Shan, S. Electrochemical functionalization of vertically aligned carbon nanotube arrays with molybdenum oxides for the development of a surface-charge-controlled sensor. <u>Nanotechnology</u> 17(15) (2006): 3994.

[78]   Ikuta, N., et al. Analysis of the enhanced stability of r(+)-alpha lipoic Acid by the complex formation with cyclodextrins. <u>Int J Mol Sci</u> 14(2) (2013): 3639-55.

[79]   Corduneanu, O., Garnett, M., and Brett, A.M.O. Anodic Oxidation of α-Lipoic Acid at a Glassy Carbon Electrode and Its Determination in Dietary Supplements. Analytical Letters 40(9) (2007): 1763-1778.

[80]   Miranda, M.P., del Rio, R., del Valle, M.A., Faundez, M., and Armijo, F. Use of fluorine-doped tin oxide electrodes for lipoic acid determination in dietary supplements. Journal of Electroanalytical Chemistry 668 (2012): 1-6.

[81]   Litescu, S.-C., David, I.-G., Radu, G.-L., and Aboul-Enein, H.Y. VOLTAMMETRIC DETERMINATION OF COENZYME Q10 AT A SOLID GLASSY CARBON ELECTRODE. Instrumentation Science & Technology 29(2) (2001): 109-116.

[82]   Yang, H.-y. and Song, J.-f. High-sensitive determination of coenzyme Q10 in iodinate–β-cyclodextrin medium by inclusion reaction and catalytic polarography. Analytical Biochemistry 348(1) (2006): 69-74.

[83]   Michalkiewicz, S. Voltammetric determination of coenzyme Q10 in pharmaceutical dosage forms. Bioelectrochemistry 73(1) (2008): 30-36.

[84]   Li, D., et al. Electrochemical Investigation of Coenzyme Q10 on Silver Electrode in Ethanol Aqueous Solution and Its Determination Using Differential Pulse Voltammetry. J Lab Autom 21(4) (2016): 579-89.

[85]   Sugawara, K., Tanaka, S., Hasebe, K., and Taga, M. Electroanalysis of lipoic acid using a carbon paste electrode modified with nickel[II]-cyclohexylbutyrate. Journal of Electroanalytical Chemistry 347(1) (1993): 393-398.

[86]   Mathew, L., Reddy, M.L.P., Rao, T.P., Iyer, C.S.P., and Damodaran, A.D. Differential pulse anodic stripping voltammetric determination of ziram (a dithiocarbamate fungicide). Talanta 43(1) (1996): 73-76.

VITA

NAME   Kanokwan Charoenkitamorn

DATE OF BIRTH   21 September 1989

PLACE OF BIRTH   Bangkok, Thailand

INSTITUTIONS ATTENDED   2011 – 2018   Ph.D., Analytical Chemistry,
Chulalongkorn University, Thailand
2015 - 2018   Ph.D., Materials Science, Japan Advanced
Institute Science and Technology, Japan
2013 – 2015   M.Sc., Materials Science, Japan Advanced
Institute Science and Technology, Japan
2007 – 2011   B.Sc., first class honor, Chemistry,
Srinakharinwirot University, Thailand

HOME ADDRESS   232 Soi Phetkasem 4, Phetkasem Rd., Bangkokyai, Bangkok,
10600 Thailand

PUBLICATION   Charoenkitamorn, K., Siangproh, W., Chailapakul, O.,
Development of gold nanoparticles modified screen-
printed carbon electrode for the analysis of thiram,
disulfiram and their derivative in food using ultra-high
performance liquid chromatography. Talanta, 132 (2015),
416–423.
Charoenkitamorn, K., Chaiyo, S., Siangproh, W.,
Chailapakul, O., Low-cost and disposable coenzyme Q10
and α-Lipoic acid sensor using manganese (IV) oxide
modified screen-printed graphene electrode., Analytica
Chimica Acta, 1004 (2018), 22-31.
Charoenkitamorn, K., Tue, P. T., Kawai, K., Chailapakul, O.,
Takamura, Y., Electrochemical Immunoassay using Open
Circuit Potential Detection labeled by Platinum

Nanoparticles. Sensors, 18 (2018), 444.

Charoenkitamorn, K., Tue, P. T., Chikae, M., Chailapakul, O., Takamura, Y., Gold Nanoparticles Labeled Electrochemical Immunoassay using Open Circuit Potential for Human Chorionic Gonadotropin Detection., Electroanalysis, 30 (2018), 1766 –1772.

AWARD RECEIVED

January 2014   Outstanding Poster Presentation award, for Pure and Applied Chemistry International Conference 2014 (PACCON2014) Organized by Department of Chemistry, Faculty of Science, Khon Kaen University and Chemical Society of Thailand under the Patronage of Her Royal Highness Princess Chulabhorn Mahidol

December 2016   Best poster, Session: Flow-based Analysis, for 13th Asian Conference on Analytical Science (ASIANALYSIS XIII) Organized by Center of Excellence for Innovation in Analytical Science and Technology, Faculty of Science, Chiang Mai University

June 2018   Outstanding Poster Presentation, for the Nineteenth Royal Golden Jubilee Ph.D. Congress (RGJ-Ph.D. Congress 19) Organized by the Royal Golden Jubilee Ph.D. Program under The Thailand Research Fund